THE NATURE AND DISTRIBUTION OF THE METAL CENTERS IN CYTOCHROME C OXIDASE

Thesis by

Gary Wayne Brudvig

In Partial Fulfillment of the Requirements

For the Degree of

Doctor of Philosophy

California Institute of Technology

Pasadena, California 91125

1981

(Submitted August 21, 1980)

To Colleen and Lars

ACKNOWLEDGEMENTS

Our work on cytochrome c oxidase has been a group effort throughout the past four years. Many of the ideas that led up to the work in this thesis came out of discussions between Dr. Sunney Chan, Dr. David Bocian, Tom Stevens and myself. I am indebted to all of these people, Tom Stevens for his biochemical insight, David Bocian for his physical chemical insight, and particularly Sunney Chan for his advice and insistence on excellence. Without these colleagues I am sure we would not have progressed as far in our work on cytochrome c oxidase.

I would also like to thank all my other colleagues and coworkers who have aided me during my graduate work. In particular I would like to thank Professor Harry Gray and the members in his group for the generous gift of the "blue" copper proteins used in this work, Professor Steven Boxer for allowing me to use his pulsed EPR instrumentation to measure electron relaxation times, and Randy Morse for his help in the work presented in chapter III.

Finally, I would like to thank my wife, Colleen, whose love and support has been my foundation here at Caltech.

ABSTRACT

Cytochrome c oxidase is the terminal oxidase in the mitochondrial electron transport chain. Its function is to catalyze the four electron reduction of O_2 to water and under coupled conditions the energy released in this reaction is used in the synthesis of adenosine triphosphate. The enzyme contains four metal centers, two heme a's and two coppers, all of which are inequivalent. In this work, the structure of the metal centers and the distances between the metals has been investigated by the use of electron paramagnetic resonance (EPR) and optical spectroscopy.

Cytochrome a_3 and Cu_{a_3} together form the O_2 binding site. In the fully oxidized enzyme these two metals do not exhibit an EPR signal due to the strong antiferromagnetic exchange interaction between these closely associated metal ions. NO has been used as a spin probe to uncouple Cu_{a_3} from cytochrome a_3. In the course of these studies it was found that the enzyme catalyzed both the oxidation and reduction of NO. The analysis of these reactions has provided a new insight into the catalytic function of cytochrome c oxidase and the implications of these experiments on the mechanism of O_2 reduction is discussed. It also was found that NO binds specifically to one conformation of the oxidized enzyme. This specificity has allowed the conformations of the oxidized enzyme to be investigated. Three conformations were found to form sequentially when the reduced enzyme was reoxidized by O_2. It is proposed that these conformations

differ in the nature of the ligand bridging between cytochrome $\underline{a}_3$ and Cu_{a_3}; the final state being one in which a μ-oxo ligand bridges between the two metal ions.

Cu_a is involved in transferring electrons from cytochrome $\underline{c}$ to the O_2 binding site. The structure of Cu_a has been of considerable interest because this site has very unusual EPR properties. The effect of sulfhydryl binding reagents on the Cu_a center EPR signal has been examined. These experiments together with an analysis of the EPR parameters of the native site, indicate that Cu_a is best described as a Cu(I)-sulfur radical complex in the oxidized enzyme. A model for the Cu_a center is proposed in which a Cu(I) is ligated to two neutral histidine nitrogens and two cysteine sulfurs, one a cysteinate and the other a thiyl radical, in a near tetrahedral geometry.

The distance between the metal centers was investigated by examining the electron spin relaxation properties of the Cu_a center by the method of continuous saturation. The dipolar interaction of a rapidly relaxing site (either of the two hemes) can dramatically increase the relaxation rate of a slowly relaxing site (the Cu_a center) if the sites are in close proximity. It is concluded that cytochrome $\underline{a}$ is within 13 Å of the Cu_a center, and that the cytochrome $\underline{a}_3$-Cu_{a_3} site is more than 10 Å from either the Cu_a center or cytochrome $\underline{a}$.

TABLE OF CONTENTS

CHAPTER I: INTRODUCTION

Cytochrome c oxidase[1,2] (ferrocytochrome c: oxygen oxidoreductase; EC 1.9.3.1) is the terminal oxidase in the mitochondrial electron transport chain. It catalyzes the four electron reduction of O_2 to water and under coupled conditions the energy released in this reaction is conserved and used in the synthesis of ATP.* The use of O_2 as the terminal electron acceptor is a great advantage to aerobic organisms since more than five-fold more energy can be obtained in the oxidation of organic molecules over that obtained by anaerobic organisms.

The interest in cytochrome c oxidase lies in two properties of the enzyme. First of all, it efficiently catalyzes the four electron reduction of O_2 to water. It can well be imagined that nature will have designed an optimal configuration for the active site of O_2 reduction. The second property of interest is the fact that this enzyme conserves a portion of the energy released in the transfer of electrons from cytochrome c to O_2. At the present time the mechanism of O_2 reduction and the mechanism by which the electron transfer reactions are coupled to the synthesis of ATP are not understood. In order to address these questions, it is necessary to determine the structure and function of each of the four metal centers within the enzyme. It is also important to know the relative proximity of each metal center to

*Abbreviations used in this work: ATP, adenosine triphosphate; EPR, electron paramagnetic resonance; NMR, nuclear magnetic resonance; MCD, magnetic circular dichroism; ENDOR, electron nuclear double resonance; PPD, p-phenylenediamine; p-HMB, p-hydroxymercuribenzoate; b-tbsCu, bis(N-t-butylsalicylaldiminato) Cu(II); EXAFS, extended x-ray absorption fine structure.

one another and their location within the cytochrome c oxidase complex. In this work we have investigated the structure of the metal centers and the distances between the metals by the use of spectroscopic techniques. Studies on the structure of the site of O_2 reaction in cytochrome c oxidase provide information that may be used in the synthesis of an inorganic catalyst of the reduction of O_2 to water. Such a catalyst is of major interest since at the present time the utility of fuel cells using H_2 and O_2 as reactants is limited by the lack of an efficient and durable O_2 electrode. Information on the mechanism of coupling electron transfer reactions to the synthesis of ATP also can be applied to areas other than mitochondrial function. For example, information on the mechanism of this process in cytochrome c oxidase may also provide an insight into the coupling of other forms of energy, such as solar energy, to the synthesis of high-energy compounds.

Cytochrome c oxidase is an oligomeric protein containing two heme a's and two coppers, and is embedded in and spans the inner mitochondrial membrane.[1] In recent years considerable progress has been made in the biochemical characterization of the enzyme complex. It now appears that the complex contains ten polypeptide subunits: eight different subunits present in one copy each and two copies of a ninth subunit.[3] The molecular weights of the individual subunits are shown in Table 1 and give a combined molecular weight of the cytochrome c oxidase complex of about 130,000. This molecular weight is very close to that estimated from the heme a/protein ratio obtained from the most

Table 1: Subunit Composition of Cytochrome c Oxidase

Subunit	Molecular Weight[a] SDS Gel Electrophoresis	Molecular Weight[b] Sequence Data	Synthetic Origin[c]
I	35,400		Mitochondria
II	24,100	26,795	Mitochondria
III	21,000		Mitochondria
IV	16,800		Cytoplasm
V	12,400	12,436	Cytoplasm
VI	8,200		Cytoplasm
VII	4,400		Cytoplasm
VIII	4,400		Cytoplasm
IX	4,400		Cytoplasm
	131,100		

a. References 4 and 5

b. Reference 6

c. Reference 7

pure preparations of the enzyme. The Hartzel and Beinert[8] preparation can yield a heme a/protein ratio of about 14 which implies a molecular weight of 140,000 based on two heme a/enzyme.

One finding of considerable interest is that the three largest subunits are synthesized in the mitochondria, whereas the remaining subunits are synthesized in the cytoplasm.[7] The cytochrome c oxidase complex is apparently assembled in the inner mitochondrial membrane by the proteolysis of one large cytoplasmically synthesized polypeptide into the smaller subunits in a complex process of protein assembly.[9,10]

It has been possible to obtain some information on the three-dimensional structure of oxidized cytochrome c oxidase by electron microscopy.[11] Under the appropriate conditions the oxidized enzyme will associate into a membranous two-dimensional lattice. Analysis of this lattice by electron microscopy at various angles has led to a three-dimensional structure[12] of oxidized cytochrome c oxidase with a resolution of about 20 Å. The structure obtained is shown in Figure 1.

Capaldi's group and others have also investigated the position of the individual subunits within the three-dimensional structure.[4,13,14] Although the overall picture is not yet complete, it appears that subunits 2 and 3 span the inner mitochondrial membrane, passing through the membrane a number of times via α-helical stretches of hydrophobic amino acid residues. Subunits 4, 5, 7, 8 and 9 appear to be located on the inner surface of the inner mitochondrial membrane (matrix-side) while subunits 1 and 6 appear to be within the protein and not

FIGURE 1

(A) a schematic representation of a mitochondria. Three domains are present: the matrix within the inner mitochondrial membrane, the intercristal space between the inner and outer mitochondrial membranes, and the cytoplasm outside the mitochondria. (B) an enlargement of (A) to show the structure of oxidized cytochrome c oxidase at a resolution of about 20 Å (obtained from reference 12). Note that two small protein domains extend into the matrix and one large protein domain extends into the intercristal space.

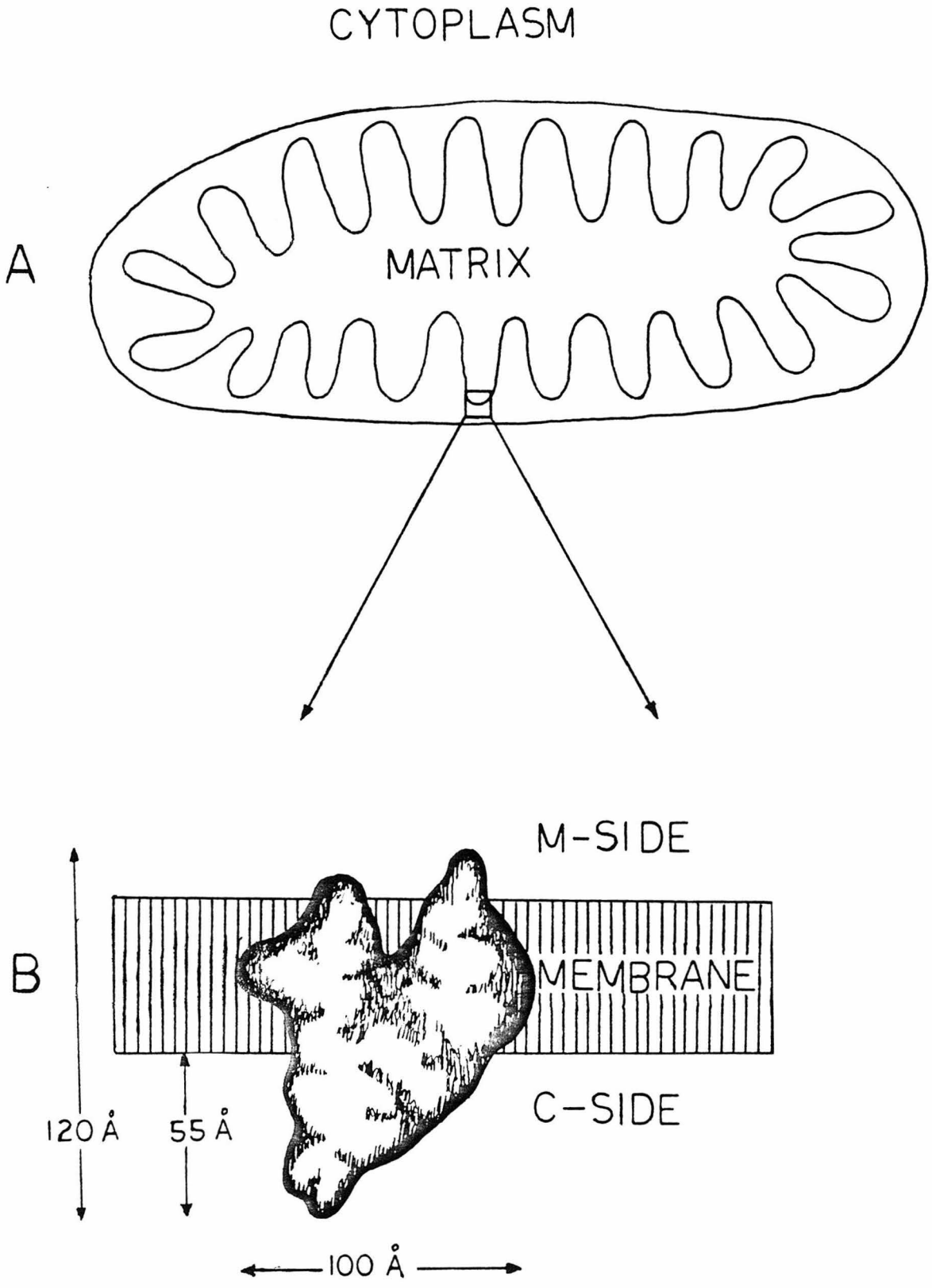
CYTOPLASM
A
MATRIX
M-SIDE
B
MEMBRANE
C-SIDE
120 Å
55 Å
100 Å

accessible to water soluble reagents. Again these results were obtained on the oxidized enzyme.

Although the general shape of the enzyme was determined, these studies have not provided any information concerning the structure of the metal centers or their location within the three-dimensional structure. However, spectroscopic studies have provided information on the immediate environment of the metal centers and on the chemical properties of each metal center.

A variety of spectroscopic techniques have been used to study the metal centers. These techniques have been useful in probing the metal centers themselves, but generally provide little information on the overall structure of the enzyme. However, in many ways this is an advantage since the complexity of a large oligomeric complex can be reduced to the level of four metal coordination sites. Presumably, the metal centers are the active sites of the enzyme and, hence, knowledge of their structure and function should provide information on the function of the overall complex.

Cytochrome c oxidase was originally recognized on the basis of optical experiments.[15] In these studies, the ligand binding center within mitochondria was designated as cytochrome a_3. It was also recognized that another cytochrome with an optical spectrum similar to that of cytochrome a_3 was present in mitochondria. This cytochrome, which does not bind ligands, was designated cytochrome a. When the cytochrome c oxidase complex was eventually purified, it was realized that both cytochrome a and a_3 were part of the same overall complex.[16] At the time cytochrome c oxidase was purified, it was also

apparent that copper was associated with the complex. Originally many investigators believed that this copper was adventitious, but kinetic experiments[17] demonstrated that copper was, indeed, a functional component of the cytochrome c oxidase complex.

The work on the structure and function of the metal centers has been reviewed recently by Malmström.[18] The enzyme contains a heme a and one copper that apparently are closely associated with each other and together form the ligand binding site. The heme component of the ligand binding site has been designated cytochrome a_3. However, a number of designations have been given the copper component of the ligand binding site including: Cu_u (to refer to the fact that this copper is "undetectable" by EPR), Cu_B (to be noncommital about the nature of this copper) and Cu_{a_3} (to refer to the fact that this copper is associated with cytochrome a_3). We prefer the designation of Cu_{a_3} to the copper component of the ligand binding site because it allows an obvious association between the two components of the ligand binding site, cytochrome a_3 and Cu_{a_3}.

Neither of the remaining heme a and copper in cytochrome c oxidase binds exogenous ligands. The heme a that does not bind exogenous ligands has been designated cytochrome a and again the copper that does not bind exogenous ligands has been referred to by several names including: Cu_d (for EPR "detectable" copper), Cu_A and Cu_a. We prefer the designation Cu_a because it allows an association to be drawn between the heme a and copper which do not bind exogenous ligands (the evidence for which is presented in Chapter V).

This work is directed toward determining the nature and distribution of the metal centers in cytochrome c oxidase. In Chapter II, we investigate the structure and function of the cytochrome a_3 - Cu_{a_3} site. We have used NO as a spin probe to study the structure of the ligand binding site by EPR. In the course of these studies it was found that the enzyme catalyzes both the oxidation and reduction of NO. The analysis of these reactions has provided a new insight into the catalytic function of cytochrome c oxidase and the implications of these experiments on the mechanism of O_2 reduction is discussed. We also found that NO binds specifically to one conformation of the oxidized enzyme. This specificity has allowed us to investigate the conformations of the oxidized enzyme and these studies are presented in Chapter III.

The nature of Cu_a is discussed in Chapter IV. We have obtained results which suggest that Cu_a is best described as a Cu(I)-sulfur radical complex in the oxidized enzyme. Finally, in Chapter V, we present results on the distribution of the metal centers within cytochrome c oxidase. The dipolar enhancement of the electron spin relaxation rate of a slowly relaxing center (Cu_a) by a rapidly relaxing site (cytochrome a or cytochrome a_3) was investigated. In Chapter VI the overall picture of the metal centers in cytochrome c oxidase, as suggested by this work, is presented.

References

1. Capaldi, R.A. and M. Briggs (1976), in "The Enzymes of Biological Membranes", vol. 4 (A. Martinosi, ed.), Plenum Press, New York, N.Y., 87.
2. Lemberg, M.R. (1969), Physiol. Rev. 49, 48.
3. Capaldi, R.A. (in press), in "Proceedings of the Symposium on Interaction Between Iron and Proteins in Oxygen and Electron Transport", (C. Ho, ed.), Elsevier, Amsterdam.
4. Briggs, M. and R.A. Capaldi (1977), Biochemistry 16, 73.
5. Capaldi, R.A., R.L. Bell and T. Branchek (1977), Biochem. Biophys. Res. Comm. 74, 425.
6. Yasunobu, K.T., M. Tanaka, M. Haniu, M. Sameshima, N. Reimer, T. Eto, T.E. King, C. Yu, L. Yu and Y. Wei (1979), in "Cytochrome Oxidase", (T.E. King, Y. Orii, B. Chance and K. Okunuki, eds.), Elsevier, Amsterdam, 91.
7. Schatz, G. and T.L. Mason (1974), Ann. Rev. Biochem. 43, 51.
8. Hartzell, C.R. and H. Beinert (1974), Biochim. Biophys. Acta 368, 318.
9. Poyton, R.O. and E. McKemmie (1979), J. Biol. Chem. 254, 6763.
10. Poyton, R.O. and E. McKemmie (1979), J. Biol. Chem. 254, 6772.
11. Henderson, R., R.A. Capaldi and J.S. Leigh, Jr. (1977), J. Mol. Biol. 112, 631.

12. Deatherage, J.F., R. Henderson and R.A. Capaldi (in press), in "Proceedings of the Symposium on Interaction Between Iron and Proteins in Oxygen and Electron Transport", (C. Ho, ed.), Elsevier, Amsterdam.

13. Ludwig, B., N.W. Downer and R.A. Capaldi (1979), Biochemistry 18, 1401.

14. Bisson, R., C. Montecucco, H. Gutweniger and A. Azzi (1979), J. Biol. Chem. 254, 9962.

15. Keilen, D. and E.F. Hartree (1939), Proc. Roy. Soc. (London) B127, 167.

16. Griffiths, D.E. and D.C. Wharton (1961), J. Biol. Chem. 236, 1850.

17. Beinert, H. and G. Palmer (1964), J. Biol. Chem. 239, 1221.

18. Malmström, B.G. (1979), Biochim. Biophys. Acta 549, 281.

CHAPTER II: STRUCTURE AND FUNCTION OF CYTOCHROME $\underline{a}_3$ - Cu_{a_3}: REACTIONS WITH NO

1. INTRODUCTION

Cytochrome $\underline{a}_3$ has long been recognized as the ligand binding center in cytochrome $\underline{c}$ oxidase[1] and is generally assumed to be the site where O_2 binds. However, EPR studies[2,3] have shown that Cu_{a_3} is closely associated with cytochrome $\underline{a}_3$. Neither cytochrome $\underline{a}_3$ nor Cu_{a_3} exhibit EPR signals in the fully oxidized resting enzyme. It was initially suggested that cytochrome $\underline{a}_3$ and Cu_{a_3} are not observed by EPR due to a strong exchange interaction between these two metals.[4] This suggestion has been strongly supported by magnetic susceptibility measurements[5] which have shown that cytochrome $\underline{a}_3$ and Cu_{a_3} together form an S=2 site, indicating that the two metals are strongly antiferromagnetically coupled in the oxidized enzyme ($-J \geq 200\ cm^{-1}$). The close association of Cu_{a_3} with cytochrome $\underline{a}_3$ suggests that Cu_{a_3} is involved in the binding of ligands as well as the catalysis of the reduction of O_2 to water.

A variety of techniques has been used to study the structure and function of cytochrome $\underline{a}_3$ and Cu_{a_3}. By far the most often used has been optical spectroscopy. This technique has been used to determine ligand binding constants,[6] redox potentials,[7] conformational states,[8] and the kinetics of the reaction with O_2 and ligands.[9] MCD has been used in conjunction with optical spectroscopy in these types of experiments;[10] the advantage of MCD being that cytochrome $\underline{a}_3$ can be readily

distinguished from cytochrome a because of their different spin states.

Optical spectroscopy has been successfully utilized to monitor the reaction of the reduced enzyme with O_2 at low temperature.[11] In order to carry out this experiment the CO-bound reduced enzyme is dissolved in an H_2O/ethylene glycol solution and cooled to -40°C. At this temperature the rate of dissociation of CO from the enzyme is sufficiently slow that an O_2 saturated solution can be mixed with the reduced CO-bound enzyme and the solution frozen before O_2 reacts with the enzyme. Then at 77k the CO can be flashed off the enzyme and replaced by O_2. When the O_2-bound reduced enzyme is warmed incrementally, temperatures are reached wherein individual steps in the reaction of O_2 with the reduced enzyme occur. Three such reaction steps have been observed and the products have been named compound A, B, and C, respectively.[11] Although the exact species comprising each of these compounds is not known, it has been proposed that compound A is formed upon binding of O_2 to the reduced enzyme, compound B is formed when one electron is transferred to the bound O_2, and compound C is formed when a second electron is transferred to the bound O_2. The possible states formed in the reaction of O_2 with the reduced enzyme will be elaborated on in section 4.

The major disadvantage of optical spectroscopy and MCD is that Cu_{a_3} cannot be observed and its role in each of the above experiments must be inferred. EPR spectroscopy has proved to be more useful in determining the structure of both

cytochrome $\underline{a}_3$ and Cu_{a_3}. However, EPR studies of the cytochrome $\underline{a}_3$ - Cu_{a_3} pair have been limited by the fact that the interaction between the metal centers must be eliminated or modified before an EPR signal can be observed. Two methods have been used to break the coupling between the metals: 1) selective reduction[12] of cytochrome $\underline{a}_3$ or Cu_{a_3}, and 2) use of the spin probe NO.[2,13,14]

When cytochrome $\underline{c}$ oxidase is partially reduced or partially reoxidized under anaerobic conditions, EPR signals can be observed* from high-spin cytochrome $\underline{a}_3$.[3,12,15] The signals arise from protein molecules in which Cu_{a_3} is reduced and cytochrome $\underline{a}_3$ is oxidized. It has been possible to observe EPR signals from cytochrome $\underline{a}_3$ coordinated to hydroxide,[4] cyanide,[16] azide,[4] sulfide,[12,17] and a number of larger molecules containing one of these three functional groups (Table 1). These EPR signals are consistent with cytochrome $\underline{a}_3$ having one unoccupied axial position (or an axial ligand that can be displaced by cyanide, azide, or sulfide in the partially reduced enzyme) and one endogenous imidazole axial ligand.[19] However, these studies cannot provide information on the structure of the oxygen binding site in the fully oxidized or fully reduced enzyme, since in these states none of the above ligands induce EPR

*There is still some uncertainty as to whether the high-spin heme EPR signals observed from partially reduced cytochrome $\underline{c}$ oxidase are entirely due to cytochrome $\underline{a}_3$. Upon partial reoxidation of the reduced enzyme, all of the high-spin heme EPR signals have been shown[12] to arise from cytochrome $\underline{a}_3$. However, upon partial reduction of the oxidized enzyme, a large number of different high-spin heme EPR signals have been observed (see Table 1), some of which may be due to cytochrome $\underline{a}$ having undergone a transition from low-spin to high-spin.

Table 1: EPR Signals Observed from Partially Reduced Cytochrome c Oxidase in the Absence and Presence of Ligands (EPR Active Site is Underlined)

Species	EPR Signal (g-values)
ferricytochrome a	3.03, 2.29, 1.45[a]
oxidized Cu_a center	2.18, 2.03, 1.99[a]
$Fe^{+3}_{a_3}$-L···$Cu^{+}_{a_3}$ (L is an unknown and possibly variable ligand)	6.42, 5.37, 2.0[a] 6.27, 5.49, 2.0[a] 5.99, 5.79, 2.0[a] 6.10, 5.84, 2.0[b]
$Fe^{+3}_{a_3}$-OH^{-}···$Cu^{+}_{a_3}$	2.6, 2.2, 1.87[c] 2.5, 2.2, 1.88[c]
$Fe^{+3}_{a_3}$-CN^{-}···$Cu^{+}_{a_3}$	3.58, ? , ?[d]
$Fe^{+3}_{a_3}$-N_3^{-}···$Cu^{+}_{a_3}$	2.9, 2.2, 1.67[c] 2.75, 2.2, 1.76[c]
$Fe^{+3}_{a_3}$-SH^{-}···$Cu^{+}_{a_3}$	2.54, 2.23, 1.87[e] 2.77, 2.23, 1.71[f]
$Fe^{+2}_{a_3}$-CO···$Cu^{+2}_{a_3}$	2.28, 2.06, 2.03[g]

a. Reference 3
b. Reference 15
c. Reference 4
d. Reference 16
e. Reference 17
f. Reference 12
g. Reference 18

signals from the enzyme.

In the absence of added ligands or in the presence of cyanide, azide, or sulfide (all of which are electron rich ligands), the reduction potential of Cu_{a_3} is apparently much larger than that of cytochrome $\underline{a}_3$, making it impossible to observe states in which cytochrome $\underline{a}_3$ is reduced while Cu_{a_3} is oxidized. Thus, it has not been possible to observe Cu_{a_3} by EPR during anaerobic reductive or oxidative titrations. However, recently it was found that in the presence of both CO and O_2 an EPR signal could be observed from Cu_{a_3} in the partially reduced enzyme.[18] Presumably under the conditions of this experiment CO binds to cytochrome $\underline{a}_3$ and alters the reduction potential of cytochrome $\underline{a}_3$ such, that its reduction potential is higher than that of Cu_{a_3} (CO, NO, and O_2 are electron deficient ligands that would be expected to raise the reduction potential of a heme when bound, in contrast to cyanide, azide, and sulfide which are electron rich ligands and would be expected to lower the reduction potential of a heme when bound). This allows a state of the enzyme to be prepared in which Cu_{a_3} is oxidized and carboxycytochrome $\underline{a}_3$ is reduced. The EPR signal observed from Cu_{a_3} ($g=2.28, 2.11, 2.05$; $A_{11}=0.010\ cm^{-1}$) is quite similar to that of copper in superoxide dismutase ($g=2.26, 2.10, 2.03$; $A_{11}=0.013\ cm^{-1}$).[20] A crystal structure has been obtained for superoxide dismutase[21] and the copper was found to be ligated to four imidazoles; three of the ligands form a plane with the copper, while the fourth ligand is bent slightly out-of-plane. One axial position was

available for the coordination of exogenous ligands. It is reasonable to assume, then, that the structure of Cu_{a_3} may be similar to that of the copper in superoxide dismutase.

One disadvantage of observing EPR signals from partially reduced states of the enzyme is that the sample is heterogeneous. In general more than one partially reduced state contributes to the EPR spectrum, making interpretation of the EPR signals difficult. The second technique, which circumvents this problem, is the use of NO as a spin probe to uncouple cytochrome $\underline{a}_3$ and Cu_{a_3}.

The binding of NO to ferrous hemoproteins is well known.[22] In the case of fully reduced cytochrome $\underline{c}$ oxidase, NO binds to cytochrome $\underline{a}_3$ and the nitrosylferrocytochrome $\underline{a}_3$ site exhibits an EPR signal[14] with g-values of 2.091, 2.006, and 1.97. In contrast, the fully reduced enzyme alone does not exhibit an EPR spectrum. When ^{14}NO is bound to reduced cytochrome $\underline{c}$ oxidase, the EPR signal of the complex exhibits a nine-line superhyperfine pattern, which can be interpreted in terms of the superposition of three sets of three lines arising from two non-equivalent nitrogens (I=1) interacting with the unpaired electron.[14] When ^{15}NO is used in this experiment, the ^{15}NO-bound enzyme exhibits an EPR spectrum with g-values identical to those of the ^{14}NO-bound species, but with a superhyperfine pattern of two sets of three lines.[13] This pattern is consistent with one ^{14}N and one ^{15}N bound axially to cytochrome $\underline{a}_3$. These observations indicate that in the fully reduced enzyme cytochrome $\underline{a}_3$ has one endogenous axial nitrogen ligand and one

axial site available for binding NO.

The endogenous axial nitrogen ligand on ferrocytochrome $\underline{a}_3$ could be contributed by any of a number of amino acid groups including histidine, arginine, lysine, and peptide nitrogen. However, Kon and Kataoka[23] have shown that the g-values and nitrogen superhyperfine splittings of the EPR signals of NO-bound hemin are dependent on the Π-bonding capability of the axially bound nitrogen ligand opposite NO. Only with strong Π-bonding ligands, such as pyridine, did the EPR signals exhibit rhombic symmetry and resolved nitrogen superhyperfine splitting from the nitrogen ligand opposite NO as observed for nitrosyl-ferrocytochrome $\underline{a}_3$. These results suggest that the endogenous axial nitrogen ligand of cytochrome $\underline{a}_3$ is a strong Π-bonding ligand, with the imidazole group from a histidine residue being the only reasonable candidate.

Histidine is known to be an endogenous axial ligand to iron in the hemoproteins cytochrome $\underline{c}$ and hemoglobin.[24] The similarities in the EPR spectra of NO-bound ferrocytochrome $\underline{c}$, ferrohemoglobin and ferrocytochrome $\underline{a}_3$ have led Van Gelder and Blokzijl-Homan[14] to suggest that the endogenous axial ligand to cytochrome $\underline{a}_3$ is also a histidine. This conclusion is consistent with the conclusion based on the cyanide, azide, and sulfide bound cytochrome $\underline{a}_3$ EPR signals observed in the partially reduced enzyme.[19] Therefore, it appears very likely that cytochrome $\underline{a}_3$ has one endogenous axial histidine ligand in both the partially and fully reduced enzyme.

NO has also been observed to bind to oxidized cytochrome $\underline{c}$

oxidase.[2] In this case, NO reversibly binds to $Cu_{a_3}^{+2}$ and uncouples Cu_{a_3} from cytochrome $\underline{a}_3$. The resulting complex exhibits a rhombic high-spin heme EPR signal from cytochrome $\underline{a}_3$. This EPR signal is typical of those observed from other high-spin ferrihemes and indicates that NO does not interact with cytochrome $\underline{a}_3$ and that the $Cu_{a_3}^{+2}$-NO site does not perturb the spin state of ferricytochrome $\underline{a}_3$ (for example, no dipolar or exchange interaction is evident between $Cu_{a_3}^{+2}$-NO and ferricytochrome $\underline{a}_3$). These results suggest that the spins on $Cu_{a_3}^{+2}$ and NO are strongly coupled and the $Cu_{a_3}^{+2}$-NO complex is diamagnetic.

Although NO itself does not appear to bind to cytochrome $\underline{a}_3$ in the oxidized enzyme, several other ligands were found to bind to cytochrome $\underline{a}_3$, while NO remained coordinated to Cu_{a_3}.[2] When cyanide was added to the oxidized enzyme in the presence of NO, a low-spin EPR signal was observed, characteristic of cyanide-bound ferricytochrome $\underline{a}_3$. Fluoride also was found to bind to cytochrome $\underline{a}_3$, although in this case cytochrome $\underline{a}_3$ remained high-spin and exhibited an axial EPR signal in the presence of NO.

A model for the cytochrome $\underline{a}_3$ - Cu_{a_3} site was proposed which explains the EPR observations of the NO-bound oxidized enzyme.[25] In this model, the strong antiferromagnetic exchange interaction between cytochrome $\underline{a}_3$ and Cu_{a_3} is facilitated through a bridging ligand bound equatorially to a tetragonal Cu_{a_3}. For a d^9 copper with a tetragonal geometry, the unpaired electron is in a $d_{x^2-y^2}$ orbital with the orbital lobes directed

towards the ligands in the square plane. The attachment of a strong field ligand, such as NO, to an axial position of Cu_{a_3} should place the unpaired electron in a square plane containing the stronger field ligand. When this occurs, the antiferromagnetic exchange interaction between Cu_{a_3} and cytochrome $\underline{a}_3$ would be greatly reduced, while a strong interaction between Cu_{a_3} and the coordinated NO would be possible.

Another interesting characteristic of the interaction of NO with the oxidized enzyme was observed when N_3^- was added to the NO-bound oxidized enzyme. In this case N_3^- did not simply bind to cytochrome $\underline{a}_3$, as did CN^- and F^-, but instead reacted with NO at the oxygen binding site to form the one-quarter reduced NO-bound enzyme.[2] This reaction was shown to produce N_2O and N_2 and generate a state of the enzyme which exhibited a triplet EPR signal. The triplet state arises from the dipolar coupling of nitrosylferrocytochrome $\underline{a}_3$ (S=1/2) and $Cu^{+2}_{a_3}$ (S=1/2). The observed EPR signal exhibits copper hyperfine splitting on the half-field transition; the magnitude of the splitting is characteristic of a tetragonal geometry for Cu_{a_3}.

Although this triplet EPR signal is of considerable interest itself, the observation that cytochrome $\underline{c}$ oxidase catalyzes a reaction of N_3^- and NO suggests that NO could be utilized to investigate the catalytic function of the enzyme. In this chapter we investigate the interactions of NO with cytochrome $\underline{c}$ oxidase more closely and find that several reactions of NO are catalyzed by this enzyme, both to oxidize

and reduce NO.[26] These reactions were sufficiently slow that the states of the enzyme formed in the course of reaction could be monitored by EPR. The elucidation of these reactions as well as the nature of the states generated has revealed new information on the structure of the oxygen binding site.

The implications of the results on the reactions of NO with the enzyme for the mechanism of O_2 binding and reduction are discussed. These implications suggest a sequence by which the reduced enzyme reacts with O_2 to form the oxidized state.

2. MATERIALS AND METHODS

2.1 Preparation of Cytochrome c Oxidase Complexes. Beef heart cytochrome c oxidase was isolated by the procedure of Hartzell and Beinert.[27] The purified protein was dissolved in 50 mM Tris/acetate buffer, 0.5% Tween 20, pH 7.4 and stored at -85°C until use. The concentration of the enzyme was determined by the pyridine hemochromogen assay[28] and the concentrations quoted in this work were based on two heme a/enzyme. The preparations used in this work contained 9-11 nmoles heme a/mg protein.

Nitric oxide (^{14}N), obtained from Matheson, is known to be contaminated with other nitrogen oxides and was therefore scrubbed with a dry ice/ethanol trap before being added to the enzyme samples. ^{15}NO (99.2% isotopic enrichment, Prochem) was found to be essentially free of other nitrogen oxides and was used as received. $K^{15}N^{14}N_2$ (99.4% isotopic enrichment), $Na^{15}NO_2$ (99.1% isotopic enrichment), and $K^{15}NO_3$ (99.1% isotopic

enrichment) were all obtained from Prochem. All other reagents used were of the highest purity commercially available.

Four complexes of cytochrome c oxidase were prepared in this work: (i) oxidized enzyme plus NO, (ii) oxidized enzyme plus azide and NO, (iii) reduced enzyme plus NO, and (iv) reduced enzyme plus nitrite. The samples were first made anaerobic by three cycles of evacuation and flushing with argon. Then NO was added to the samples through an inlet to the vacuum line so as to completely exclude oxygen. Denaturation of the protein (vide infra) was observed if strict anaerobic conditions were not maintained.

The oxidized enzyme plus NO complex was prepared by the addition of NO to a pressure of one atmosphere to an anaerobic sample of the oxidized enzyme in the absence of added ligands. The oxidized enzyme plus azide and NO complex was prepared by adding NaN_3 to the oxidized enzyme to a concentration of 100 mM, making the sample anaerobic, and then adding NO to a pressure of one atmosphere. The reduced enzyme plus NO complex was prepared by adding the reductant (10 mM sodium ascorbate plus 5 mM PPD or 5 mM sodium dithionite) to the anaerobic oxidized protein from a sidearm, incubating for 10 minutes to allow for complete reduction, and then adding NO to a pressure of one atmosphere. The reduced enzyme plus nitrite complex was prepared by adding 10 mM sodium ascorbate plus 5 mM PPD and 50 mM $NaNO_2$ to the anaerobic oxidized protein from a sidearm. When ^{15}NO was added to the enzyme the same procedures were followed except that the pressure of ^{15}NO added to the samples

was not measured but was approximately one atmosphere.

2.2 Activity Assays. The activity of cytochrome c oxidase was measured polarographically using a YSI Model 53 oxygen electrode in a medium containing 50 mM phosphate buffer, 0.3 mg/ml cytochrome c, 1% Tween 80, and 30 mM ascorbate at pH 7.4 and 30.5°C. The activity was measured before and after incubation of the oxidized enzyme for 24 hrs. at 4°C while mixing with an atmosphere of NO. In order to assay the activity of the enzyme which had been incubated with NO, it was necessary to extensively degas the sample, since exposure of the enzyme in the presence of NO to air resulted in denaturation of the enzyme. The NO was removed from the sample by five cycles of evacuation and flushing with argon. The activity was 114 ±10 before NO incubation and 137 ±20 after the incubation, in units of moles cytochrome c oxidized/mole cytochrome c oxidase/sec. This control demonstrates that NO does not irreversibly alter the catalytic activity of the enzyme.

2.3 EPR Spectroscopy. EPR spectra were typically recorded on 0.2 ml samples containing the enzyme at a concentration of 0.25 mM. The exact concentration of the enzyme for each experiment is given in the figure legends. The EPR spectra were recorded on a Varian E-line century series X-band spectrometer equipped with an Air-Products Heli-Trans low temperature system. All of our spectra were recorded between 10-20 K to achieve maximal resolution of the signals.

2.4 Optical Spectroscopy. The samples which were used for optical spectroscopy were prepared in a cuvette which was

fitted with a ground glass stopcock. We used 1 mm or 2 mm path length cells so that the high concentrations of the enzyme used in the EPR experiments could also be used to record optical spectra. All optical measurements were carried out at room temperature on a Beckman Acta CIII spectrometer.

2.5 Mass Spectroscopy. The samples for mass spectroscopy were prepared in a 5 ml glass bulb which was fitted with a ground glass stopcock. A 1.0 ml aliquot of cytochrome c oxidase was used in each experiment. After the addition of NO, a magnetic stir bar inside the bulb was used to mix the sample with the NO atmosphere. The reaction was then allowed to proceed for the specified length of time and, thereafter, the gas above the sample was fed directly through a ground glass inlet into a DuPont 21-492B mass spectrometer. With this procedure, only the gaseous nitrogen compounds NH_3, N_2, NO, and N_2O could be monitored, since the other gaseous nitrogen compounds, in particular NO_2, are not stable at room temperature in the presence of water. In these experiments, atmospheric CO_2 and N_2 were the major contaminants and interfered with the observation of the N_2O and N_2 parent peaks. To alleviate this problem, ^{15}NO was substituted for ^{14}NO and/or $^{15}N^{14}N^-_2$ was substituted for $^{14}N^-_3$. The parent peaks due to $^{15}N_2O$, $^{14}N^{15}NO$, $^{15}N_2$, and $^{15}N^{14}N$ could be observed without interference. In each experiment, a blank was also prepared which was identical to the sample except that the enzyme was omitted. All mass spectral data quoted in this work were corrected for the background observed in the blank.

2.6 NMR Spectroscopy. The samples, which were used for NMR spectroscopy, were prepared in a 10 mm NMR tube which was constricted near the top and fitted with a ground glass stopcock. In order to minimize the effect of sample vortexing, we used 4 ml samples. The samples contained 25% D_2O, which was used for an internal lock, and the enzyme concentration was 0.12 mM. After ^{15}NO was added to the anaerobic samples to a pressure of approximately one atmosphere, the sample plus ^{15}NO gas was frozen in liquid nitrogen and the NMR tube was sealed and removed from the stopcock at the constriction. Then the sample was thawed and placed on a motor-driven carousel at 4°C which repeatedly inverted the sample to provide mixing of the solution with the NO atmosphere. After the desired period of incubation, the ^{15}N NMR spectrum of the solution was recorded at 30°C on a JOEL FX90 NMR spectrometer.

These NMR spectroscopy experiments are complementary to the mass spectroscopy experiments described in the previous section in that gaseous reaction products were observed by mass spectroscopy and non-gaseous products were observed by NMR. However, the sensitivity of ^{15}N NMR is considerably lower than that of mass spectroscopy and a product concentration of approximately 5 mM or more was required before the NMR signal of a reaction product could be observed. For this reason much longer reaction times were required for the NMR experiments (generally several days at 4°C).

3. RESULTS

In the presence of NO, EPR signals can be observed from all

four metal centers in cytochrome c oxidase, depending on the oxidation and/or ligation state of the enzyme. We have summarized in Table 2 the states of the enzyme which have previously been observed in the presence of NO plus those which we will describe in this work. Cytochrome a and Cu_a exhibit EPR signals in the oxidized state which are eliminated upon reduction of these sites. Neither of these metal centers interact directly with NO. It is not quite as straightforward to determine the oxidation and ligation states of cytochrome a_3 and Cu_{a_3} by EPR spectroscopy. In the oxidized enzyme, these two metal centers are strongly antiferromagnetically coupled,[5] while in the reduced enzyme no EPR signals are expected from the high-spin cytochrome a_3. However, in the presence of NO, three states do exhibit diagnostic EPR signals: (i) ferricytochrome a_3, $Cu^{+2}_{a_3}$-NO (high-spin cytochrome a_3 EPR signal), (ii) nitrosyl-ferrocytochrome a_3, $Cu^{+2}_{a_3}$ (triplet EPR signal), and (iii) nitrosylferrocytochrome a_3, $Cu^{+}_{a_3}$ (nitrosylferrocytochrome a_3 EPR signal).

In this work, we utilized EPR spectroscopy to determine the states of the metal centers which are formed during the reactions with NO. As we will demonstrate, NO can both oxidize and reduce cytochrome c oxidase. Under the appropriate conditions, a cycle was established in which the oxidation state of the enzyme oscillated as NO was consecutively oxidized and reduced. It was possible to follow these reaction cycles by EPR only because the rate of consumption of NO was quite slow. This allowed us to initiate the reaction by adding NO, incubate the sample for a

Table 2: EPR Signals Observed for Cytochrome c Oxidase and Its NO Complexes

Complex	Species Present	EPR Signals (g-values)
oxidized enzyme[a] or	ferricytochrome a	3.03, 2.21, 1.45
'oxygenated' enzyme + NO[b]	oxidized Cu_a center	2.18, 2.03, 1.99
	ferricytochrome a_3 - $Cu^{+2}_{a_3}$	EPR silent
oxidized enzyme + NO[b]	ferricytochrome a	3.03, 2.21, 1.45
	oxidized Cu_a center	2.18, 2.03, 1.99
	ferricytochrome a_3	6.16, 5.82, 2.0
	$Cu^{+2}_{a_3}$ - NO	EPR silent
oxidized enzyme + N_3^- + NO[b]	ferricytochrome a	3.03, 2.21, 1.45
	oxidized Cu_a center	2.18, 2.03, 1.99
	nitrosylferro-cytochrome a_3 - $Cu^{+2}_{a_3}$	Triplet signal: main transition from g=2.61 to g=1.69, half-field transition at g=4.3
reduced enzyme[a]	ferrocytochrome a	EPR silent
	reduced Cu_a center	EPR silent
	ferrocytochrome a_3 - $Cu^{+}_{a_3}$	EPR silent
reduced enzyme + limited NO[c]	ferrocytochrome a	EPR silent
	reduced Cu_a center	EPR silent
	$Cu^{+}_{a_3}$	EPR silent
	nitrosylferrocytochrome a_3	2.09, 2.00, 1.97 (9 line hyperfine structure on g=2.00)
reduced enzyme + excess NO[d]	ferrocytochrome a	EPR silent
	reduced Cu_a center	EPR silent
	nitrosylferrocytochrome a_3, $Cu^{+}_{a_3}$ - NO	EPR silent
NO dissolved in buffer[b]	NO	1.97, 1.97, 1.7

a. Reference 3
b. Reference 2
c. Reference 14
d. This work

specified length of time at 20°C, quickly freeze the sample by placing it in the Air Products Heli-trans dewar at 10 K to trap the states present, and then monitor the state of the enzyme by EPR. At each instant in time the major steady state species observed should be the one which just preceded the slowest step in the reaction cycle. Depending on the concentration of the dissolved NO, this slowest step in the reaction cycle could be either a redox reaction if excess NO was present, or the binding of NO to the enzyme if the NO was limited. It was possible to vary the NO concentration by incubating the sample without mixing, since the rate at which NO diffused from the gas above the sample into the unstirred solution was insignificant compared to the rate at which NO was consumed by the reactions. By this procedure we, therefore, observed the steady state species as a function of NO concentration.

3.1 Reduced Cytochrome c Oxidase + NO. (1) Dithionite as Reductant. In most of the previous work done on the nitrosyl derivative of reduced cytochrome c oxidase, dithionite was used to reduce the enzyme.[13,14] We also initially employed dithionite to reduce the enzyme. However, we have noted that the enzyme was unstable in the presence of both dithionite and NO as the enzyme precipitated within minutes after the addition of NO. Moreover, when NO was added to the enzyme reduced by dithionite, no EPR signal was observed from the NO dissolved in the buffer, even when the sample was mixed and rapidly frozen; only the EPR signal from nitrosylferrocytochrome a_3 was observed. This observation demonstrates that a reaction was occurring which

reduced the concentration of dissolved NO to a level which was too small to be detected by EPR.

In order to determine what reaction took place to consume the NO, we examined the mass spectrum of the products formed from the incubation of 100 mM sodium dithionite in 50 mM Tris/acetate, pH 7.4 under an NO atmosphere at room temperature. It was found that essentially all of the NO was converted into N_2O within 20 minutes. We followed the rate of NO consumption by dithionite manometrically (after correcting for the N_2O evolved). The results (Figure 1) show that two moles of NO were rapidly consumed per mole of dithionite and, thereafter, a slower reaction continued to consume NO. In addition, we have noted a change in pH of the sample resulted from the reaction of NO with dithionite. In the presence of excess NO, the pH dropped from 5.8 (the pH of a solution of 50 mM Tris/acetate buffered to pH 7.4 plus 0.5 M sodium dithionite) to 2.2 after incubation of the sample for 24 hours at room temperature. In contrast, when the mole ratio of NO to dithionite was equal to one, the pH of the solution dropped only from 5.8 to 5.6.

All of the above can be explained by reactions (1) and (2), provided that reaction (1) is much more rapid than reaction (2).

$$S_2O_4^{-2} + 2NO + H_2O \rightarrow 2HSO_3^- + N_2O \qquad (1)$$

$$HSO_3^- + 2NO \rightarrow SO_4^{-2} + N_2O + H^+ \qquad (2)$$

The first reaction should not lower the pH much below pH 6, since the pK_a of HSO_3^- is 6.9. However, reaction (2) would decrease the pH significantly below pH 6, since the pK_a of HSO_4^- is 1.9. These reactions account for the instability of cytochrome c

FIGURE 1

Manometric measurement of NO consumption when excess NO was added to an anaerobic solution of 100 mM sodium dithionite and 50 mM Tris/acetate at pH 7.0. A 3.0 ml solution was stirred constantly and maintained at 30.0°C by a temperature regulated water bath. The consumption of NO was noted to be biphasic, and the data were fitted to the sum of two exponentials: (i) a rapid reaction which consumed two moles of NO per mole of dithionite, which has been attributed to reaction (1); and (ii) a slow reaction, which has been attributed to reaction (2). See text for details.

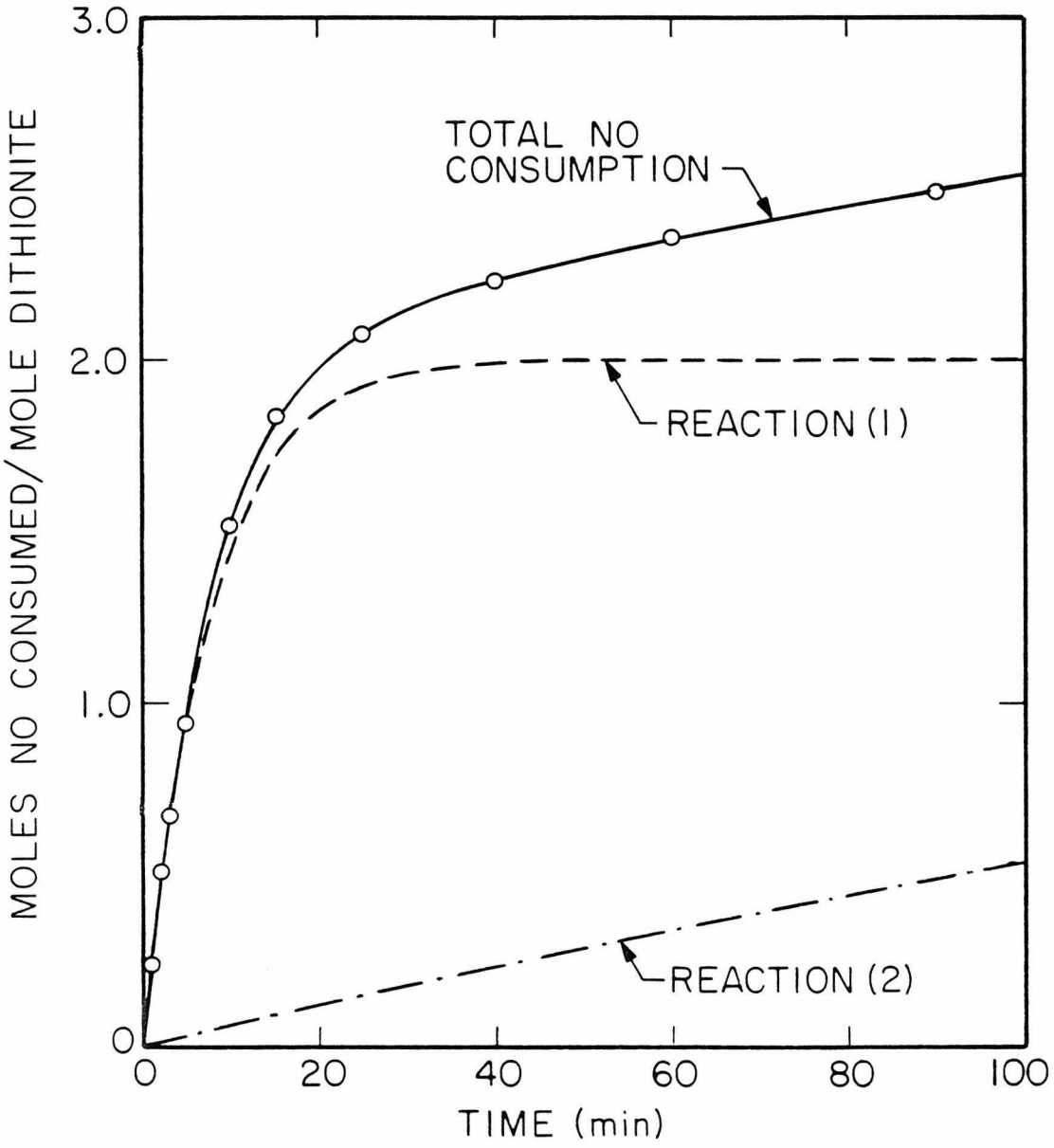
3.0
2.0
1.0
0
MOLES NO CONSUMED/MOLE DITHIONITE
TOTAL NO
CONSUMPTION
REACTION (1)
REACTION (2)
0
20
40
60
80
100
TIME (min)

oxidase in the presence of dithionite and NO. Since dithionite is the limiting reagent in most reduction studies on cytochrome c oxidase, its rapid reaction with NO would produce a large pH drop in the sample, which then causes the enzyme to precipitate. Therefore, NO-binding studies involving dithionite as the reducing agent should not be carried out unless the sample is strongly buffered.

(2) Ascorbate + PPD as Reductant. Ascorbate with PPD as the mediator can also be used to reduce cytochrome c oxidase. In order to ascertain whether the ascorbate plus PPD reduction of the enzyme was complicated by side reactions such as those with dithionite, we first examined the rate of reaction of ascorbate plus PPD with NO. The mass spectra of the products formed after the reaction of ^{15}NO with 60 mM ascorbate plus 5 mM PPD in 50 mM Tris/acetate buffer, pH 7.4, in the presence and absence of cytochrome c oxidase are shown in Figure 2. Even after 11 1/2 hours of incubation, the reaction of ascorbate plus PPD with NO was not pronounced; however, a small amount of N_2O was formed. $^{15}N_2O$ was produced when ^{15}NO was used and $^{14}N_2O$ was produced when ^{14}NO was used. The production of N_2O is probably due to the slow reduction of NO to N_2O by ascorbate (reaction (3)).

$$\text{Ascorbate} + 2NO \rightarrow \text{Dehydroascorbate} + N_2O + H_2O \qquad (3)$$

In the presence of cytochrome c oxidase, however, the amount of N_2O produced was two-fold greater. Therefore, reaction (3) appears to be catalyzed by cytochrome c oxidase.

When NO was added to cytochrome c oxidase which was reduced

FIGURE 2

Mass spectra of (A) the gaseous compounds obtained after 1.0 ml of 80 μM cytochrome c oxidase plus 60 mM ascorbate and 5 mM PPD was incubated with ^{15}NO for 11 1/2 hours; and (B) the gaseous compounds obtained in a sample identical to that in (A) except without the enzyme. The ^{15}NO parent peaks (M/e = 31) are attenuated ten-fold from the rest of the peaks.

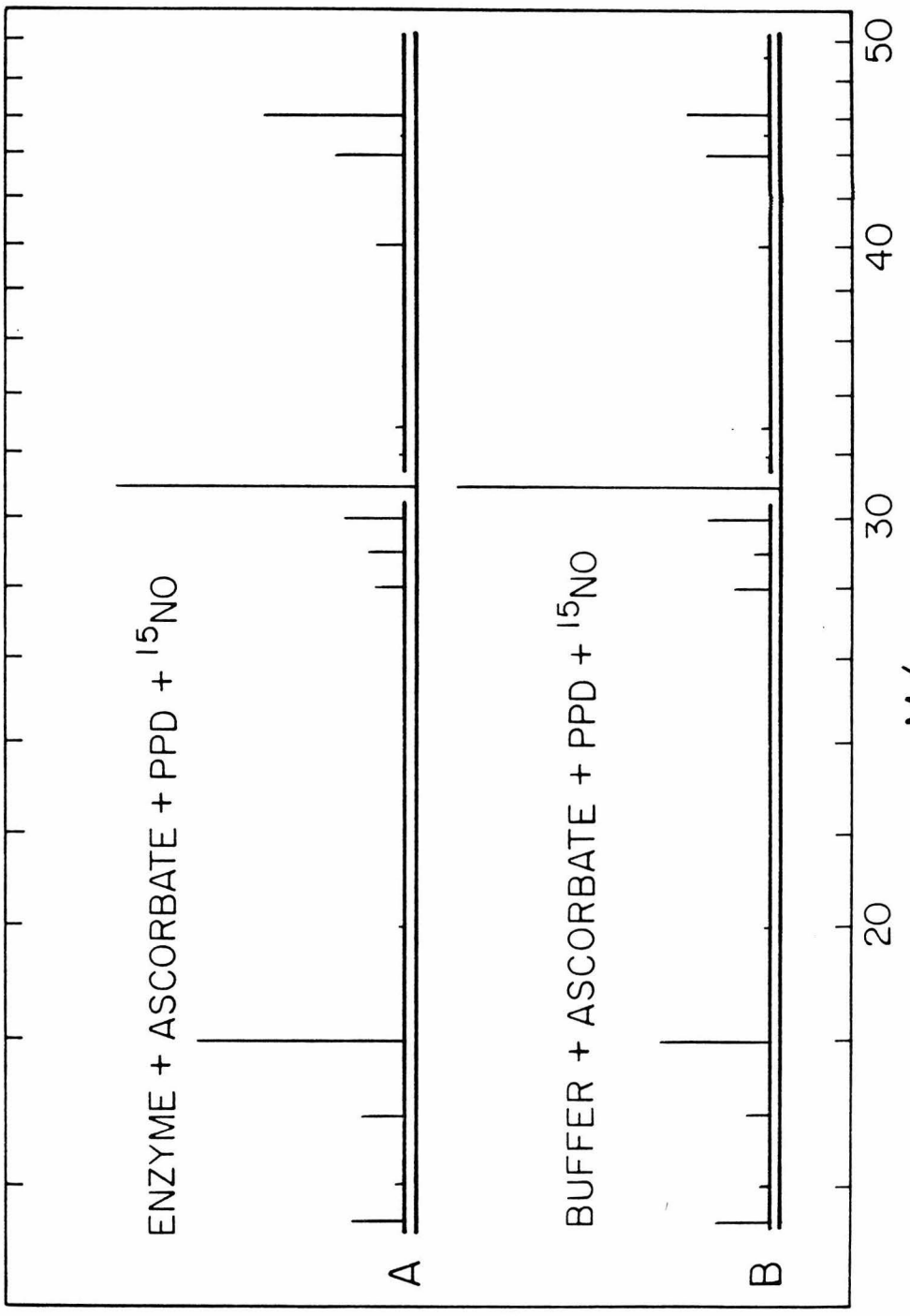
ENZYME + ASCORBATE + PPD + ^{15}NO
A
BUFFER + ASCORBATE + PPD + ^{15}NO
B
20
30
40
50
M/e

by dithionite, the enzyme exhibited a nitrosylferrocytochrome $\underline{a}_3$ EPR signal and no EPR signal from the NO dissolved in the buffer. In contrast, when NO was added to the enzyme which was reduced by ascorbate plus PPD, we observed a large EPR signal from the NO dissolved in the buffer, but essentially no EPR signal from the enzyme (Figure 3A). However, when this sample was then allowed to incubate without mixing at room temperature, the NO dissolved in the buffer was consumed, as evidenced by the gradual disappearance of the NO EPR signal at g = 1.97. As the concentration of NO in solution decreased, the nitrosyl-ferrocytochrome $\underline{a}_3$ EPR signal increased in intensity (Figure 3B). The EPR signal observed from nitrosylferrocytochrome $\underline{a}_3$ prepared in this manner was identical to that observed when NO was added to the enzyme which was reduced with dithionite. Remixing the sample restored the large NO EPR signal at g = 1.97 and eliminated the nitrosylferrocytochrome $\underline{a}_3$ EPR signal. As long as both excess NO and excess reducing agent were available, the cycle could be repeated. However, when NO was in excess over the amount of ascorbate plus PPD and the reductant was ultimately completely consumed, the enzyme exhibited an EPR signal identical to that of the native oxidized enzyme, indicating that cytochrome $\underline{a}$ and Cu_a became reoxidized.

We examined the optical spectrum of cytochrome $\underline{c}$ oxidase reduced with ascorbate plus PPD in the presence of NO. The optical spectrum of the reduced enzyme which had just been mixed with NO is shown in Figure 4. The spectrum exhibited a characteristic[2] split Soret peak with maxima at 441 nm, due to

FIGURE 3

EPR spectra of (A) 0.20 mM cytochrome c oxidase reduced with 1.5 mM ascorbate and 1.5 mM PPD, then mixed with one atmosphere NO and rapidly frozen; (B) sample (A) incubated for 2 hours at 20°C without mixing; and (C) sample (A) incubated 22 hours at 4°C while mixing. Conditions: temperature, 15 K; microwave power, 0.05 mW (A, B) and 0.2 mW (C); modulation amplitude, 5 G (A, B) and 16 G (C); microwave frequency, 9.25 GHz.

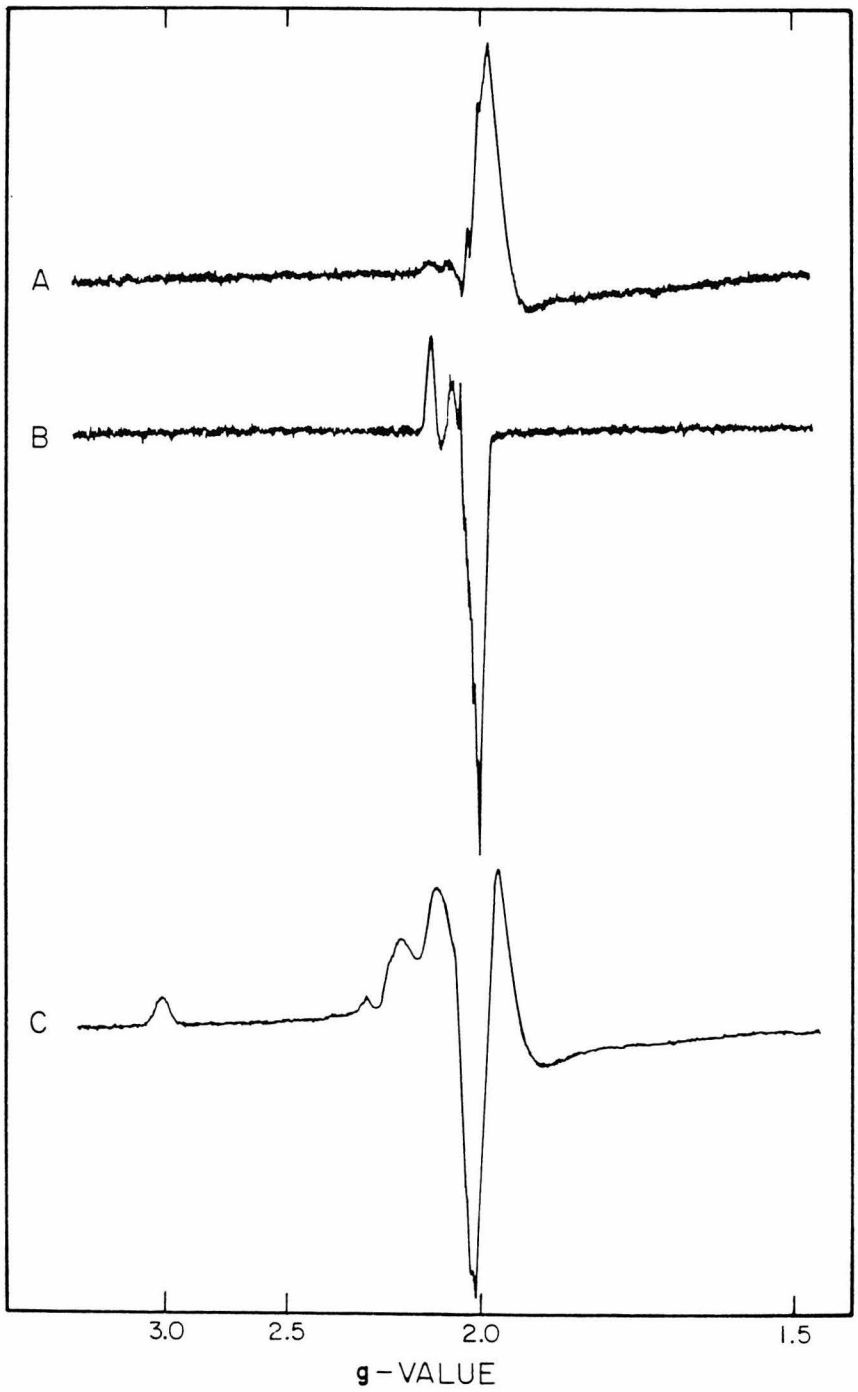
A
B
C
3.0
2.5
2.0
1.5
g – VALUE

FIGURE 4

Optical spectra of 90 μM cytochrome c oxidase reduced with 1.0 mM ascorbate plus 0.5 mM PPD immediately after mixing with one atmosphere NO (solid line); and after incubation at 4°C for 24 hours while mixing until a steady state was achieved (dashed line). The spectra were recorded in a 2 mm path length cell at 20°C.

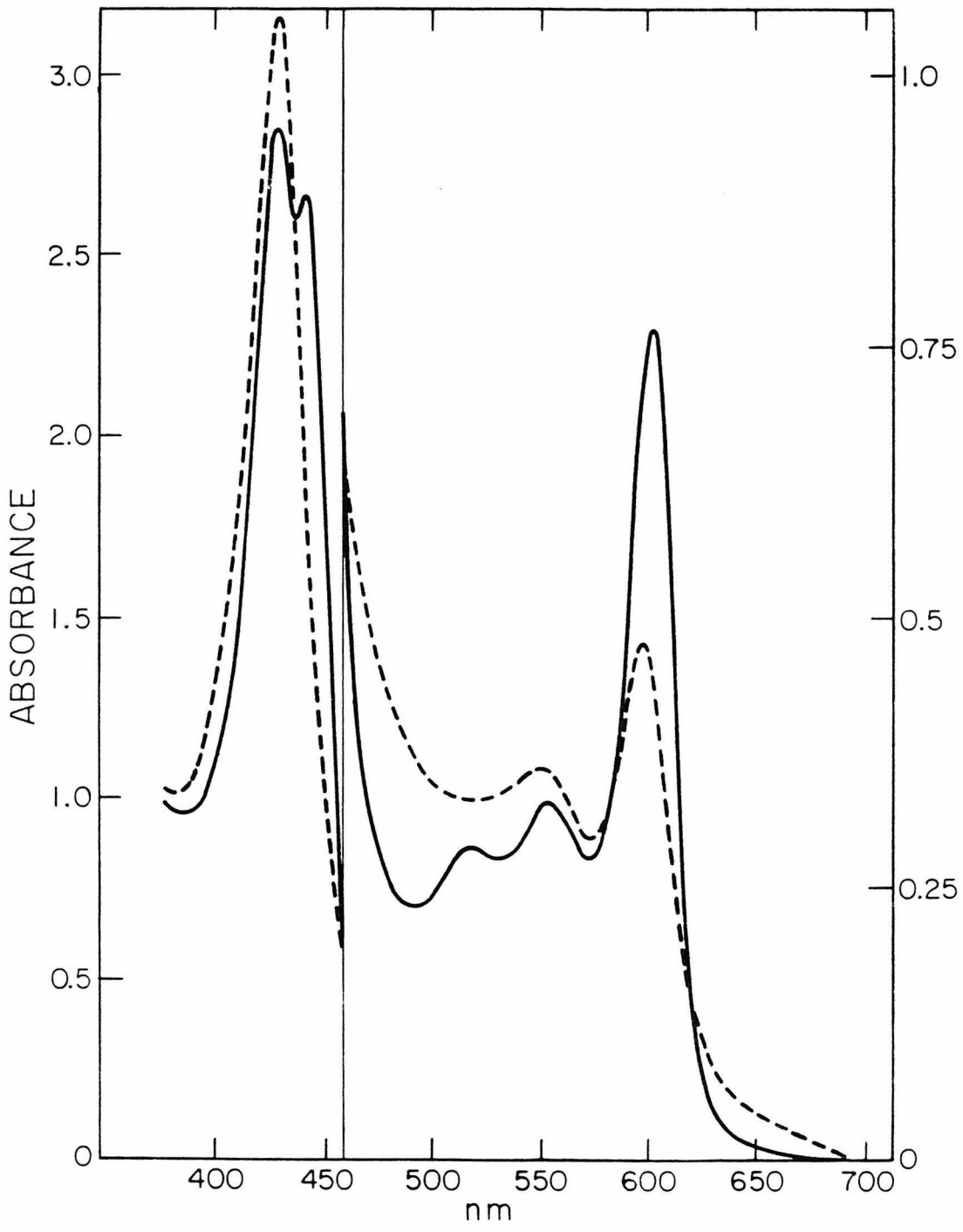
ABSORBANCE
3.0
2.5
2.0
1.5
1.0
0.5
0
1.0
0.75
0.5
0.25
0
400
450
500
550
600
650
700
nm

ferrocytochrome $\underline{a}$, and at 428 nm, due to nitrosylferrocytochrome $\underline{a}_3$. However, incubation of this sample until the dissolved NO was used up (a procedure which yields the nitrosylferrocytochrome $\underline{a}_3$ EPR signal only) did not alter the optical spectrum from that shown in Figure 4. As in our EPR studies, we were able to observe the reoxidation of the enzyme optically after prolonged mixing of the sample with NO (Figure 4). However, the optical spectrum of the enzyme reoxidized by NO was not characteristic of the fully oxidized enzyme, but rather a mixture of fully oxidized molecules with molecules in which cytochrome $\underline{a}$ was oxidized and cytochrome $\underline{a}_3$ reduced with NO bound. This point will be elaborated on in a later section in which we discuss the interaction of NO with the oxidized enzyme.

Our EPR results showed that one NO binds to cytochrome $\underline{a}_3$ tightly; even when the concentration of NO in solution was too small to be detected by EPR the nitrosylferrocytochrome $\underline{a}_3$ EPR signal was observed. However, when the concentration of dissolved NO was increased the nitrosylferrocytochrome $\underline{a}_3$ EPR signal disappeared, although the optical spectrum of the reduced enzyme in the presence of excess NO indicated that NO remained bound to ferrocytochrome $\underline{a}_3$. In order to eliminate the EPR signal from nitrosylferrocytochrome $\underline{a}_3$ without changing the oxidation or ligation state of cytochrome $\underline{a}_3$, it is necessary to magnetically couple another paramagnetic site to the nitrosyl-ferrocytochrome $\underline{a}_3$ site. If Cu_{a_3} were oxidized, the site should exhibit a triplet signal as is observed when NO and azide are added to the oxidized enzyme (Table 2). Therefore, we propose

that a second NO was bound to Cu_{a_3} at higher NO concentrations and presumably was magnetically coupled to the nitrosyl-ferrocytochrome $\underline{a}_3$ site such that the enzyme no longer exhibited an EPR signal. As a further check, we examined the effect of nitrite and nitrous oxide (possible reaction products of NO) on the nitrosylferrocytochrome $\underline{a}_3$ EPR signal and found no evidence that either of these molecules interact with the reduced NO-bound enzyme.

When two NO molecules are bound, the enzyme can donate two electrons to reduce two NO molecules according to reaction (4).

$$2NO + 2e^-(\text{enzyme}) + 2H^+ \rightarrow N_2O + H_2O \qquad (4)$$

In this manner, the cytochrome $\underline{c}$ oxidase catalyzed reduction of NO may be understood.

It, therefore, seems that a cycle is established when NO is added to the reduced enzyme, with ascorbate plus PPD providing the enzyme with two electrons which the enzyme then uses to reduce NO. This cycle is schematically shown in Figure 5. State A is the fully reduced enzyme; state B is formed when the first NO binds to the enzyme and exhibits the nitrosylferrocytochrome $\underline{a}_3$ EPR signal; state C has two NO molecules bound and is EPR silent; and state D is the transient species formed when two electrons are transferred to NO. We have not observed state D directly. It is probable that electron redistribution within the enzyme occurs rapidly. Thereafter the binding of NO to cytochrome $\underline{a}_3$ and the full reduction of the enzyme by ascorbate plus PPD would occur. Since we do not observe any EPR signals from the enzyme in the presence of excess NO, the rate determining

FIGURE 5

The proposed reaction cycle which occurs when cytochrome c oxidase is incubated with NO in the presence of ascorbate and PPD. In this cycle cytochrome a and Cu_a remain reduced except possibly during electron redistribution in the transient state D. An oxidation state has not been assigned to Cu_a itself, but rather to the Cu_a center, in view of the possibility that Cu_a remains in the cuprous state in both the oxidized and reduced enzyme while an associated sulfur ligand accepts electrons (see chapter IV for additional discussion).

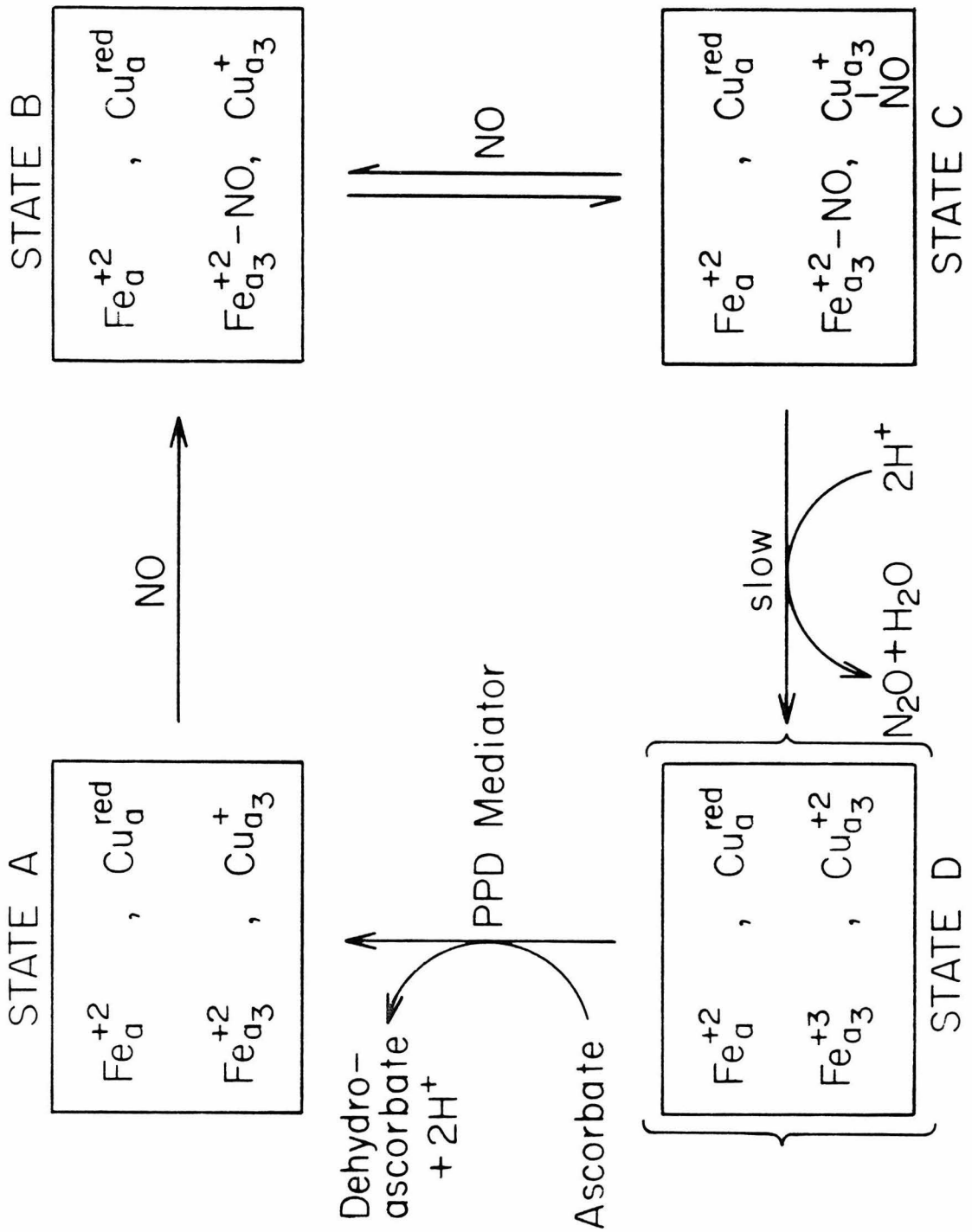
STATE A
Fe_a^{+2} , Cu_a^{red}
$Fe_{a_3}^{+2}$, $Cu_{a_3}^{+}$
NO
STATE B
Fe_a^{+2} , Cu_a^{red}
$Fe_{a_3}^{+2}$–NO, $Cu_{a_3}^{+}$
NO
STATE C
Fe_a^{+2} , Cu_a^{red}
$Fe_{a_3}^{+2}$–NO, $Cu_{a_3}^{+}$
NO
slow
$2H^+$
$N_2O + H_2O$
STATE D
Fe_a^{+2} , Cu_a^{red}
$Fe_{a_3}^{+3}$, $Cu_{a_3}^{+2}$
PPD Mediator
Dehydro-ascorbate $+ 2H^+$
Ascorbate

step in the overall cycle must be the step between states C and D.

3.2 Oxidized Cytochrome c Oxidase + N_3^- + NO. In our earlier work it was shown that when NO is added to oxidized cytochrome c oxidase in the presence of azide, cytochrome a_3 is reduced and a triplet species[2] is formed from the interaction of nitrosyl-ferrocytochrome a_3 (S = 1/2) with $Cu^{+2}_{a_3}$ (S = 1/2). In this earlier work, it was concluded that the reduction of cytochrome a_3 occurred via reaction (5).

ferricytochrome a_3 + NO + N_3^- → ferrocytochrome a_3 + N_2O + N_2 (5)

This conclusion was made on the basis of an analysis of the reaction products by mass spectroscopy.

We have now examined this reaction in greater detail by the use of both ^{15}NO and $^{15}N^{14}N_2^-$ isotopic labeling. In particular, we have made a quantitative analysis of the isotopic labeling in the N_2O and N_2 reaction products. These results are shown in Figure 6 and summarized in Table 3.

On the basis of reaction (5), we would expect that the NO-nitrogen along with one of the outer azide-nitrogens would be incorporated into the N_2O produced and the remaining two azide-nitrogens to be incorporated into dinitrogen. If only this reaction occurred, then the use of ^{15}NO and $^{14}N_3^-$ should produce only $^{14}N^{15}NO$ and $^{14}N_2$. However, as seen in Figure 6B, we observed the production of $^{15}N_2O$ in equal amounts to $^{14}N^{15}NO$, while $^{14}N_2$ was the only dinitrogen product. This interesting observation can be explained if reaction (5) occurred

FIGURE 6

Mass spectra of the gaseous compounds obtained after 10 hours of incubation at 20°C of 1.0 ml samples of the oxidized enzyme with azide and NO. Each sample contained 100 mM azide and the enzyme concentration was 0.25 mM. The background spectra were identical to spectra of the NO gas alone and representative spectra are shown in (C) for ^{15}NO and (E) for ^{14}NO. The NO parent peaks are attenuated one-hundred-fold from the rest of the peaks.

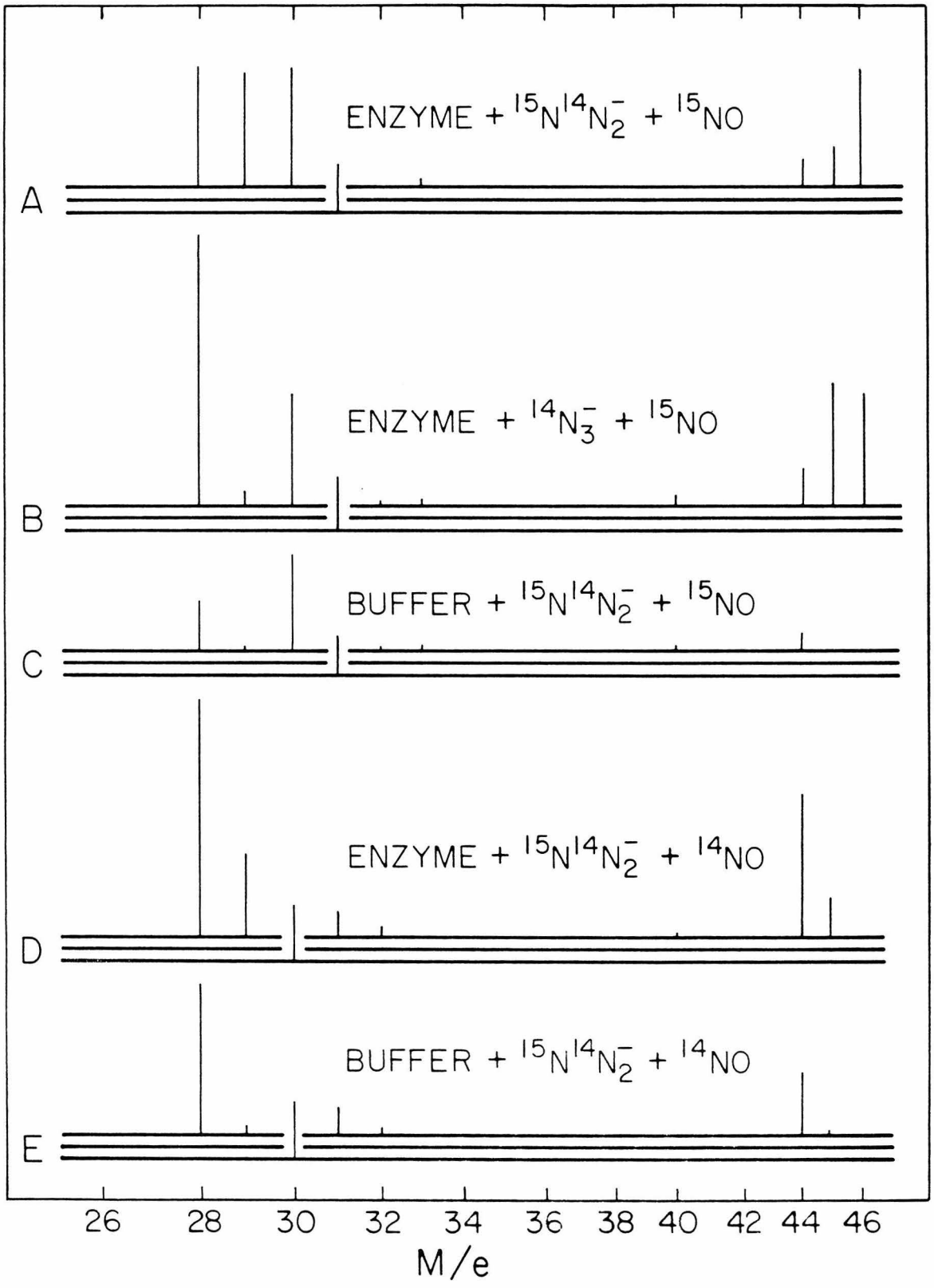
ENZYME + $^{15}N^{14}N_2^-$ + ^{15}NO
A
ENZYME + $^{14}N_3^-$ + ^{15}NO
B
BUFFER + $^{15}N^{14}N_2^-$ + ^{15}NO
C
ENZYME + $^{15}N^{14}N_2^-$ + ^{14}NO
D
BUFFER + $^{15}N^{14}N_2^-$ + ^{14}NO
E
26 28 30 32 34 36 38 40 42 44 46
M/e

Table 3: Summary of Mass Spectral Data: Comparison of the Isotopic Distribution Among the N_2 and N_2O Parent Peaks Observed with That Predicted on the Basis of the Reaction Cycles Discussed in the Text

	$^{14}N_2$		$^{15}N^{14}N$		$^{15}N_2$		$^{14}N_2O$		$^{14}N^{15}NO$ + $^{15}N^{14}NO$		$^{15}N_2O$	
	obs.	pred.	obs.	pred.	obs.	pred.	obs.	pred.	obs.	pred.	obs.	pred.
Reduced Cytochrome c Oxidase												
a) + ^{14}NO	0	0	0	0	0	0	1.00	1.00	0	0	0	0
b) + ^{15}NO	0	0	0	0	0	0	0	0	0	0	1.00	1.00
Oxidized Cytochrome c Oxidase												
a) + $^{14}N_3^-$ + ^{14}NO	1.00	1.00	0	0	-	0	1.00	1.00	0	0	0	0
b) + $^{14}N_3^-$ + ^{15}NO	0.96	1.00	0.01	0	0.03	0	.02	0	0.47	0.50	0.51	0.50
c) + $^{15}N^{14}N^{14}N^-$ + ^{14}NO	0.53	0.5	0.47	0.5	-	0	0.69	0.75	0.31	0.25	0	0
d) + $^{15}N^{14}N^{14}N^-$ + ^{15}NO	0.37	0.5	0.54	0.5	0.09	0	.04	0	0.24	0.25	0.72	.75

an equal number of times as reaction (4). Furthermore, the use of isotopically labeled NO in combination with labeled azide gave the intensity ratios of labeled products expected if reactions (4) and (5) each occur an equal number of times (Table 3).

It is evident from the above results that, in the presence of azide, NO can first reduce and then oxidize the enzyme. However, reaction (5) provides only one electron while reaction (4) consumes two electrons. Another one electron step which does not generate any gaseous products must occur to balance the overall reaction. To resolve this point, we examined the ^{15}N NMR spectrum of the reaction products formed in the reaction of ^{15}NO and $^{15}N^{14}N_2^-$ with the oxidized enzyme. The results are shown in Figure 7. After 48 hours of incubation at 4°C, we observed a peak 509.8 ppm downfield from $^{15}N^{14}N_2^-$ which can be assigned to nitrite. This peak was only observed in the sample containing the enzyme. Thus, nitrite was formed as part of the reaction cycle, suggesting reaction (6).

$$Cu^{+2}_{a_3} + NO + H_2O \rightarrow Cu^{+}_{a_3} + NO_2^- + 2H^+ \qquad (6)$$

The cycle formed then was: (i) the reduction of cytochrome $\underline{a}_3$ via reaction (5), (ii) the reduction of Cu_{a_3} via reaction (6), and (iii) the oxidation of both Cu_{a_3} and cytochrome $\underline{a}_3$ via reaction (4).

The above conclusions were verified by examination of the EPR spectra of cytochrome $\underline{c}$ oxidase samples which were allowed to incubate at room temperature in the presence of azide and NO for variable lengths of time. The results are shown in Figure 8.

FIGURE 7

^{15}N FT NMR spectra of (A) 0.12 mM oxidized cytochrome c oxidase plus 100 mM $Na^{15}N^{14}N_2$ and approximately one atmosphere ^{15}NO incubated 48 hours at 4°C; (B) a sample identical to that in (A) except without the enzyme; and (C) an aqueous solution of 10 mM $Na^{15}NO_2$ and 100 mM $Na^{15}N^{14}N_2$ with an insert containing a 70% solution of HNO_3. Conditions: temperature, 30°C; rf frequency, 9.04 MHz; pulse angle, 60°; acquisition time, 0.682 sec.; spectral width, 6000 Hz; transients, 70,000 (A), 72,000 (B), 21,000 (C).

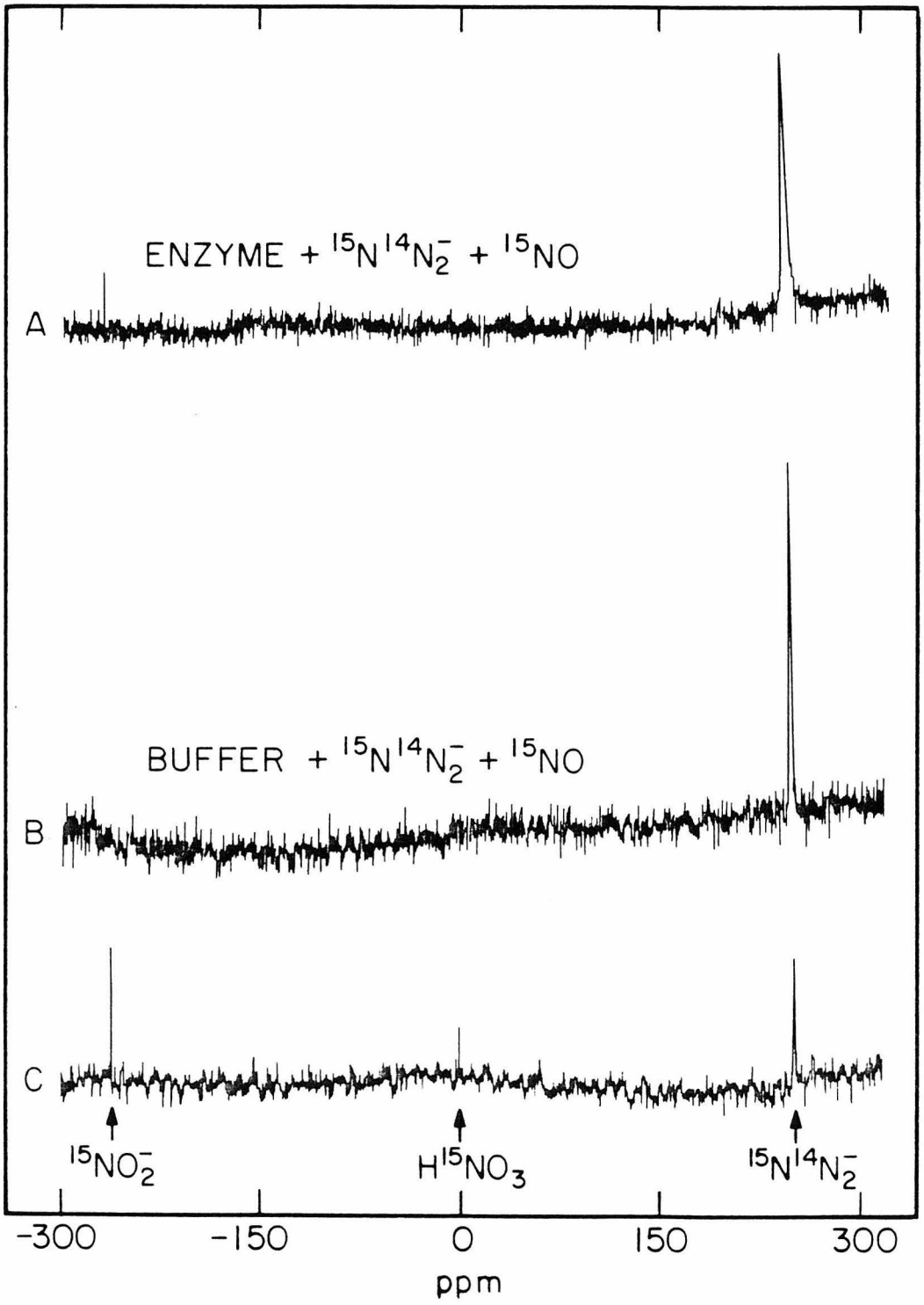
ENZYME + $^{15}N^{14}N_2^-$ + ^{15}NO
A
BUFFER + $^{15}N^{14}N_2^-$ + ^{15}NO
B
C
$^{15}NO_2^-$
$H^{15}NO_3$
$^{15}N^{14}N_2^-$
-300
-150
0
150
300
ppm

FIGURE 8

EPR spectra of (A) 0.25 mM oxidized cytochrome c oxidase plus 100 mM azide and one atmosphere NO which was mixed, incubated 10 minutes, remixed, and rapidly frozen; (B) sample (A) incubated 30 minutes at 20°C without mixing; and (C) sample (A) incubated a total of 60 minutes at 20°C without mixing. Conditions: temperature, 15 K; microwave power, 0.05 mW; modulation amplitude, 5 G; microwave frequency, 9.25 GHz. The low field portions of the spectra were recorded with a 4-fold higher modulation amplitude and a 9-fold higher microwave power to give a 12-fold greater intensity compared to the high field portion.


×12
A
×12
B
g = 2.09
×12
C
6.0 5.0 4.0 3.5 3.0 2.5 2.0 1.5
g-VALUE

We observed the triplet EPR signal characteristic of nitrosylferrocytochrome $\underline{a}_3$, $Cu^{+2}_{a_3}$, in the presence of excess NO (Figure 8A). When the sample was then allowed to incubate at room temperature, the NO dissolved in the buffer was slowly consumed as evidenced by the disappearance of the signal at g = 1.97. Concomitant with the disappearance of the dissolved NO was the appearance of a nitrosylferrocytochrome $\underline{a}_3$ EPR signal with its characteristic sharp maximum at g = 2.09 indicating the reduction of Cu_{a_3}. As the nitrosylferrocytochrome $\underline{a}_3$, EPR signal increased in intensity, the nitrosylferrocytochrome $\underline{a}_3$, $Cu^{+2}_{a_3}$ triplet EPR signal intensity decreased. The triplet EPR signal, however, never completely disappeared, even after prolonged incubation of the sample at room temperature reduced the concentration of dissolved NO to a level no longer detectable by EPR. Again, remixing the sample with NO restored the spectrum shown in Figure 8A (remixed spectrum not shown).

The above results suggest the reaction cycle, depicted in Figure 9, when azide and NO are added to oxidized cytochrome $\underline{c}$ oxidase. Here state E refers to the oxidized enzyme. One-electron reduction of the oxidized enzyme via reaction (5) produced state F, the nitrosylferrocytochrome $\underline{a}_3$, $Cu^{+2}_{a_3}$ state, which exhibits the triplet EPR signal. Then Cu_{a_3} was reduced via reaction (6) to form state G, the nitrosylferrocytochrome $\underline{a}_3$, $Cu^{+2}_{a_3}$ state, which exhibits the nitrosylferrocytochrome $\underline{a}_3$ EPR signal. The binding of a second NO to the two-electron reduced enzyme formed state H in which cytochrome $\underline{a}_3/Cu_{a_3}$ are EPR silent, and finally the reoxidation of the enzyme occurred via reaction (4).

FIGURE 9

The proposed reaction cycle which occurs when oxidized cytochrome c oxidase is incubated with azide and NO.

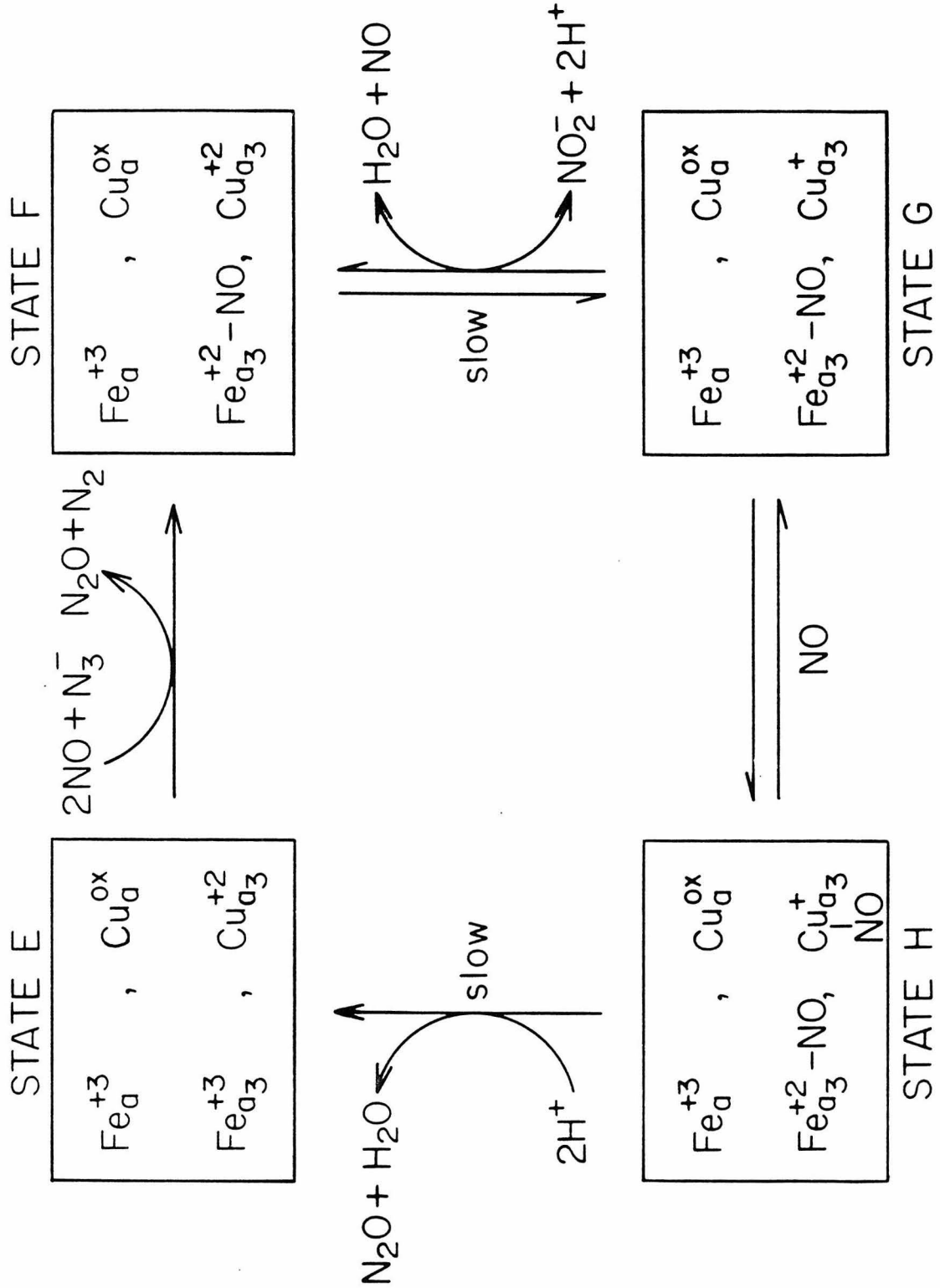
STATE F
Fe_a^{+3} , Cu_a^{ox}
$Fe_{a_3}^{+2}-NO$, $Cu_{a_3}^{+2}$
$2NO + N_3^-$ $N_2O + N_2$
$H_2O + NO$
slow
$NO_2^- + 2H^+$
STATE G
Fe_a^{+3} , Cu_a^{ox}
$Fe_{a_3}^{+2}-NO$, $Cu_{a_3}^{+}$
NO
STATE E
Fe_a^{+3} , Cu_a^{ox}
$Fe_{a_3}^{+3}$, $Cu_{a_3}^{+2}$
$N_2O + H_2O$
slow
$2H^+$
STATE H
Fe_a^{+3} , Cu_a^{ox}
$Fe_{a_3}^{+2}-NO$, $Cu_{a_3}^{+}$ NO

It is evident that, in the presence of excess NO, the reduction of Cu_{a_3} is the rate limiting step. However, when the concentration of dissolved NO was sufficiently low, the rate at which NO binds to the two-electron reduced enzyme becomes comparable to the rate of reduction of Cu_{a_3}. Accordingly a steady state is established with comparable concentrations of the nitrosylferrocytochrome $\underline{a}_3$, $Cu^{+2}_{a_3}$ and nitrosylferrocytochrome $\underline{a}_3$, $Cu^{+}_{a_3}$ species. Note that in the reaction cycle, states G and H are analogous to states B and C, respectively in Figure 5. It should also be noted that throughout this reaction cycle both cytochrome $\underline{a}$ and the Cu_a center remained fully oxidized and were observed in the EPR spectrum.

3.3 Reduced Cytochrome $\underline{c}$ Oxidase + NO_2^-. In the previous section it was noted that NO can reduce Cu_{a_3} with the formation of nitrite (reaction (6)). On the basis of the free energy associated with this reaction under standard conditions, we expect excess nitrite to react with reduced cytochrome $\underline{c}$ oxidase to form NO and, in the presence of excess reductant, the nitrosylferrocytochrome $\underline{a}_3$, $Cu^{+}_{a_3}$ state. We found that nitrite did react with cytochrome $\underline{c}$ oxidase reduced with ascorbate and PPD (reaction (7)) to form the nitrosylferrocytochrome $\underline{a}_3$, $Cu^{+}_{a_3}$ state. This state of the enzyme exhibited an EPR signal from nitrosylferrocytochrome $\underline{a}_3$ which was identical to that observed when NO was added to the dithionite-reduced enzyme, or when limited NO was added to the enzyme reduced by ascorbate plus PPD.

$$NO_2^- + e^- \text{ (enzyme)} + 2H^+ \rightarrow NO + H_2O \qquad (7)$$

Yonetani et al.[22] previously utilized the reaction of dithionite plus nitrite to generate NO in their preparation of nitrosylferroheme complexes. It is possible that ascorbate and PPD also react with nitrite to produce free NO. However, this reaction is quite slow. It was found that no nitrosyl-ferrocytochrome c EPR signal was generated when nitrite plus ascorbate and PPD were added to cytochrome c, even after 4 hours of incubation at room temperature. In addition no EPR signal from NO dissolved in the buffer was observed in this sample. These experiments demonstrate that in the case of cytochrome c oxidase the reduction of nitrite to NO occurred at the oxygen binding site of the enzyme.

3.4 Oxidized Cytochrome c Oxidase + NO. When NO is added to oxidized cytochrome c oxidase a high-spin cytochrome a_3 EPR signal is observed. The formation of this complex was discussed by Stevens et al.,[2] and it was proposed that NO binds to Cu_{a_3} and breaks the antiferromagnetic coupling between Cu_{a_3} and cytochrome a_3. Although for short incubation times, NO binds reversibly to the oxidized enzyme, subsequent work has shown that prolonged incubation of the oxidized enzyme with NO leads to reduction of cytochrome a_3 and Cu_{a_3}.

The EPR spectrum of the oxidized enzyme which has been mixed with NO and immediately frozen is shown in Figure 10A. A high-spin cytochrome a_3 EPR signal at g = 6 was observed in addition to the cytochrome a, Cu_a, and NO EPR signals. When the sample was incubated at 20°C without mixing, the NO in solution was slowly consumed. Paralleling the consumption of

FIGURE 10

EPR spectra of (A) 0.25 mM oxidized cytochrome c oxidase plus one atmosphere NO, mixed and rapidly frozen; (B) sample (A) incubated at 20°C without mixing for 8 hours; and (C) sample (B) remixed with NO and rapidly frozen. The EPR spectrum obtained after rapid removal of NO and immediate freezing of sample (C) exhibited a signal at $g = 2.09$ of the same intensity as in (B). Conditions: temperature, 11 K; microwave power, 0.02 mW; modulation amplitude, 10 G; microwave frequency, 9.25 GHz.

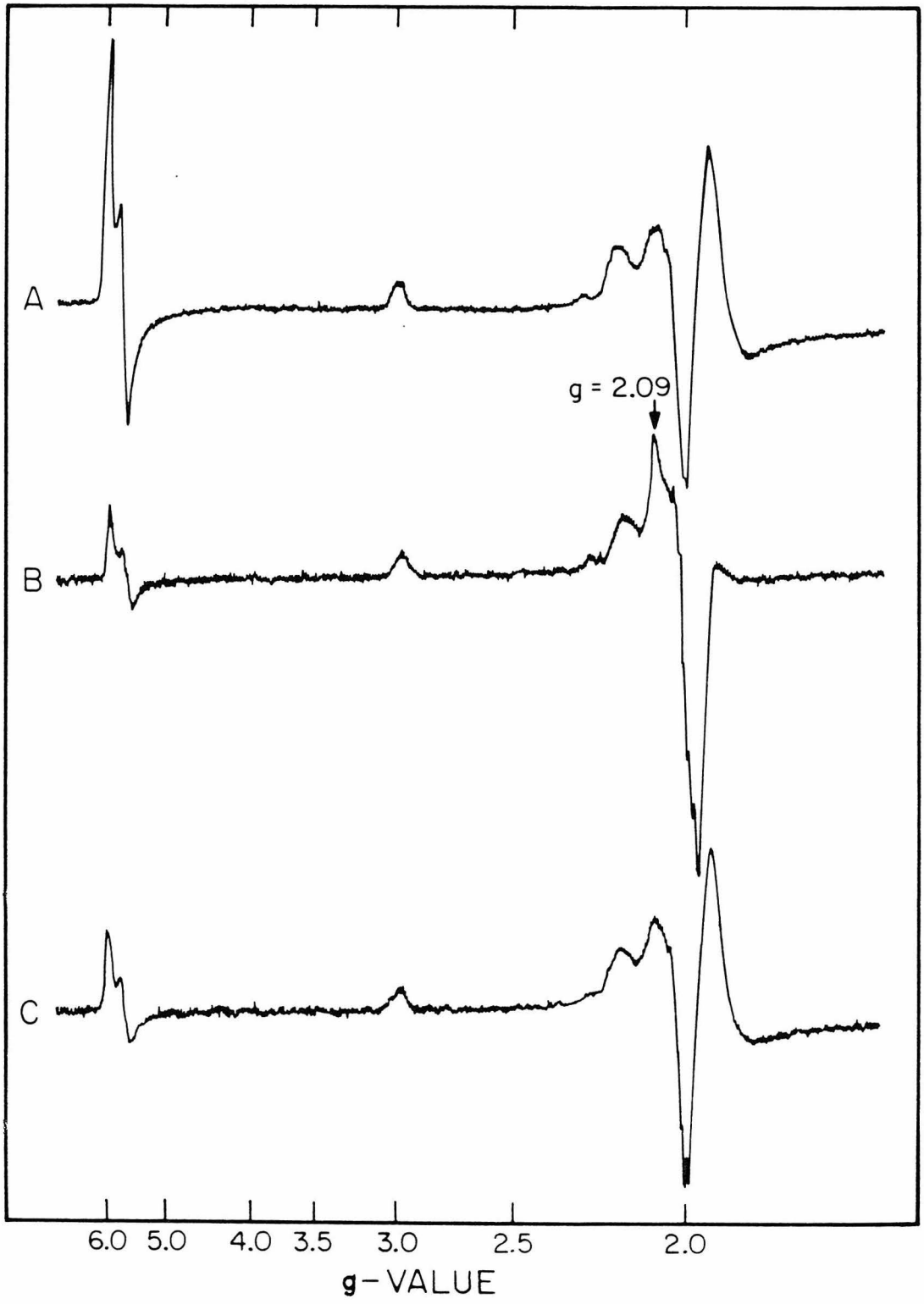
A
g = 2.09
B
C
6.0
5.0
4.0
3.5
3.0
2.5
2.0
g-VALUE

NO was a decrease in intensity of the high-spin cytochrome $\underline{a}_3$ EPR signal. Finally the nitrosylferrocytochrome $\underline{a}_3$ EPR signal appeared when the concentration of NO in solution was lowered significantly (Figure 10B). While remixing the sample with NO eliminated the nitrosylferrocytochrome $\underline{a}_3$ EPR signal, it did not restore the high-spin cytochrome $\underline{a}_3$ EPR signal (Figure 10C). Rapid removal of NO from the sample at this point, however, restored the nitrosylferrocytochrome $\underline{a}_3$ EPR signal.

The intensity of the nitrosylferrocytochrome $\underline{a}_3$ EPR signal after removal of the NO from the sample is a measure of the fraction of molecules in which both cytochrome $\underline{a}_3$ and Cu_{a_3} are reduced. Thus, the time course of the reduction of these metal centers can be followed by first incubating the sample with NO for a specified length of time, then rapidly removing the NO from the sample, and finally freezing the sample to monitor the EPR spectrum. The intensity of the nitrosylferrocytochrome $\underline{a}_3$ EPR was observed to increase with the time of incubation with NO. However, in the steady-state, which was reached after about 10 hours of incubation at room temperature, only about 10 - 30% of the enzyme molecules were in a state which exhibited this EPR signal. This fraction was estimated from the intensity of the g = 2.09 EPR signal from nitrosylferrocytochrome $\underline{a}_3$.

These observations are consistent with the slow reduction of the oxidized enzyme by NO. However, we observed the reduction of only cytochrome $\underline{a}_3$ and Cu_{a_3}; cytochrome $\underline{a}$ and Cu_a remained fully oxidized even after long incubation times. Moreover, it appears that the reduction proceeds via a two-electron step,

since no one-electron reduced intermediates (e.g. nitrosyl-ferrocytochrome $\underline{a}_3$, $Cu^{+2}_{a_3}$) were observed.

The reduction of the oxidized enzyme by NO was confirmed by following the optical spectrum. For incubation times less than 30 minutes, NO had no effect on the optical spectrum of the oxidized enzyme (Figure 11). Thereafter, the optical spectrum slowly changed with time. The spectrum obtained after several hours of incubation at room temperature is shown in Figure 11. This spectrum, which has a Soret band at 426 nm and an α-band at 597 nm, is nearly identical to that which was observed when the reduced enzyme was reoxidized by NO (cf. Figure 4). The intensity of the α-band in this spectrum was intermediate between that in the fully oxidized enzyme and the one-quarter reduced enzyme.[2] In the light of the EPR results presented earlier, these optical results are best interpreted in terms of a steady state containing a mixture of the fully oxidized enzyme and the two-electron reduced NO-bound enzyme.

It is interesting to compare the reduction of cytochrome $\underline{c}$ oxidase by NO in the presence and absence of azide. In the former case, it was shown that the enzyme was reduced via two consecutive one-electron steps (reactions (5) and (6)). However, in the latter case, the enzyme was reduced either via a two-electron step or via two one-electron steps which occur in rapid succession, since no one-electron reduced states were observed. Earlier in this work we showed that the enzyme can catalyze the oxidation of NO to nitrite (reaction (6)). However, this one-electron step was quite slow, and it would not be

FIGURE 11

Optical spectra of 90 μM oxidized cytochrome c oxidase plus one atmosphere NO which was mixed and immediately recorded (— · —); and incubated at 4°C for 24 hours while mixing until a steady state was achieved (——). For comparison the spectrum of the one-quarter reduced NO-bound enzyme is also shown (---). The one-quarter reduced enzyme was prepared by the reaction of azide and NO with the oxidized enzyme. The spectra were recorded in a 2 mm path length cell at 20°C.

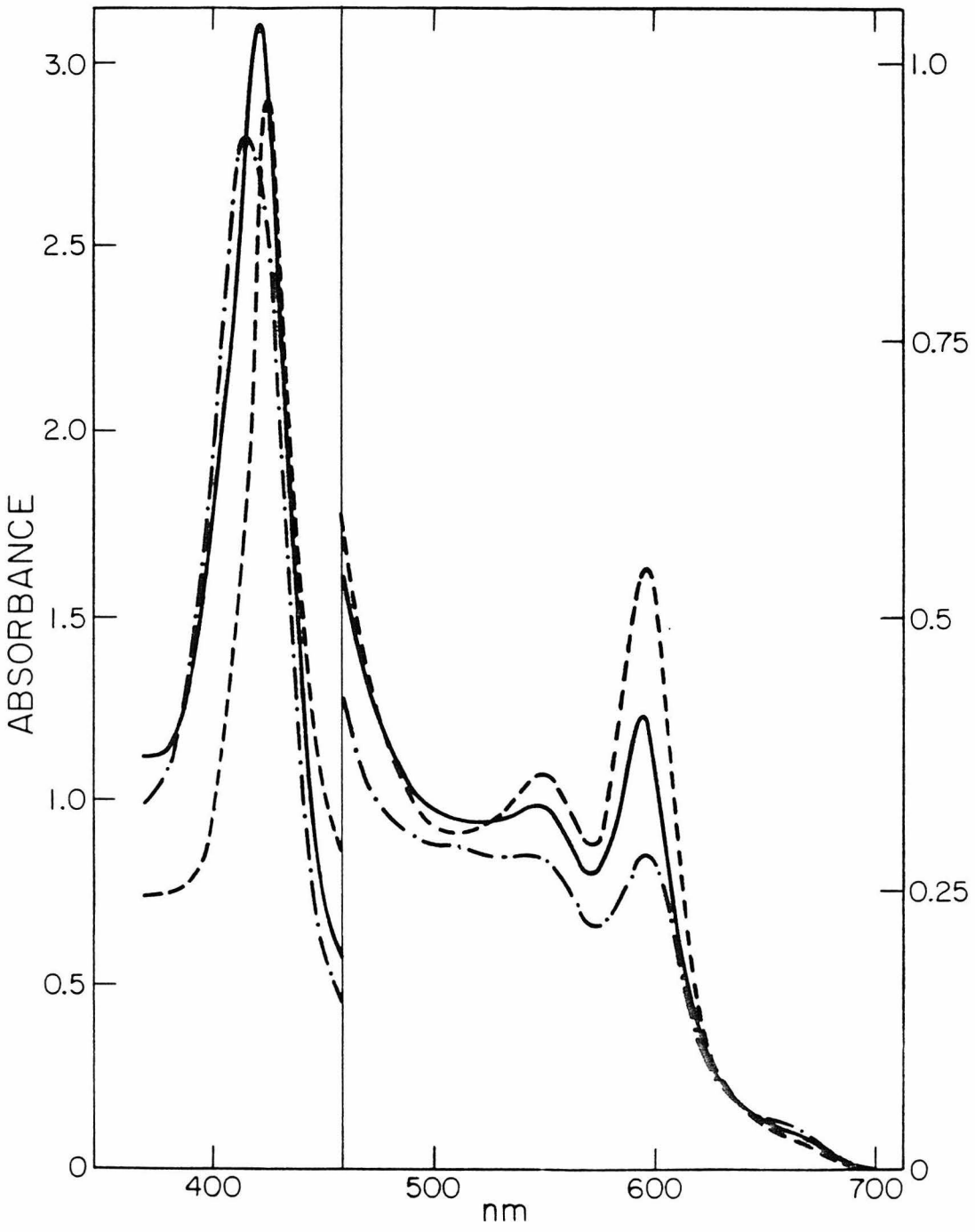
ABSORBANCE
3.0
2.5
2.0
1.5
1.0
0.5
0
1.0
0.75
0.5
0.25
0
400
500
600
700
nm

expected to occur twice in rapid succession. Therefore, the reduction of the oxidized enzyme must have occurred via a two-electron process. One possibility is reaction (8).

$$NO + H_2O \rightarrow NO_2 + 2H^+ + 2e^- \text{ (enzyme)} \qquad (8)$$

Unfortunately, due to the slow rate of reduction of the oxidized enzyme by NO, we have been unable to detect any products by mass or NMR spectroscopy which would allow us to verify this redox process. However, we were able to observe the production of N_2O by mass spectroscopy which indicates that the enzyme was reoxidized via reaction (4).

Alternatively, the enzyme could be reduced by endogenous reductants which may be present as impurities in preparations of the enzyme.[29] To investigate this possibility, we examined the EPR spectrum as a function of time of a sample of the anaerobic oxidized enzyme which was incubated at 4°C. Even after 4 days of incubation, we found no indication that auto-reduction had occurred. In particular, we observed no reduction in the cytochrome *a* or Cu_a EPR signal intensities or increase in high-spin heme EPR signals from cytochrome a_3 which are known to appear when the enzyme is partially reduced.[30] Although this experiment would seem to rule out the possibility of reduction by endogenous reductants, this point cannot be totally settled until the nature and presence of such endogenous reductants[29] are better defined.

Regardless of the source of electrons which reduce cytochrome *c* oxidase, it is clear that the enzyme undergoes a cycle of oxidation and reduction in the presence of NO. Such a cycle is

depicted in Figure 12. This cycle is analogous to that which occurred when azide and NO were added to the oxidized enzyme except that here the reduction of the enzyme occurs via reaction (8) or possibly, although less likely, via endogenous reductants. Both our EPR and optical results indicated that the steady state, in the presence of excess NO, contained a mixture of states E and H. Therefore, in this case both the reduction and the oxidation of the enzyme by NO must have been comparably slow.

4. DISCUSSION

We have found that cytochrome c oxidase catalyzes:

(i) the reduction of two NO molecules to N_2O (reaction (4)),

(ii) the reaction of NO plus azide to form N_2O and N_2 (reaction (5)),

(iii) the reversible oxidation of NO to nitrite (reactions (6) and (7)),

and probably also

(iv) the oxidation of NO to NO_2 (reaction (8)).

Both reactions (4) and (7) have been observed to be catalyzed by other metalloproteins. Hemocyanin[31] and cytochrome cd[32] in particular are known to catalyze the reduction of two NO molecules to N_2O. In addition, under anaerobic conditions a number of bacterial organisms are capable of utilizing NO as the terminal electron acceptor. In these bacteria it is believed that the reductive pathway[33] consists of a sequential reduction of nitrate → nitrite → NO → N_2O → N_2. Although the enzymes involved in this denitrification process

FIGURE 12

The proposed reaction cycle which occurs when oxidized cytochrome c oxidase is incubated with NO.

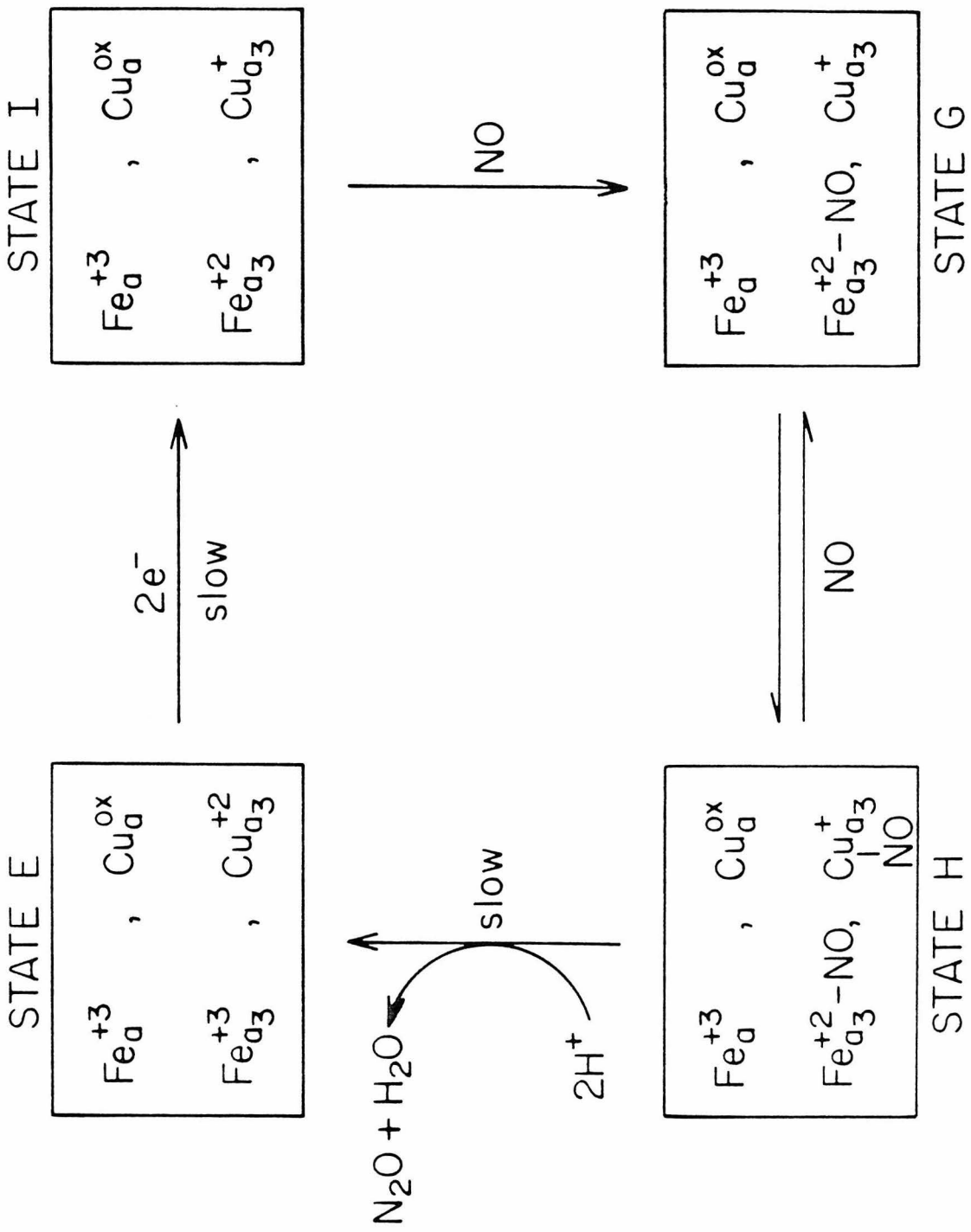
STATE I
Fe_a^{+3} , Cu_a^{ox}
$Fe_{a_3}^{+2}$, $Cu_{a_3}^{+}$
NO
STATE G
Fe_a^{+3} , Cu_a^{ox}
$Fe_{a_3}^{+2}$–NO, $Cu_{a_3}^{+}$
$2e^-$
slow
NO
STATE E
Fe_a^{+3} , Cu_a^{ox}
$Fe_{a_3}^{+3}$, $Cu_{a_3}^{+2}$
slow
$N_2O + H_2O$
$2H^+$
STATE H
Fe_a^{+3} , Cu_a^{ox}
$Fe_{a_3}^{+2}$–NO, $Cu_{a_3}^{+}$
NO

have not been well characterized, it appears that many are cytochromes.[34] Hence, although the primary function of cytochrome c oxidase is to reduce oxygen to water, it is not surprising that this enzyme also possesses some rudimentary nitric oxide reductase and nitrite reductase activity.

Nonetheless, these reactions provide new information on the catalytic activity of cytochrome c oxidase. In all of the reactions of NO observed in this work, a stable product was formed after a one- or two-electron step. These reactions can be contrasted to the reduction of dioxygen to water by the enzyme, which involves four electrons. In the latter process, partially reduced species are not released from the enzyme. These one- and two-electron reactions of NO, therefore, may shed some light on the initial one- or two-electron reduction of dioxygen. In particular, the states of cytochrome c oxidase which are formed in the course of reaction with NO and monitored by EPR may be indicative of the states formed during the reduction of dioxygen to water.

The reactions of NO with the enzyme occur exclusively at the cytochrome a_3/Cu_{a_3} site with no apparent involvement of either cytochrome a or Cu_a. For example, in the reaction of the oxidized enzyme with azide and NO, the reduction and reoxidation of cytochrome a_3 and Cu_{a_3} occurs with no detectable effect on the EPR signals of either cytochrome a or Cu_a. This result supports the view that the cytochrome a_3-Cu_{a_3} site is not intimately interacting with the other two metal centers during the catalytic process.

Our NO experiments have also provided some definite information on the structure of the oxygen binding site. In the oxidized enzyme, NO readily binds to Cu_{a_3}, even while fluoride or cyanide remain bound[2] to cytochrome $\underline{a}_3$. Thus, the ligand binding pocket in the oxidized enzyme must be large enough to accommodate both NO and cyanide. It is possible that cyanide or fluoride bridges between cytochrome $\underline{a}_3$ and Cu_{a_3} in these complexes with NO occupying a second binding site on Cu_{a_3} as suggested by Chan et al.[25]

Of greater significance to the catalytic function of the enzyme is the structure of the oxygen binding site in the reduced protein. Our results indicate that two NO molecules can bind to the reduced enzyme; one is tightly bound to cytochrome $\underline{a}_3$ and the other is weakly bound to Cu_{a_3}. It is clear that in the di-NO complex the two bound NO molecules interact strongly, since this state is EPR silent. Thus, the binding sites on cytochrome $\underline{a}_3$ and Cu_{a_3} must be quite close to each other.

It is possible to estimate the distance between cytochrome $\underline{a}_3$ and Cu_{a_3} from the magnitude of D, the zero field splitting, in the nitrosylferrocytochrome $\underline{a}_3$, $Cu^{+2}_{a_3}$ triplet state. A value has been obtained for $|D|$ of about 0.07 cm^{-1} from the breadth of the $\Delta M_s \pm 1$ transition for this triplet.[2] Assuming a purely dipolar interaction between the two spins, we calculate a distance of 3.4 Å between the two spin centers.[35] However, spin-orbit and exchange interactions can also contribute to the zero-field splitting in triplets. These contributions are of the order $(\Delta g/g)J_i$ and $(\Delta g/g)^2 J_i$, respectively,[36] where J_i is

the isotropic super-exchange energy. Using the average of the g-values[14,18] for nitrosylferrocytochrome $\underline{a}_3$ and Cu_{a_3}, $\Delta g/g$ can be estimated to be 0.04. There is, however, a major uncertainty in the magnitude of J_i. The temperature dependence[37] of the triplet signal shows no deviation from the expected Boltzmann distribution of the spins among the triplet sublevels from 7 - 80K. This result may be taken to infer that $|J| \leq 5\ cm^{-1}$, where J is the singlet-triplet splitting. However, the zero-field splitting of the triplet depends on the exchange interaction, J_i, between the ground state of one site and an excited state, which is coupled to the ground state through spin-orbit coupling, of the second site.[36] The magnitude of J_i is expected to be much less than J, particularly for a triplet involving a nitrosylferroheme species. Accordingly, the spin-orbit and exchange contributions to the zero-field splitting in the nitrosylferrocytochrome $\underline{a}_3$, $Cu^{+2}_{a_3}$ triplet state are likely to be quite small. Taking these considerations into account and the fact that the spin on nitrosylferrocytochrome $\underline{a}_3$ lies substantially on the nitrogen of NO, we estimate that the distance between cytochrome $\underline{a}_3$ and Cu_{a_3} is $\sim$5 Å, which is close to that expected if dioxygen bridges between the two metals.

The close proximity of the two metals may be important in the stabilization and anchoring of reactive intermediates which are formed during the reduction of dioxygen to water. This close proximity is undoubtedly also important in the catalysis of the reactions with NO discussed in this work. In particular, reactions (4) and (5) must be catalyzed by the binding of two

molecules in close proximity and maintaining this close association at the oxygen binding site for a sufficiently long time to allow for the redox reactions to occur.

Finally, we consider the implications of our NO experiments on the mechanism of oxygen reduction. In this regard, it is important to compare the reduction of the protein under aerobic and anaerobic conditions. When cytochrome c oxidase is reduced anaerobically, Cu_{a_3} is reduced before cytochrome a_3. Also when the fully reduced enzyme is reoxidized anaerobically, cytochrome a_3 is oxidized before Cu_{a_3}. These differences in reduction potentials between the two metal centers have allowed cytochrome a_3 to be observed by EPR as a high-spin heme in a state where cytochrome a_3 is oxidized while Cu_{a_3} is reduced.[12] However, it is clear from this work that in the presence of NO, the reduction potential of cytochrome a_3 becomes higher than that of Cu_{a_3}. This raises the question of whether or not the reduction potentials measured on the anaerobic enzyme have any direct bearing on the enzyme during its reaction with dioxygen. Presumably the coordination of dioxygen to the enzyme would also greatly perturb the reduction potential of cytochrome a_3. In fact it is possible that the nitrosylferrocytochrome a_3, $Cu^{+2}_{a_3}$ triplet state, which is stabilized by NO, resembles a state formed during the reaction of the enzyme with dioxygen. Thus the role of cytochrome a_3 may be to anchor dioxygen to the enzyme while remaining in the ferrous state, and the role of Cu_{a_3} may be to receive electrons from cytochrome a/Cu_a and sequentially transfer them to dioxygen.

In the light of these considerations, we propose the mechanism for oxygen reduction shown in Figure 13. The reduction of oxygen is proposed to proceed in five steps. 1) Dioxygen binds to ferrocytochrome $\underline{a}_3$ and forms a bridge with Cu_{a_3}. 2) In this state the electron on Cu_{a_3} is rapidly delocalized onto the oxygen. 3) Cu_{a_3} then accepts an electron from cytochrome $\underline{a}$ or Cu_a. 4) This reduction of Cu_{a_3} results in the immediate splitting out of one water molecule and the formation of a ferrylcytochrome a_3-O^{-2} state. This state involving an Fe(IV) is proposed to be only a transient intermediate formed during the reduction of dioxygen, and as such has been proposed before in a number of systems including cytochrome $\underline{c}$ oxidase.[11,38] 5) Finally, another electron from cytochrome $\underline{a}$ or Cu_a is transferred to cytochrome $\underline{a}_3$ to fully oxidize the enzyme and form a μ-oxo bridge between cytochrome $\underline{a}_3$ and Cu_{a_3}. As was suggested by Blumberg and Peisach,[19] this μ-oxo bridge between cytochrome $\underline{a}_3$ and Cu_{a_3} could facilitate the strong antiferromagnetic exchange interaction between these two metal centers in the oxidized enzyme.

It is interesting to compare the results of Chance et al.[11] on the intermediates formed in the reaction of O_2 and reduced cytochrome $\underline{c}$ oxidase with our proposed mechanism. As was described in the introduction, three intermediates were observed at low temperature by optical spectroscopy: compound A, proposed to be formed when O_2 binds to the reduced enzyme; compound B, proposed to be formed when one electron is transferred to the coordinated O_2; and compound C, proposed to be formed

FIGURE 13

Proposed mechanism for the reduction of dioxygen to water by cytochrome c oxidase. Compounds A, B, and C refer to the intermediates observed by Chance et al.[11] in the low-temperature reaction of O_2 with reduced cytochrome c oxidase which we have identified as three of the intermediates in this mechanism.

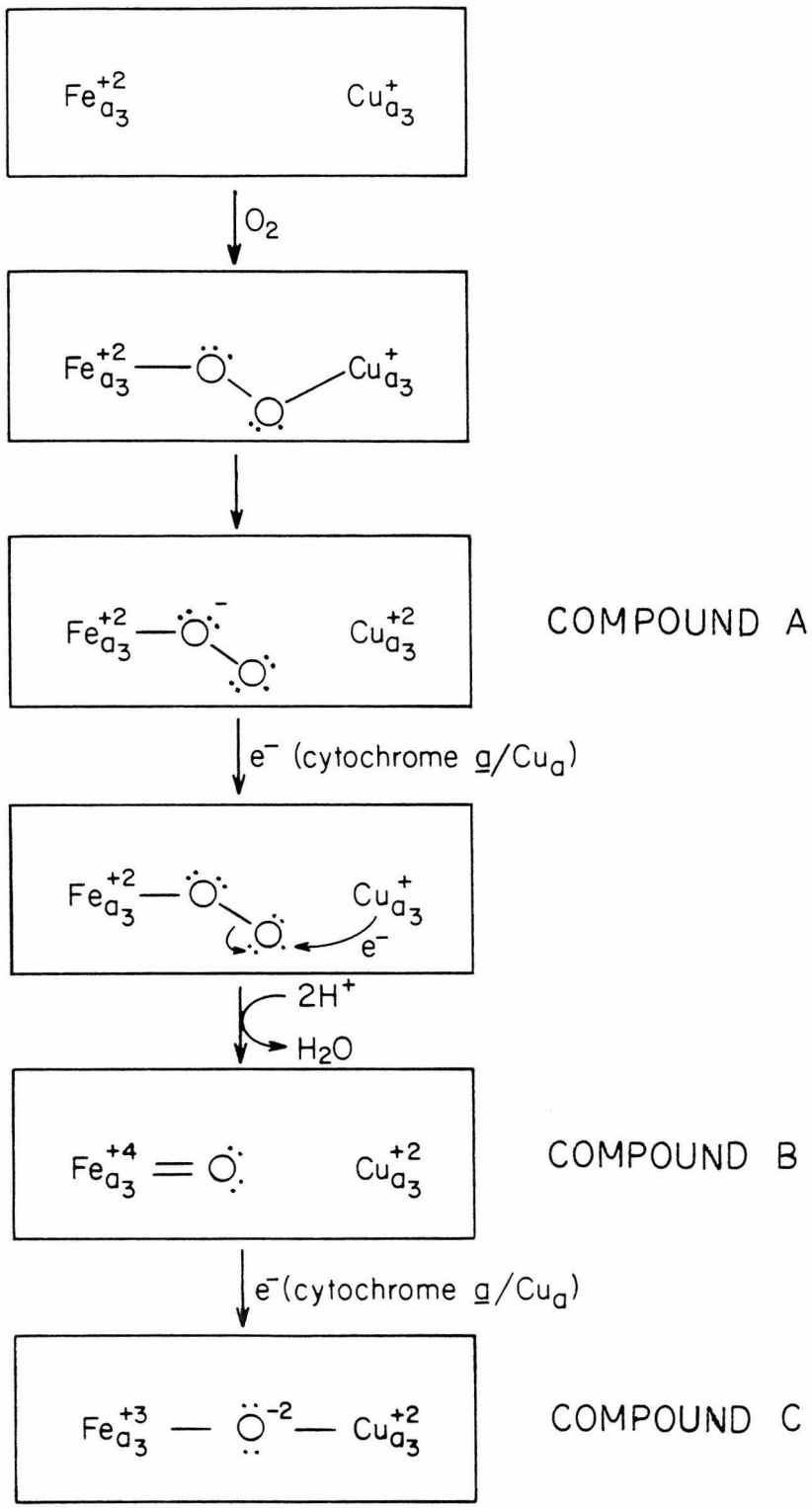
$Fe^{+2}_{a_3}$
$Cu^{+}_{a_3}$
O_2
$Fe^{+2}_{a_3}$
$Cu^{+}_{a_3}$
$Fe^{+2}_{a_3}$
$Cu^{+2}_{a_3}$
COMPOUND A
e^- (cytochrome a/Cu_a)
$Fe^{+2}_{a_3}$
$Cu^{+}_{a_3}$
e^-
$2H^+$
H_2O
$Fe^{+4}_{a_3}$
$Cu^{+2}_{a_3}$
COMPOUND B
e^-(cytochrome a/Cu_a)
$Fe^{+3}_{a_3}$
O^{-2}
$Cu^{+2}_{a_3}$
COMPOUND C

when a second electron is transferred to the coordinated O_2. Identification of compounds A, B, and C as three of the intermediates in our proposed mechanism (Figure 13) is consistent with the results of Chance et al.[11] and, moreover, agrees well with the work of Clore et al.[39] in which EPR spectra in conjunction with optical spectra were recorded during the low temperature reaction of O_2 with the reduced enzyme.

Our proposed mechanism differs from previously proposed mechanisms in that a μ-peroxo intermediate state is not formed during the reduction of dioxygen to water. It may be that the oxygen binding site in cytochrome c oxidase involves two non-equivalent metal centers to avert the formation of a μ-peroxo species.

References

1. Keilen, D. and E.F. Hartree (1939), Proc. Roy. Soc. (London) B127, 167.
2. Stevens, T.H., G.W. Brudvig, D.F. Bocian and S.I. Chan (1979), Proc. Natl. Acad. Sci. USA 76, 3320.
3. Aasa, R., S.P.J. Albracht, K.E. Falk, B. Lanne and T. Vänngård (1976), Biochim. Biophys. Acta 422, 260.
4. Van Gelder, B.F. and H. Beinert (1969), Biochim. Biophys. Acta 189, 1.
5. Tweedle, M.F., L.J. Wilson, L. Garĉia-Iñiguez, G.T. Babcock and G. Palmer (1978), J. Biol. Chem. 253, 8065.
6. Nicholls, P. (1976), Biochim. Biophys. Acta 430, 13.
7. Wikström, M., H.J. Harmon, W.J. Ingledew and B. Chance (1976), FEBS Lett. 65, 259.
8. Muijsers, A.O., R.H. Tiesjema and B.F. Van Gelder (1971), Biochim. Biophys. Acta 234, 481.
9. Gibson, Q.H. and C. Greenwood (1965), J. Biol. Chem. 240, 2694.
10. Babcock, G.T., L.E. Vickery and G. Palmer (1978), J. Biol. Chem. 253, 2400.
11. Chance, B., C. Saronio and J.S. Leigh, Jr. (1975), J. Biol. Chem. 250, 9226.
12. Shaw, R.W., R.E. Hansen and H. Beinert (1978), Biochim. Biophys. Acta 504, 187.
13. Stevens, T.H., D.F. Bocian and S.I. Chan (1979), FEBS Lett. 97, 314.

14. Blokzijl-Homan, M.F.J. and B.F. Van Gelder (1971), Biochim. Biophys. Acta 234, 493.

15. Rosén, S., R. Bränden, T. Vänngård and B.G. Malmström (1977), FEBS Lett. 74, 25.

16. Dervartanian, D.V., I.Y. Lee, E.C. Slater and B.F. Van Gelder (1974), Biochim. Biophys. Acta 347, 321.

17. Wever, R., B.F. Van Gelder and D.V. Dervartanian (1975), Biochim. Biophys. Acta 387, 189.

18. Reinhammar, B., R. Malkin, P. Jensen, B. Karlsson, L. Andréasson, R. Aasa, T. Vänngård and B.G. Malmström (1980), J. Biol. Chem. 255, 5000.

19. Blumberg, W.E. and J. Peisach (1979), in "Cytochrome Oxidase", (T.E. King, Y. Orii, B. Chance and K. Okunuki, eds.), Elsevier, Amsterdam, 153.

20. Fielden, E.M., P.B. Roberts, R.C. Bray, D.J. Lowe, G.N. Mautner, G. Rotilio and L. Calabrese (1974), Biochem. J. 139, 49.

21. Richardson, J.S., K.A. Thomas, B.H. Rubin and D.C. Richardson (1975), Proc. Natl. Acad. Sci. USA 72, 1349.

22. Yonetani, T., H. Yamamoto, J.E. Erman, J.S. Leigh, Jr. and G.H. Reed (1972), J. Biol. Chem. 247, 2447.

23. Kon, H. and N. Kataoka (1969), Biochemistry 8, 4757.

24. Dickerson, R.E. and I. Geis (1969), "The Structure and Action of Proteins", Benjamin, Inc.

25. Chan, S.I., T.H. Stevens, G.W. Brudvig and D.F. Bocian (1980), in "Proceedings of the International Symposium on Frontiers in Protein Chemistry", (T. Liu, K. Yasunobu and G. Mamiya, eds.), Elsevier, Amsterdam, in press.

26. Brudvig, G.W., T.H. Stevens and S.I. Chan (1980), Biochemistry 19, in press.

27. Hartzell, C.R. and H. Beinert (1974), Biochim. Biophys. Acta 368, 318.

28. Takemori, S. and T.E. King (1965), J. Biol. Chem. 240, 504.

29. Powers, L., W.E. Blumberg, B. Chance, C.H. Barlow, J.S. Leigh, J. Smith, T. Yonetani, S. Vik and J. Peisach (1979), Biochim. Biophys. Acta 546, 520.

30. Hartzell, C.R. and H. Beinert (1976), Biochim. Biophys. Acta 423, 323.

31. Verplaetse, J., P. Van Tornout, G. Defreyn, R. Witters and R. Lontie (1979), Eur. J. Biochem. 95, 327.

32. Matsubara, T. and H. Iwasaki (1972), J. Biochem. 72, 57.

33. St. John, R.T. and T.C. Hollocher (1977), J. Biol. Chem. 252, 212.

34. Cox, C.D., Jr., W.J. Payne and D.V. Dervartanian (1971), Biochim. Biophys. Acta 253, 290.

35. Symons, M. (1978), "Chemical and Biochemical Aspects of Electron Spin Resonance Spectroscopy", Wiley, N.Y., 108.

36. Abragam, A. and B. Bleaney (1970), "Electron Paramagnetic Resonance of Transition Ions", Oxford, London, 491.

37. Martin, C.T., personal communication.

38. Collman, J., C. Elliott, T. Halbert and B. Tovrog (1977), Proc. Natl. Acad. Sci. USA 74, 18.

39. Clore, G.M., L. Andréasson, B. Karlsson, R. Aasa and B. Malmström (1980), Biochem. J. 185, 139.

CHAPTER III: STRUCTURE AND FUNCTION OF CYTOCHROME $\underline{a}_3$ - Cu_{a_3}: CONFORMATIONS OF THE OXIDIZED ENZYME

1. INTRODUCTION

In chapter II we presented results which indicated that NO reacts with cytochrome c oxidase, both to oxidize and reduce the enzyme. However, these reactions were quite slow, particularly when NO was added to the oxidized enzyme. In fact, for short incubation times NO was found to reversibly bind to Cu_{a_3} and uncouple Cu_{a_3} from cytochrome $\underline{a}_3$.[1] The uncoupled state exhibited a high-spin ferricytochrome $\underline{a}_3$ EPR signal that was typical of other high-spin ferrihemes. The observation of an EPR signal from cytochrome $\underline{a}_3$ in the presence of NO opened a number of avenues for the study of the structure of the cytochrome $\underline{a}_3$-Cu_{a_3} site. For example, cyanide and fluoride were found to bind to ferricytochrome $\underline{a}_3$, while NO was coordinated to $Cu^{+2}_{a_3}$. These observations led Chan et al.[2] to propose the model for the cytochrome $\underline{a}_3$-Cu_{a_3} site shown in Figure 1. In this model, the strong antiferromagnetic exchange interaction between Cu_{a_3} and cytochrome $\underline{a}_3$ is facilitated through a bridging ligand bound equatorially to a tetragonal Cu_{a_3}. The attachment of a strong field ligand, such as NO, to an axial position of Cu_{a_3} should place the unpaired electron on Cu_{a_3} in a square plane containing the stronger field ligand. When this occurs, the antiferromagnetic exchange interaction between Cu_{a_3} and cytochrome $\underline{a}_3$ could be greatly reduced, while a strong interaction between Cu_{a_3} and the coordinated NO would be possible.

FIGURE 1

Model of the oxidized cytochrome $\underline{a}_3$-Cu_{a_3} site proposed by Chan et al.[2] on the basis of NO-binding studies of cytochrome c oxidase. For Cu(II) in a tetragonal crystal field, as shown, the unpaired electron resides in a $3d_{x^2-y^2}$ orbital which is dipicted by the lobes pointing toward the ligands in the square plane. Here R_1, R_2, R_3, and R_4 denote endogenous ligands to Cu_{a_3} and L denotes the ligand bridging between Cu_{a_3} and cytochrome $\underline{a}_3$ which may or may not be an endogenous ligand.

A

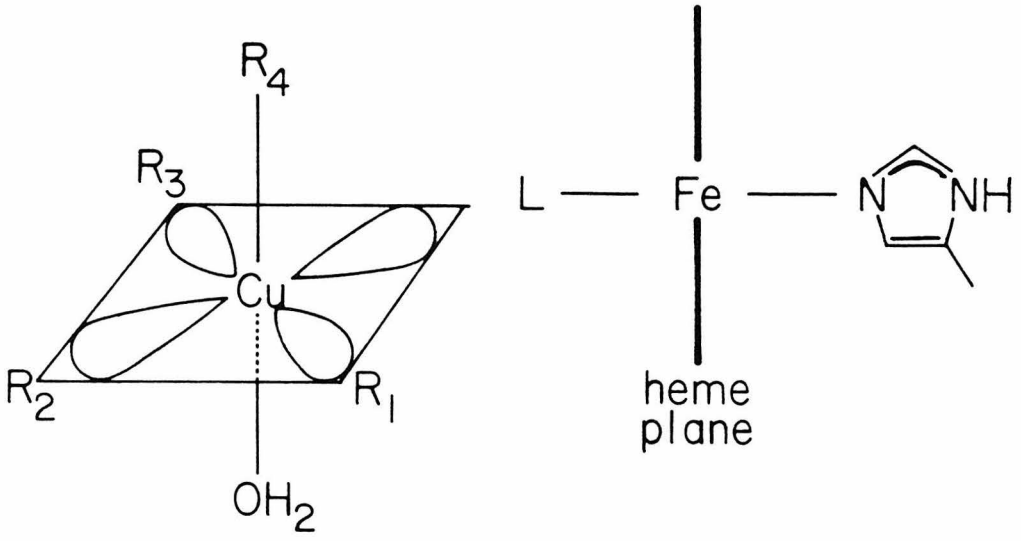

B

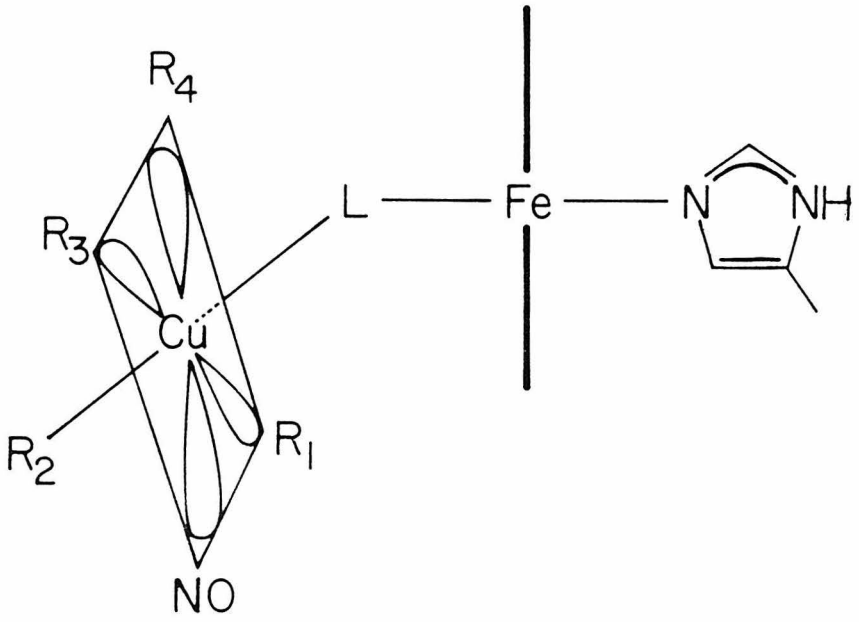

One complication in the studies on the binding of NO to the oxidized enzyme was that the intensity of the high-spin ferricytochrome $\underline{a}_3$ EPR signal observed never corresponded to 100% of cytochrome $\underline{a}_3$.[1] In fact the intensity of this EPR signal varied among preparations of the enzyme; in some preparations no cytochrome $\underline{a}_3$ EPR signal was observed when NO was added to the oxidized enzyme. It appears that more than one conformation of the fully oxidized enzyme may exist and the model described above (Figure 1) may pertain to only a subset of the possible conformations. If, indeed, the oxidized enzyme is heterogeneous, then the nature of such heterogeneity must be understood. Much of what is known about cytochrome $\underline{c}$ oxidase has been obtained from studies of the oxidized enzyme; and if the oxidized enzyme contains multiple conformations, then many of these studies may require reinterpretation. In this regard, NO provides a method by which one specific conformation of the oxidized enzyme can be detected. We have utilized this specificity of NO to investigate the conformations of the oxidized enzyme in this chapter. Four distinct conformations of the oxidized enzyme have been identified. The ligand binding and EPR properties of these conformations indicate that the differences between the conformations can be understood by differences in the structure of the O_2 binding site. The mechanism by which these conformations interconvert and the functional significance of each is discussed.

2. MATERIALS AND METHODS

Beef heart cytochrome c oxidase was isolated by the procedures of Hartzell and Beinert[3] and Yu et al..[4] The purified protein was dissolved in 50 mM Tris/acetate buffer, pH 7.4, 0.5% Tween 20 (Hartzell and Beinert preparation) and in 50 mM phosphate, pH 7.4, 0.5% cholate (Yu et al. preparation).

The addition of NO to the samples is described in chapter II. In addition to the oxidized enzyme plus NO (the preparation of this sample is described in chapter II), five other complexes of cytochrome c oxidase were prepared in this work: (i) oxidized enzyme plus cyanide, (ii) oxidized enzyme plus cyanide and NO, (iii) oxidized enzyme plus fluoride, (iv) oxidized enzyme plus fluoride and NO, and (v) 'oxygenated' enzyme.[5]

The oxidized enzyme plus cyanide complex was prepared by the addition of a 1:2 mole ratio mixture of solid KCN and KH_2PO_4 to the anaerobic sample from a sidearm on the EPR tube. The amount of KCN added would have given a final KCN concentration of 100 mM. However, the major portion of the cyanide bubbled off as HCN. The actual concentration of dissolved cyanide, estimated from the partial pressure of HCN over the sample and the solubility of HCN in water, was about 2 mM. The oxidized enzyme plus cyanide and NO complex was prepared as above except that the KCN plus KH_2PO_4 mixture was added to the enzyme while the sample was under vacuum. Then NO was admitted to the sample after the desired period of incubation to give a final pressure of one atmosphere without further evacuation of the enzyme plus cyanide. It was found that a major fraction of the

cyanide in the sample was removed if the enzyme was degassed after the addition of KCN, resulting in incomplete formation of the oxidized cyanide complex.

The oxidized enzyme plus fluoride was prepared by adding an aliquot of a 1 M solution of KF to the oxidized enzyme to give the desired final fluoride concentration and then making the sample anaerobic. The oxidized enzyme plus fluoride and NO complex was prepared in the same manner as the oxidized enzyme plus fluoride with the further addition of NO to a pressure of one atmosphere.

The 'oxygenated' state[5] of the enzyme was prepared by adding a slight excess of ascorbate plus PPD to reduce the enzyme. In the experiments where the rate of decay of the 'oxygenated' enzyme was monitored by EPR, individual samples were reduced with ascorbate plus PPD and then placed in a dialysis bag and dialyzed against 1000 volumes of an aerobic buffer solution to reoxidize the enzyme and to remove the ascorbate and PPD from the sample. The beginning of the dialysis was taken as the zero of time and samples were removed at various times and immediately placed in an EPR tube and frozen in liquid nitrogen.

The EPR spectra were recorded on a Varian E-line century series X-band EPR spectrometer equipped with an Air Products Heli-Trans low temperature system. The intensity of the high-spin ferricytochrome a_3 EPR signals was determined relative to an external metmyoglobin standard (dissolved in 10 mM phosphate, pH 6.0) and also relative to the low-spin ferricytochrome a

EPR signal. The high-spin heme EPR signals were integrated by the method of Aasa et al..[6] The low-spin cytochrome *a* EPR signal was integrated by the method of Aasa and Vänngård[7] using the g = 3.0 component to determine the total area. The low-spin cytochrome *a* EPR signal has been shown to correspond to 100% of one heme,[6] and on this basis the low-spin cytochrome *a* EPR signal was used as an internal standard. The high-spin cytochrome a_3 EPR signal intensities (for the rhombic high-spin cytochrome a_3 EPR signal induced by NO) determined by using a metmyoglobin standard were found to be independent of temperature, thus indicating that the zero-field splitting parameter (D) is nearly equal for the two high-spin ferric hemes. After correction for the distribution of population among the spin sublevels of the high-spin ferric heme, the high-spin cytochrome a_3 EPR intensities determined by using the internal cytochrome *a* standard were found to agree with those determined by using the metmyoglobin standard to within 10%.

The intensity of the low-spin cyanoferricytochrome a_3 EPR signal was determined relative to the low-spin cytochrome *a* EPR signal. All three g-values of the cyanocytochrome a_3 EPR signal are not known since the signal is very anisotropic and the two high-field turning points have not been observed. Therefore, the cyanocytochrome a_3 EPR signal was integrated by the method of DeVries and Albracht[8] using the g = 3.58 component to determine the total area.

3. RESULTS

3.1 Interaction of NO with Oxidized Cytochrome c Oxidase.

In the work of Stevens et al.,[1] it was found that a rhombic high-spin cytochrome a_3 EPR signal (g = 6.16, 5.82, 2) could be observed when NO was added to the oxidized enzyme. However, the intensity of this EPR signal varied among preparations of the enzyme from less than 5% of one heme to as much as 60% of one heme. It was suggested that a conformational heterogeneity of the oxidized enzyme may exist and that NO induces a high-spin cytochrome a_3 EPR signal in only a subset of the possible conformations.

In this work we will focus on the differences in the interaction of NO with two types of preparations of the enzyme: one specific Hartzell and Beinert preparation and one specific Yu et al. preparation. These preparations differ in that NO induced a high-spin cytochrome a_3 EPR signal which accounted for 60% of one heme in the Hartzell and Beinert preparation, but only 1% of one heme in the Yu et al. preparation. It should be noted that only one particular preparation of each type was used in this work. We have found that the NO-binding properties of the oxidized enzyme varied each time a new batch of the enzyme was isolated, even when the same procedure was followed in the isolation (see reference (1)). However, for a given batch of the enzyme, the fraction of high-spin cytochrome a_3 induced by NO was constant for all the samples from this batch.

The fraction of cytochrome a_3 observed in the presence

of NO was unchanged after a variety of treatments. For example, changing the pH from 7.0 to 9.0 did not change the intensity of the cytochrome $\underline{a}_3$ EPR signal induced by NO. A variety of other treatments, such as changing the ionic strength of the buffer, changing the detergent in which the enzyme was dissolved from Tween 20 to cholate, and precipitation of the enzyme by ammonium sulfate and resolubilization of the enzyme in phosphate buffer, also did not alter the intensity of the cytochrome $\underline{a}_3$ EPR signal induced by NO.

3.2 g' = 12 EPR Signal. Cytochrome c oxidase has been observed to exhibit a fairly broad EPR signal* at g' = 12.[9] This EPR signal is quite unusual for heme or copper proteins; and, in fact, at the present time it is not known for sure that it is associated with any of the metal centers in cytochrome c oxidase, although its intensity has been observed to increase as the purification of the enzyme proceeds.[9] When NO was added to the oxidized enzyme, the intensity of the g' = 12 EPR signal did not change, even when a large high-spin cytochrome $\underline{a}_3$ EPR signal was induced. Moreover, the intensity of the g' = 12 EPR signal was about two-fold larger in the Yu et al. preparation than in the Hartzell and Beinert preparation. This observation can be contrasted to the intensity of the NO-induced cytochrome $\underline{a}_3$ EPR signal which was much larger in the Hartzell and Beinert preparation than in the Yu et al.

*The g-value for this resonance is only an effective g-value, since its value depends on the microwave frequency used to obtain the EPR signal; and, hence, we will label the g-value with a prime. This point will be discussed in section 4.3.

preparation. It appears that the g' = 12 EPR signal may arise from molecules separate from those in which NO induced a high-spin cytochrome $\underline{a}_3$ EPR signal.

3.3 Oxidized Enzyme Plus Cyanide and NO. Stevens et al.[1] found that cyanide plus NO induced a low-spin cyanocytochrome $\underline{a}_3$ EPR signal from oxidized cytochrome $\underline{c}$ oxidase. It was concluded that NO was bound to Cu_{a_3} while cyanide was bound to cytochrome $\underline{a}_3$; NO acted to uncouple Cu_{a_3} from cytochrome $\underline{a}_3$ and cyanide induced a high to low-spin transition when bound to cytochrome $\underline{a}_3$. Chan et al.[2] pointed out that the intensity of the low-spin cyanocytochrome $\underline{a}_3$ EPR signal induced by NO was equal to that of the high-spin cytochrome $\underline{a}_3$ EPR signal induced by NO. Thus, cyanide appears to bind quantitatively to cytochrome $\underline{a}_3$ in the enzyme molecules that NO induces a cytochrome $\underline{a}_3$ EPR signal.

We found that the addition of cyanide to the oxidized Yu et al. preparation of the enzyme had no effect on the g' = 12 EPR signal, provided that the sample was mixed and immediately frozen. However, when the oxidized enzyme was incubated at 4°C in the presence of cyanide the g' = 12 EPR signal gradually disappeared (Figure 2). This result demonstrates that the g' = 12 EPR signal is associated with the cytochrome $\underline{a}_3$-Cu_{a_3} site and that cytochrome $\underline{a}_3$ does not readily bind exogenous ligands in the conformation which exhibits the g' = 12 EPR signal.

FIGURE 2

EPR spectra of the Yu et al. preparation of cytochrome c oxidase in the presence of both cyanide and NO. In all cases one atmosphere of NO was added, mixed with the sample for two minutes, and then the sample was immediately frozen at 77K. The samples contained 0.2 mM cytochrome c oxidase and were preincubated with approximately 2 mM HCN at 4°C before adding NO: (A) 5 minute preincubation; (B) 30 minute preincubation; and (C) 5 hour preincubation. Conditions: temperature, 16K; microwave power, 0.5 mW; modulation amplitude, 16 G; microwave frequency, 9.23 GHz.

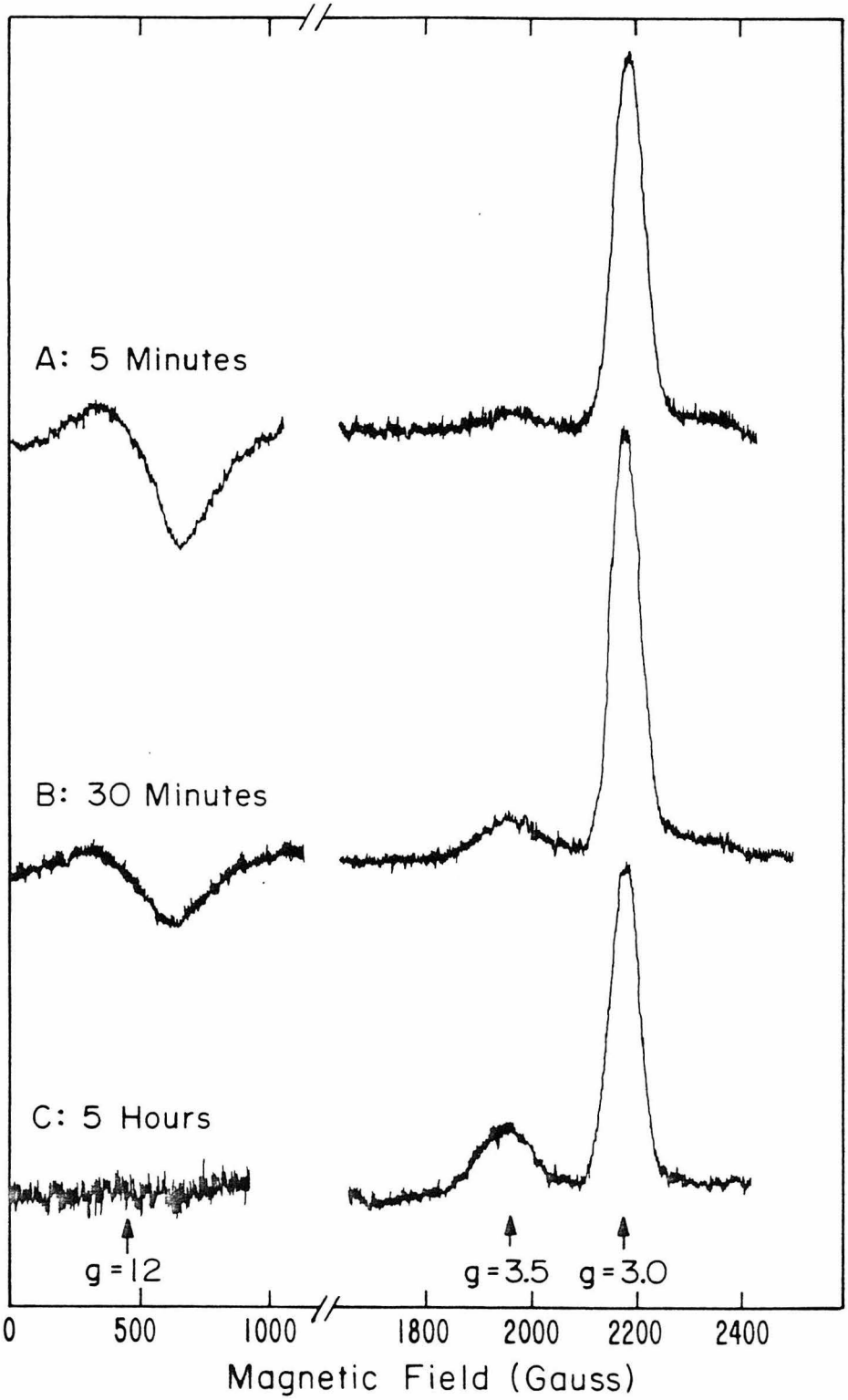
A: 5 Minutes
B: 30 Minutes
C: 5 Hours
g = 12
g = 3.5
g = 3.0
0
500
1000
1800
2000
2200
2400
Magnetic Field (Gauss)

It was possible to directly monitor the fraction of cyanide-bound enzyme molecules by adding NO to our sample of the Yu et al. preparation.* A direct parallel was found between the decrease in intensity of the g' = 12 EPR signal and the increase in intensity of the NO-induced cyanocytochrome $\underline{a}_3$ EPR signal when the oxidized enzyme was incubated with cyanide (Figures 2 and 3). After long incubation times (more than 6 hours), the g' = 12 EPR signal was completely eliminated and intensity of the NO-induced cyanocytochrome $\underline{a}_3$ EPR signal accounted for 100% of one heme. This is, in fact, the first time that 100% of both cytochrome $\underline{a}_3$ and cytochrome $\underline{a}$ have been simultaneously observed by EPR. It should be noted that the cyanocytochrome $\underline{a}_3$ EPR signal only appeared when NO was added to the sample in the presence of cyanide. Furthermore, the cyanocytochrome $\underline{a}_3$ EPR signal was completely eliminated upon removal of NO from the sample.

The direct parallel between the decrease in intensity of the g' = 12 EPR signal and the increase in intensity of the NO-induced cyanocytochrome $\underline{a}_3$ EPR signal (Figure 3) indicates that only two conformations of the enzyme were present in the Yu et al. preparation: (i) the conformation which exhibited the g' = 12 EPR signal and (ii) the conformation with cyanide bound in which NO induced a cyanocytochrome $\underline{a}_3$ EPR signal.

*In order for the intensity of the NO-induced cyanocytochrome $\underline{a}_3$ EPR signal to be a true indication of the fraction of enzyme molecules which have bound cyanide, the sample must be mixed with NO and immediately frozen. It was observed that the intensity of the NO-induced cyanocytochrome $\underline{a}_3$ EPR signal decreased when the sample was incubated at 4°C in the presence of NO. This observation can be explained if NO induced a slow reduction of the enzyme (see chapter II, section 3.4).

FIGURE 3

Fraction of the Yu et al. preparation of cytochrome *c* oxidase which exhibited an EPR signal at g' = 12 (determined from equation (1)) and the fraction in which NO induced a low-spin cyanocytochrome a_3 EPR signal at g = 3.5 as a function of time of preincubation with cyanide. The concentrations and EPR conditions were the same as in Figure 2.

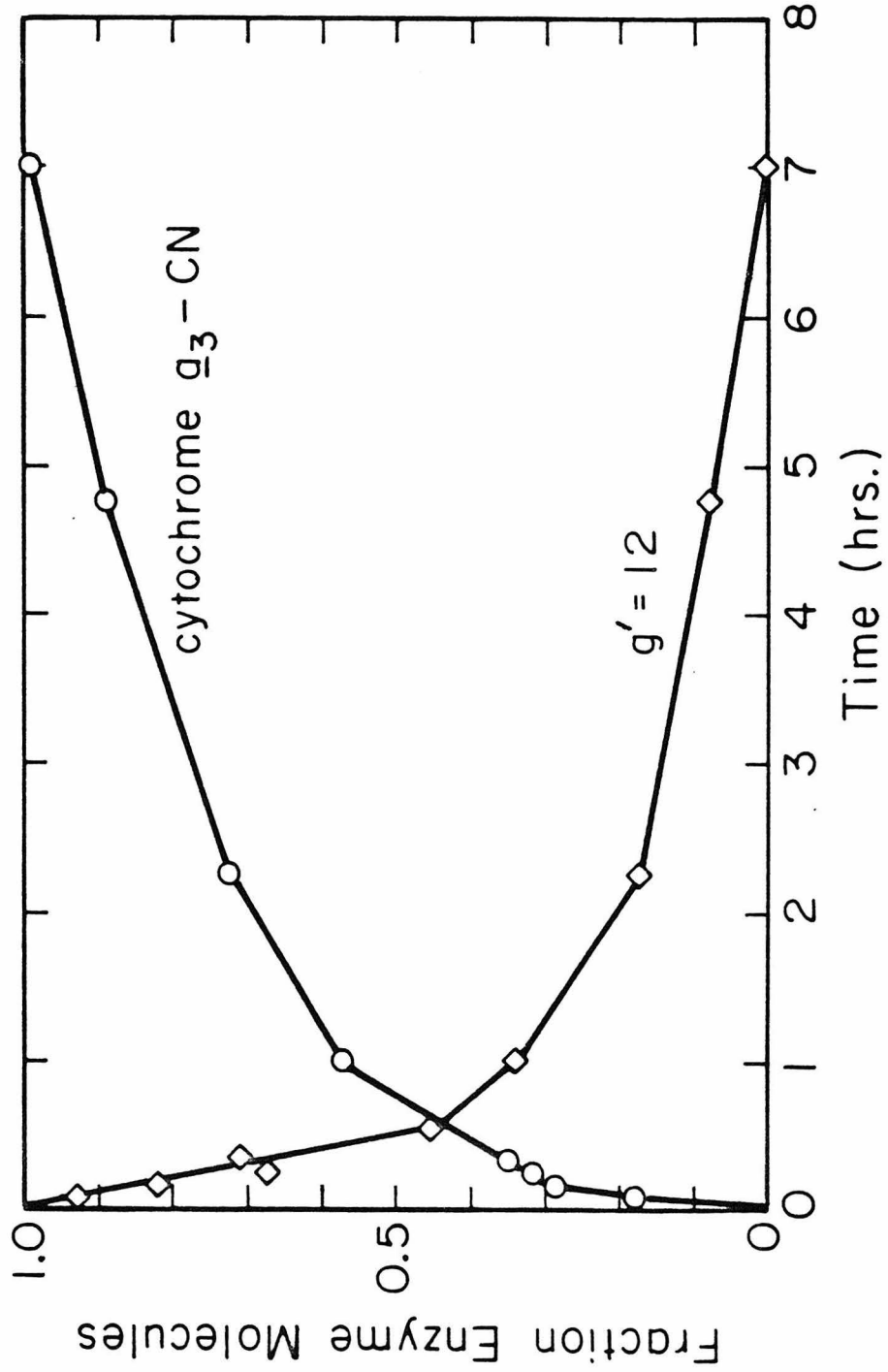
cytochrome a_3 – CN
g′= 12
Fraction Enzyme Molecules
1.0
0.5
0
0
1
2
3
4
5
6
7
8
Time (hrs.)

This result allows the intensity of the g' = 12 EPR signal to be quantitated at each time point in Figure 3 by assuming that the intensity of the g' = 12 EPR signal is proportional to the fraction of enzyme molecules unaccounted for by the NO-induced cyanocytochrome $\underline{a}_3$ EPR signal. The g' = 12 EPR signal was impossible to quantitate directly without this assumption because it is not known with certainty: (i) the spin state of the species exhibiting the g' = 12 EPR signal, and (ii) whether other resonances at higher or lower field are associated with the g' = 12 EPR signal (in this regard, the g' = 12 EPR signal does not appear to have equal area above and below the baseline).

The intensity of the g' = 12 EPR signal was measured by its maximum to minimum height. However, this height was strongly dependent on the temperature (Figure 4). This temperature dependence probably was mainly due to the g' = 12 EPR signal arising from a $S > 1/2$ species, but it also was due in part to broadening of the signal at higher temperatures. The g' = 12 peak height was scaled to 16K, by the use of Figure 4, for each time point in Figure 3. Then this peak height was divided by the area of the g = 3 component of the cytochrome $\underline{a}$ EPR signal to normalize the g' = 12 EPR signal intensity, since the cytochrome $\underline{a}$ EPR signal remained constant during the incubation of the enzyme with cyanide and represented one heme/enzyme. The following formula was obtained for the fraction, F, of the enzyme molecules exhibiting the g' = 12 EPR signal:

FIGURE 4

The maximum to minimum height of the EPR signal centered at g' = 12 versus the temperature. Conditions: microwave power, 0.2 mW; modulation amplitude, 16 G; microwave frequency, 9.24 GHz.

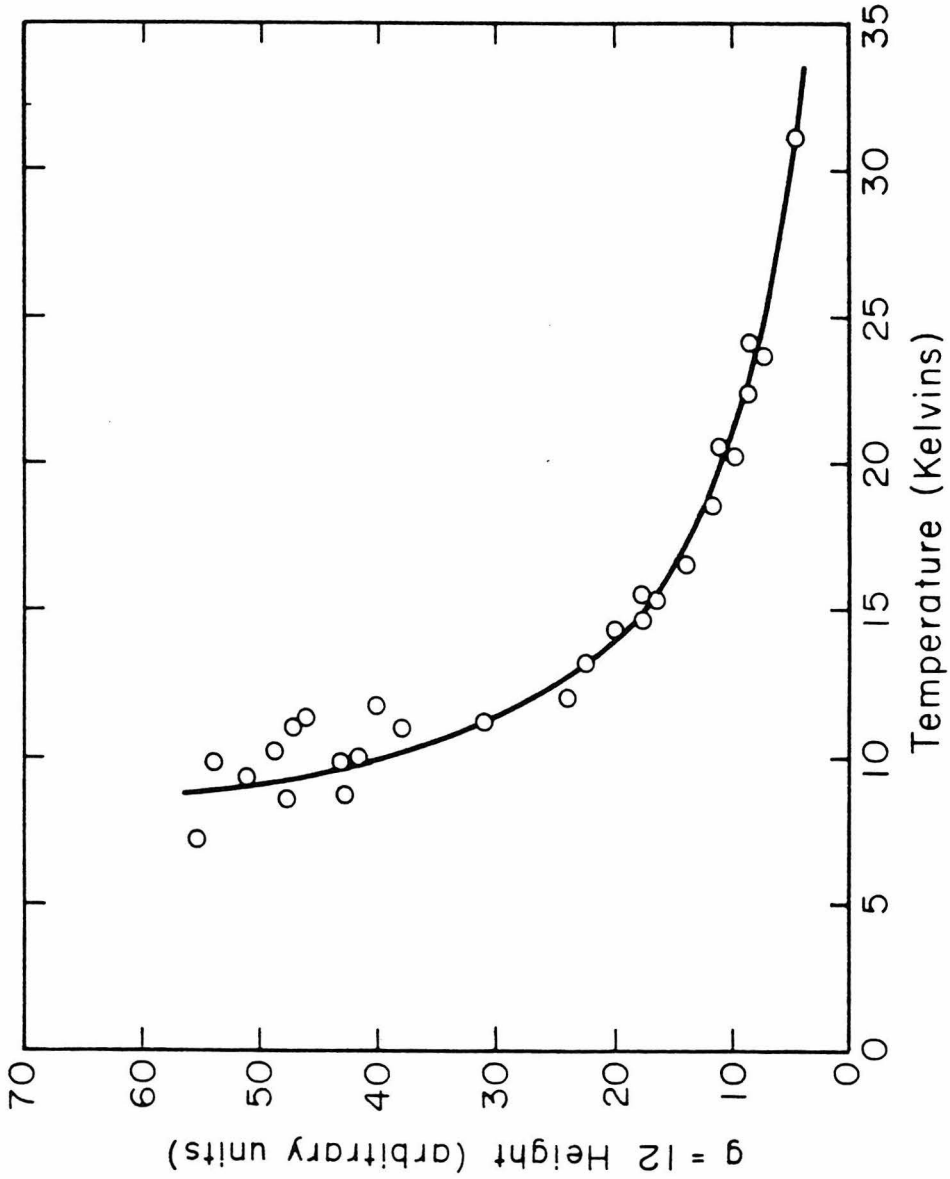
g = 12 Height (arbitrary units)
0
10
20
30
40
50
60
70
0
5
10
15
20
25
30
35
Temperature (Kelvins)

$$F = (17)\left[\frac{H(g' = 12)}{A(g = 3)}\right]\left[\frac{16}{T}\right] \qquad (1)$$

where H(g' = 12) is the maximum to minimum height in mm of the g' = 12 EPR signal scaled to 16K by the use of Figure 4, A(g = 3) is the area of the g = 3.0 component of the cytochrome a EPR signal calculated by summing the peak heights in mm at 10 G spacings, and T is the temperature in Kelvins at which the spectrum was recorded. It was found that the fraction of enzyme molecules exhibiting the g' = 12 EPR signal [as calculated from equation (1)] plus the fraction exhibiting the NO-induced cyanocytochrome a_3 EPR signal was constant throughout the entire time of incubation with cyanide (sum = 0.97 ± 0.08). This result is supportive of our earlier statement that only two conformations are present in the Yu et al. preparation in the presence of cyanide. These two conformations interconvert under the influence of cyanide resulting in a homogeneous population of enzyme molecules once all have bound cyanide.

We have used formula (1) to estimate the fraction of enzyme molecules which exhibit the g' = 12 EPR signal and the intensity of the g = 6 rhombic high-spin cytochrome a_3 EPR signal to estimate the fraction of enzyme molecules in which NO uncouples Cu_{a_3} from cytochrome a_3. The results for both the Hartzell and Beinert and Yu et al. preparations are shown in Table 1. The obvious conclusion from the data in Table 1 is that the sum of the molecules exhibiting the g' = 12 EPR signal plus those exhibiting a NO-induced g = 6 EPR signal does

Table 1: Fraction of Enzyme Molecules Exhibiting g' = 12 and NO-induced g = 6 EPR Signals in Oxidized Cytochrome c Oxidase

Preparation	Fraction		Sum (g' = 12 and g = 6)
	g' = 12	g = 6	
Yu et al.	0.74	0.01	0.75
Hartzell and Beinert	0.39	0.56	0.95

not account for 100% of the enzyme molecules in the Yu et al. preparation. In fact, this sum was different for the two preparations of the enzyme, accounting for close to 100% of the enzyme molecules in the Hartzell and Beinert preparation, but only 75% in the Yu et al. preparation. We now discuss fluoride binding studies, the results of which have shed some light on the unaccounted for fraction of the oxidized enzyme molecules.

3.4 Oxidized Enzyme Plus Fluoride and NO. Fluoride was found to bind to cytochrome $\underline{a}_3$ while NO was coordinated to Cu_{a_3}.[1] In this case the high-spin fluoroferricytochrome $\underline{a}_3$ EPR signal exhibited axial symmetry. We investigated the possibility that fluoride could slowly bind to the conformation which exhibited a g' = 12 EPR signal (as did cyanide) and, after long incubation, allows 100% of the fluorocytochrome $\underline{a}_3$ EPR signal to be induced by NO.

When fluoride was added to the Yu et al. preparation in the absence of NO a new unusual EPR signal appeared. The new signal (hereafter referred to as the fluorocytochrome $\underline{a}_3$-Cu_{a_3} EPR signal) spanned at least from 800 to 2000 Gauss and had five resonances with g-values of 8.5, 6, 5, 4.3, and 3.2 (Figure 5B and E). The addition of NO to the oxidized enzyme-fluoride complex immediately eliminated the fluorocytochrome $\underline{a}_3$-Cu_{a_3} EPR signal, and in its place the high-spin fluoroferricytochrome $\underline{a}_3$ EPR signal was observed (Figure 5C). This observation demonstrates that the fluorocytochrome $\underline{a}_3$-Cu_{a_3} EPR signal is associated with the cytochrome $\underline{a}_3$-Cu_{a_3} site. Moreover, the

FIGURE 5

EPR spectra of the Yu et al. preparation of cytochrome c oxidase (A) native anaerobic enzyme; (B) 100 mM KF added to (A) and incubated 24 hrs. at 4°C; (C) one atmosphere of NO added to (B), mixed and immediately frozen. Spectra (D), (E), and (F) as the same as spectra (A), (B), and (C), respectively, with a four-fold increase in gain. Conditions: temperature, 17K; microwave power, 0.5 mW; modulation amplitude, 16 G; microwave frequency, 9.24 GHz.

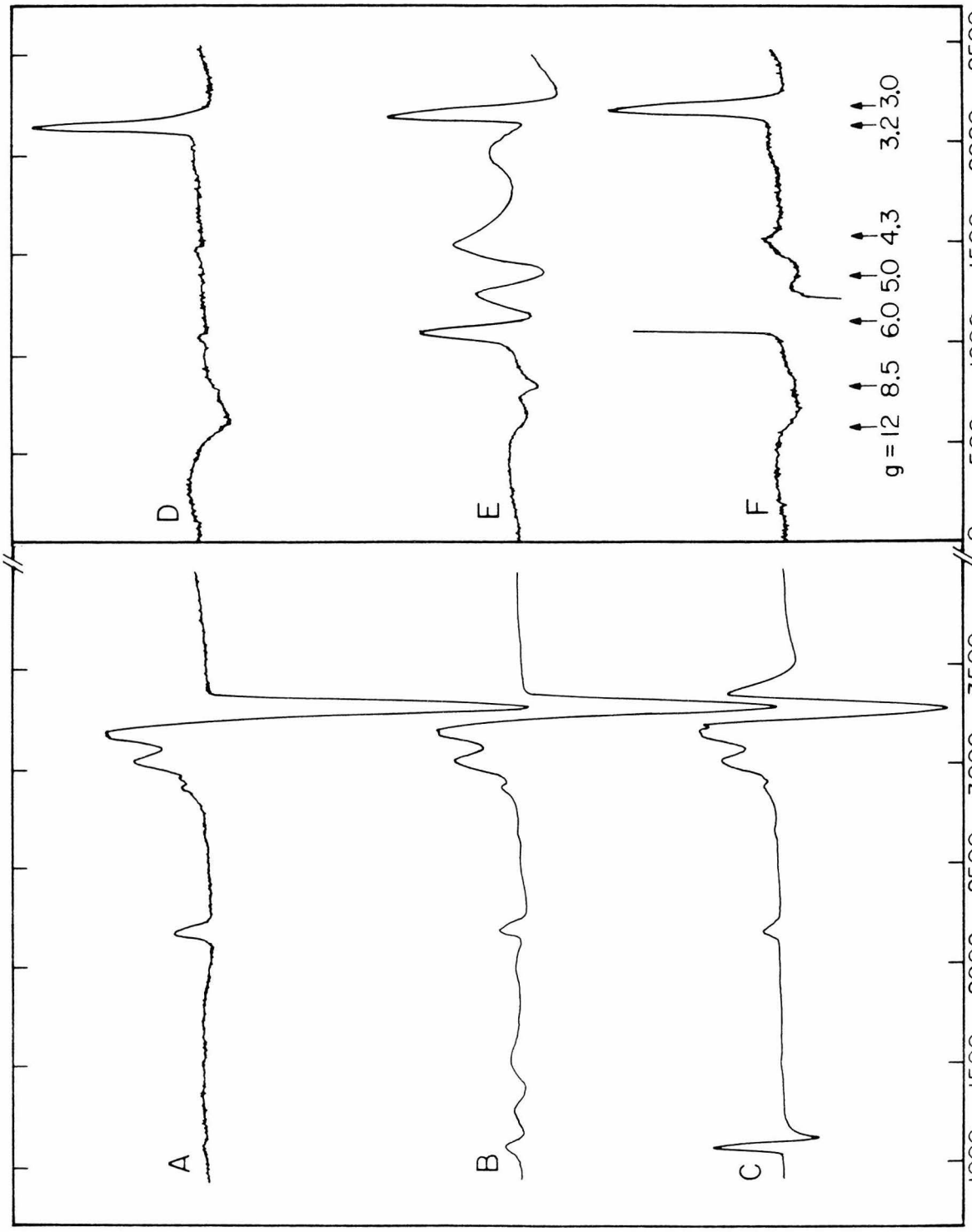
A
B
C
D
E
F
g = 12 8.5 6.0 5.0 4.3 3.2 3.0
1000 1500 2000 2500 3000 3500
0 500 1000 1500 2000 2500
Magnetic Field (Gauss)

intensity of the NO-induced high-spin fluoroferricytochrome $\underline{a}_3$ and the g' = 12 EPR signals together accounted for very close to 100% of the enzyme molecules in <u>both</u> the Yu et al. and Hartzell and Beinert preparations (Table 2).

It should be noted that on accurate estimation of the fraction of one heme represented by the g = 6 EPR signal requires either knowledge of the zero-field splitting between the $m_s = \pm 1/2, \pm 3/2$, and $\pm 5/2$ spin sublevels or measurement of the EPR spectrum at very low temperature. In the former case, the population in the $m_s = \pm 3/2$ and $\pm 5/2$ spin sublevels can be calculated for the temperature at which the EPR spectrum was recorded and the observed g = 6 EPR signal intensity can be increased appropriately. In the latter case, all of the molecules are in the $m_s = \pm 1/2$ states and the intensity of the g = 6 EPR signal corresponds to 100% of the high-spin ferriheme. For the rhombic high-spin cytochrome $\underline{a}_3$ EPR signal induced by NO in the absence of other exogenous ligands the zero-field splitting of cytochrome $\underline{a}_3$, D, was measured[2] to be 8 cm^{-1}. We have assumed that D equals 6 cm^{-1} for fluoride-bound cytochrome $\underline{a}_3$ in calculating the fraction of enzyme molecules in which a high-spin fluorocytochrome $\underline{a}_3$ EPR signal was induced by NO. This value of D for fluoroferricytochrome $\underline{a}_3$ was chosen by analogy to fluoroferrimyoglobin in which D has been measured[10] to be 6.1 cm^{-1}.

For the Hartzell and Beinert preparation, essentially 100% of the enzyme molecules were accounted for in the absence of fluoride by the sum of the intensities of the g' = 12 and NO-

Table 2: Intensities of the g' = 12 and NO-induced g = 6 EPR Signals in Oxidized Cytochrome c Oxidase Plus Fluoride

Preparation	Time of Incubation	Fraction g' = 12	Fraction g = 6	Sum (g'=12 and g=6)
Yu at al.	0	0.74	0.01 (rhombic)	0.75
	4 hr.	0.74	0.20 (axial)	0.94
	16 hr.	0.72	0.28 (axial)	1.00
Hartzell and Beinert	0	0.39	0.56 (rhombic)	0.95
	4 hr.	0.45	0.51 (axial)	0.96
	17 hr.	0.45	0.52 (axial)	0.97

induced g = 6 EPR signals (Table 1). In this preparation, fluoride appears to bind quantitatively to the fraction of enzyme molecules in which NO induced an EPR signal from cytochrome $\underline{a}_3$. However, fluoride does not bind at all to the fraction of the enzyme molecules which exhibit a g' = 12 EPR signal (Table 2).

The observations on the Hartzell and Beinert preparation can be contrasted to those on the Yu et al. preparation. In the Yu et al. preparation only 75% of the enzyme molecules were accounted for by the sum of the intensities of the g' = 12 and NO-induced g = 6 EPR signals (Table 1). Yet in the presence of <u>both</u> NO and fluoride, 100% of the enzyme molecules could be accounted for. It appears that a fraction of the oxidized Yu et al. preparation of the enzyme existed in which NO alone did not induce a cytochrome $\underline{a}_3$ EPR signal, but in which NO and fluoride in combination did.

Another observation which also indicates that the Yu et al. preparation contained a fraction of the enzyme molecules in a third conformation, that was not present in the Hartzell and Beinert preparation to a significant extent, was made on the fluoride-bound oxidized enzyme. It was pointed out in Figure 5 that fluoride induced an unusual fluorocytochrome $\underline{a}_3$-Cu_{a_3} EPR signal in the <u>absence</u> of NO from the Yu et al. preparation. However, fluoride induced very little of this EPR signal from the Hartzell and Beinert preparation (spectra not shown). Thus, the unusual fluorocytochrome $\underline{a}_3$-Cu_{a_3} EPR signal appears to be generated only in a fraction of the oxidized Yu et al. prepara-

tion which was distinct from the fractions which exhibited a g' = 12 EPR signal and a NO-induced (NO alone) g = 6 EPR signal.

3.5 Reoxidation of the Reduced Enzyme. When reduced cytochrome c oxidase is reoxidized by O_2, three distinct states have been observed by optical and EPR spectroscopy.[5,11] These states all appear to be fully oxidized states of the enzyme that are sequentially formed when the reduced enzyme is mixed with O_2 at 4°C. The state which is initially formed[11] appears very rapidly (within 5 ms) and decays with a $t_{1/2}$ of about 100s at 16°C. This state exhibits a Soret band at 428 nm, but its distinguishing characteristic is an EPR signal with resonances at g = 5, 1.78, and 1.69. The second state formed does not exhibit any EPR signals but has a Soret band at 428 nm. This state has been called the 'oxygenated' state.[5] The final state formed exhibits a Soret band at 418-420 nm, identical to the enzyme as isolated.

In our experiments, the reoxidized enzyme was monitored by EPR and optical spectroscopy. However, the time scale of these experiments was sufficiently long that the initial reoxidized state formed (that with an EPR signal with resonances at g = 5, 1.8, and 1.7) was not detected. Thus, the initial species that we observed can be identified as the 'oxygenated' enzyme.

We found that the 'oxygenated' enzyme did not exhibit an EPR signal at g' = 12. However, upon incubation at 4°C the g' = 12 EPR signal gradually increased in intensity and the

rate at which the g' = 12 EPR signal appeared, paralleled the rate at which the Soret band at 428 nm shifted to 420 nm (Figure 6). However, even after two days of incubation of the reoxidized enzyme at 4°C, no EPR signals from cytochrome a_3 were induced by NO.

The addition of fluoride to the 'oxygenated' enzyme was found to induce a large fluorocytochrome a_3-Cu_{a_3} EPR signal. Moreover, the addition of NO to the fluoride-bound 'oxygenated' enzyme induced a high-spin fluoroferricytochrome a_3 EPR signal. Thus, it appears that the 'oxygenated' conformation can be identified as the conformation which accounted for about 25% of the enzyme molecules in the Yu et al. preparation, but which was virtually absent in the Hartzell and Beinert preparation.

4. DISCUSSION

4.1 Identification of Four Conformations of Oxidized Cytochrome c Oxidase.

We have obtained evidence that at least four conformations of oxidized cytochrome c oxidase can exist. These conformations are not in rapid equilibrium; and, hence, it was possible to distinguish the EPR properties of each conformation. The EPR properties are listed in Table 3. We have named the four conformations: the "g12" conformation (that which exhibits a g' = 12 EPR signal), the "g5" conformation (that which exhibits an EPR signal with resonances at g = 5, 1.8, and 1.7), the 'oxygenated' conformation (that in which fluoride alone induces a fluorocytochrome a_3-Cu_{a_3} EPR signal), and the "resting" conformation (that in which NO alone induces a high-spin cytochrome a_3 EPR signal). The choice of these names will

FIGURE 6

Change in absorption at 428 nm and change in the fraction of enzyme molecules which exhibited a g' = 12 EPR signal with time after reoxidation of the fully reduced enzyme with air. The Hartzell and Beinert preparation was used. The concentration of cytochrome c oxidase was 0.16 mM (EPR) and 0.02 mM (optical). The EPR conditions were the same as in Figure 2.

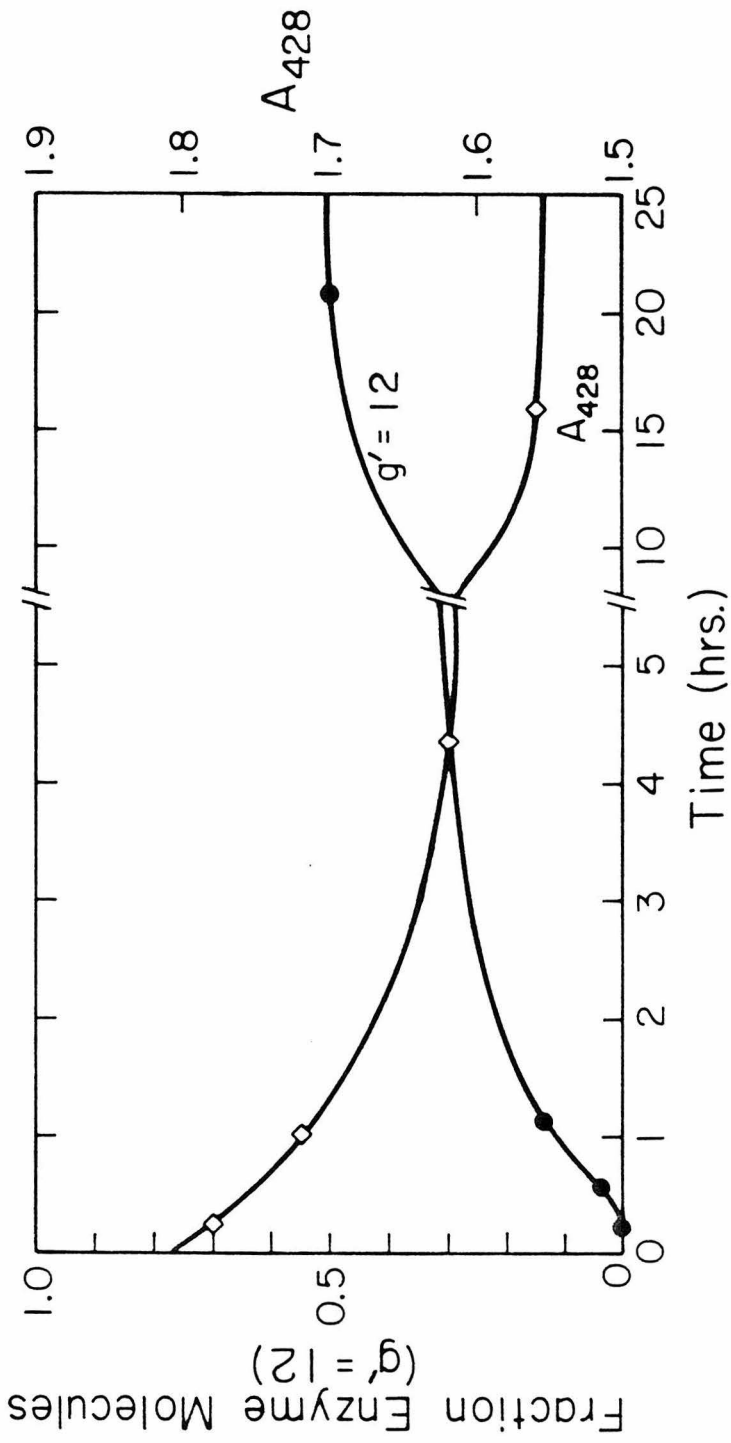
Fraction Enzyme Molecules
(g' = 12)
1.0
0.5
0
0
1
2
3
4
5
10
15
20
25
Time (hrs.)
1.9
1.8
1.7
1.6
1.5
A428
g' = 12
A428

Table 3: EPR Properties of the Conformations of Oxidized Cytochrome c Oxidase. The distinguishing property of each conformation is enclosed in a box.

State	Conformation			
	"g12"	"Resting"	'Oxygenated'	"g5"[a]
Unligated:	g'=12 EPR signal	EPR silent	EPR silent	g=5,1.8,1.7 EPR signal
Plus NO:	g'=12 EPR signal	High-spin cyt. $\underline{a}_3^{+3}$ EPR signal	EPR silent	b
Plus Fluoride:	g'=12 EPR signal	EPR silent	cyt. $\underline{a}_3^{+3}$-F^--$Cu_{a_3}^{+2}$ EPR signal	b
Plus Fluoride and NO:	g'=12 EPR signal	High-spin cyt. $\underline{a}_3^{+3}$-F^- EPR signal	High-spin cyt. $\underline{a}_3^{+3}$-F^- EPR signal	b
Plus Cyanide:	g'=12 EPR signal slowly eliminated	EPR silent	EPR silent	EPR silent
Plus Cyanide and NO:	Low-spin cyt. $\underline{a}_3^{+3}$-CN^- EPR signal slowly appears	Low-spin cyt. $\underline{a}_3^{+3}$-CN^- EPR signal	Low-spin cyt. $\underline{a}_3^{+3}$-CN^- EPR signal	b

a. Reference 11

b. Not determined

become apparent in the following discussion. The sum of these conformations accounted for 100% of the enzyme molecules in both the Hartzell and Beinert and Yu et al. preparations of the enzyme studied. This sum was also found to account for all the enzyme molecules in three separate Hartzell and Beinert preparations which were not described in this work. However, the fraction of the enzyme molecules in each conformation did vary among these preparations.

When the reduced enzyme was reoxidized with O_2 the oxidized enzyme relaxed through a series of three distinct conformations:

"g5" → 'oxygenated' → "g12"

Thus, three of the conformations that we have distinguished can be identified as states formed upon reoxidation of the reduced enzyme with O_2. However, the "resting" conformation was not formed when the enzyme was reoxidized by O_2.

4.2 "Resting" Conformation. The "resting" conformation has only been observed in the enzyme as isolated and never appeared after the enzyme was passed through a cycle of reduction and reoxidation. Perhaps a step in the isolation of the enzyme transformed a fraction of the enzyme molecules into the "resting" conformation and, thereafter, this conformation remained until the enzyme was reduced and reoxidized. In this regard, reoxidation of the reduced enzyme by ferricyanide in the absence of O_2 did not regenerate any of the "resting" conformation.

The "resting" conformation was distinguished by a high-spin cytochrome $\underline{a}_3$ EPR signal that was induced by NO only in this conformation. This high-spin cytochrome $\underline{a}_3$ EPR signal observed in the presence of NO (g = 6.16, 5.82, 2) has also been observed by Rosén et al.[12] during partial reduction of oxidized cytochrome c oxidase in the absence of NO. Rosén et al.[12] found that the conformation of the enzyme exhibiting this EPR signal did not rapidly react with O_2 when both O_2 and reductant were added to the oxidized enzyme. They concluded that this conformation was associated with the "resting" state of the enzyme. It has been observed[13] that cytochrome c oxidase can exist in two "conformations", one of which rapidly reacts with O_2 upon the simultaneous addition of both O_2 and reductant called the 'pulsed' enzyme and another which does not rapidly react with O_2 and reductant called the "resting" enzyme. In view of the observation by Rosén et al.[12] that the high-spin cytochrome $\underline{a}_3$ EPR signal with g = 6.16, 5.82, 2 is associated with the "resting" conformation, we identify the conformation that exhibits a cytochrome $\underline{a}_3$ EPR signal in the presence of NO as the "resting" conformation. It is probable that the conformation called the 'pulsed' enzyme by Antonini et al.[13] is heterogeneous, possibly including all three of the other conformations that we have identified.

The fact that NO uncouples Cu_{a_3} from cytochrome $\underline{a}_3$ in the "resting" conformation indicates that the ligand mediating the antiferromagnetic exchange interaction[14] between the two metals does not strongly influence the crystal field of Cu_{a_3}. This

allows a strong field ligand, such as NO, to reorient the crystal field of Cu_{a_3} and break the coupling between Cu_{a_3} and cytochrome $\underline{a}_3$ as shown in Figure 1. The model proposed by Chan et al.[2] for the cytochrome $\underline{a}_3$-Cu_{a_3} site, shown in Figure 1, appears to be the appropriate model for the "resting" conformation.

The question remains as to the identity of the bridging ligand, L, in the "resting" conformation. Our results indicate that this ligand is bound to cytochrome $\underline{a}_3$ less strongly than cyanide or fluoride (see Table 3). In addition, the bridging ligand, L, does not strongly influence the crystal field of Cu_{a_3}. Among the possible candidates for L are: water, hydroxyl, carboxylate, and tyrosinate. Further work, perhaps an investigation of the formation or decomposition of the "resting" conformation from/into the other conformations at high and low pH, is necessary to shed further light on the nature of the bridging ligand in the "resting" conformation.

4.3 Nature of the g' = 12 EPR Signal. We have identified the "g12" conformation by an EPR signal at g' = 12. The question remains as to the origin of this unusual EPR signal. Magnetic susceptibility measurements on oxidized cytochrome $\underline{c}$ oxidase indicate that cytochrome $\underline{a}_3$ and Cu_{a_3} together form an S = 2 site.[14] Since all the preparations of the enzyme that we have studied contained a large fraction of the enzyme molecules in the "g12" conformation (from 30-75%), it must be concluded that the g' = 12 EPR signal arises from an S = 2 state.

Griffith[15] has calculated the energy levels for an

antiferromagnetically coupled high-spin ferriheme and a cupric copper for the limits when E/D and D/J are small, where D and E are the axial and rhombic zero-field splittings and J is the isotropic superexchange interaction. These energy levels are shown in Figure 7. It is possible to observe four "allowed" transitions from an S = 2 state (solid arrows in Figure 7). However, for systems containing a high-spin heme the zero-field splitting, D, is expected to be 2 cm^{-1} or more. Since conventional EPR spectrometers are designed to operate at 2-35 GHz (0.07-1.1 cm^{-1}) with the magnetic field scanned from 0-15,000 Gauss, none of the "allowed" transitions would be observed. However, it is also possible to observe the m_s = -1 to m_s = +1 transition (dotted arrow in Figure 7). This so-called "forbidden" $\Delta m_s = 2$ transition is analogous to the half-field transition from a triplet state and is allowed for low magnetic fields when H_1 (the microwave magnetic field) is parallel to H_o (the static magnetic field).[16]

Morse[17] has extended the calculations of Griffith[15] to include cases where E/D and D/J are not small. By definition |E/D| can only vary from zero to 1/3, but there are no limits on D/J. However, the magnetic susceptibility results[14] require that $-J \geq 200\ cm^{-1}$, and the zero-field splitting induced by the high-spin heme must be larger than 2 cm^{-1}. Within these limits, it was found[17] that the only X-band EPR transition that could occur at g' = 12 was the m_s = -1 to m_s = +1 transition.

It has been observed[18] that the g' = 12 EPR signal does not disappear, while the other EPR signals do, when the microwave

FIGURE 7

The energy levels for an S = 2 state formed from the antiferromagnetic coupling of an S = 5/2 heme and an S = 1/2 copper. D and E refer to the axial and rhombic zero-field splittings and H refers to the external magnetic field. The solid lines represent $\Delta m_s = 1$ transitions and the dashed line represents the "allowed" $\Delta m_s = 2$ transition. The energy levels were calculated by Griffith.[15] The spacing between the levels is not drawn to scale.

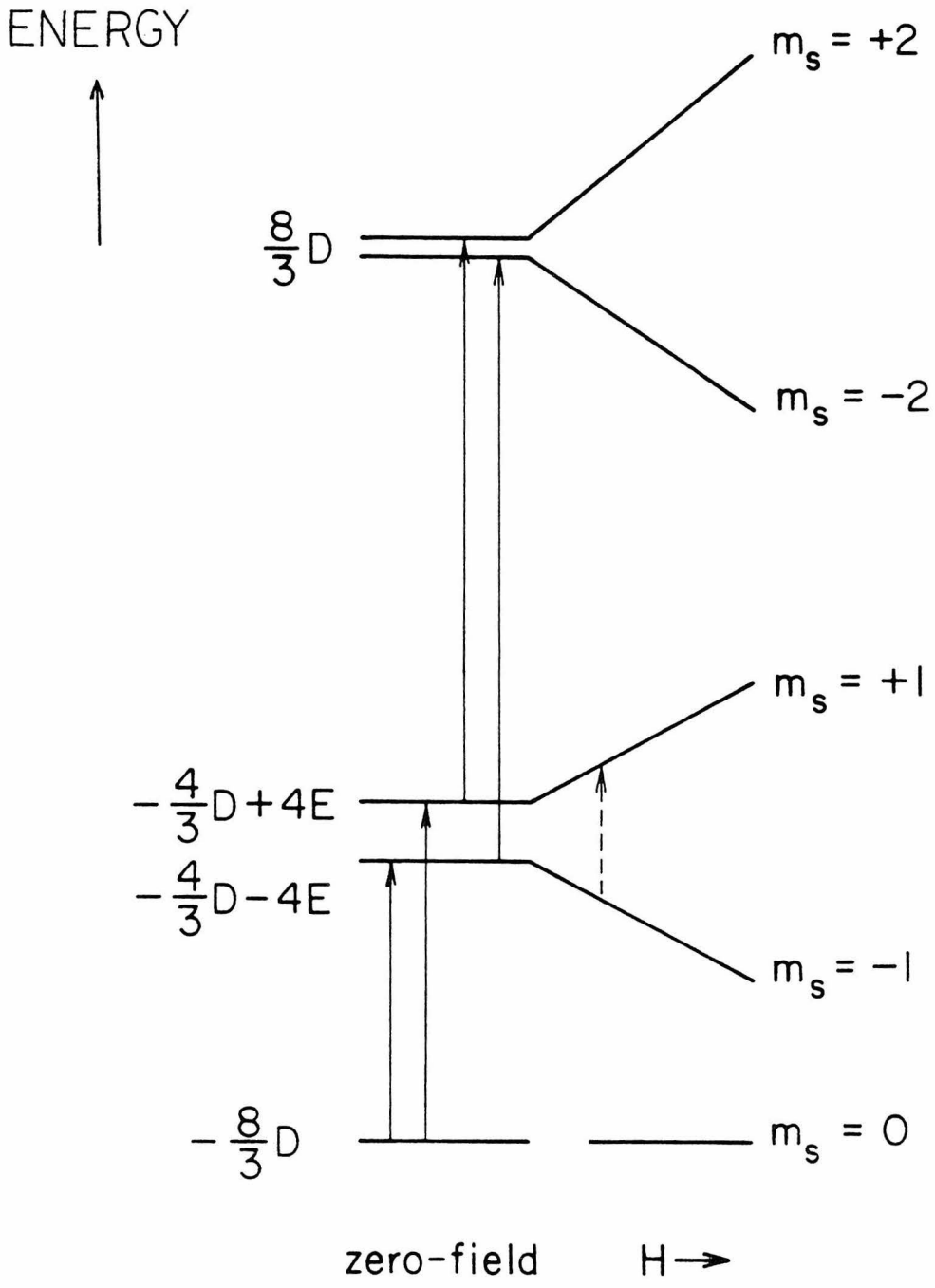
ENERGY
$m_s = +2$
$\frac{8}{3}D$
$m_s = -2$
$m_s = +1$
$-\frac{4}{3}D+4E$
$-\frac{4}{3}D-4E$
$m_s = -1$
$-\frac{8}{3}D$
$m_s = 0$
zero-field
H→

cavity is rotated in the applied magnetic field such that the microwave magnetic field, H_1, is aligned parallel to the applied magnetic field, H_o. $\Delta m_s = 1$ transitions are only allowed for $H_1 \perp H_o$. However, $\Delta m_s = 2$ transitions are allowed for $H_1 \parallel H_o$. Thus, the observation that the g' = 12 EPR signal does not disappear when the microwave cavity is rotated in the applied magnetic field to place $H_1 \parallel H_o$ is compelling evidence that the g' = 12 EPR signal arises from a $\Delta m_s = 2$ transition.

It has also been observed that the g' = 12 EPR signal observed at X-band does not occur at g = 12 when the EPR spectrum is recorded at K-band.[19] We note that the $m_s = \pm 1$ levels for an S = 2 species are split in zero-field by an energy of 8E (Figure 7). When a magnetic field is applied, the $m_s = \pm 1$ levels will be further split by an energy of $2g_e\beta H$, where g_e is the free electron g-value (it is assumed that the S = 2 state has a g-value close to the free electron g-value), β is the Bohr magneton, and H is the external magnetic field. Hence, the EPR transition will be observed when:

$$h\nu = 8E + 2g_e\beta H \qquad (2)$$

The apparent g-value, g', of the transition can be obtained by setting $h\nu = g'\beta H$. Rearranging, one obtains

$$g' = 2g_e/(1-8E/h\nu) \qquad (3)$$

At X-band (9 GHz) the transition occurs at g' = 12. Thus, E can be calculated to be 0.027 cm^{-1} from the X-band observation. However, at K-band (24 GHz) the transition will occur at g' = 5.4 and at Q-band (35 GHz) the transition will occur at g' = 4.9 for E = 0.027 cm^{-1}. Thus, the observation by Blumberg[19] that

the g' = 12 EPR signal observed at X-band changes its apparent g-value when the EPR signal is recorded at other frequencies also suggests that the g' = 12 EPR signal arises from a $\Delta m_s = 2$ transition from an S = 2 state.

4.4 "g12" Conformation. The above considerations indicate that cytochrome $\underline{a}_3$ and Cu_{a_3} together form an S = 2 site in the "g12" conformation and that cytochrome $\underline{a}_3$ has nearly axial symmetry (E is close to zero). The ligand binding properties of the "g12" conformation suggest that cytochrome $\underline{a}_3$ is six-coordinate with neither axial ligand being readily dissociable. Cyanide binds very slowly to this conformation ($t_{1/2} \approx 45$ min. when the HCN concentration is about 2 mM), while fluoride does not appear to bind at all.

Further information on the structure of the "g12" conformation is provided by the lack of effect by NO on the g' = 12 EPR signal. This result indicates that either: (i) NO does not bind to Cu_{a_3} as in Figure 1 or (ii) NO can bind to Cu_{a_3} but does not uncouple Cu_{a_3} from cytochrome $\underline{a}_3$ in the "g12" conformation. The crystal field about Cu_{a_3} is the dominant factor in determining whether or not NO can uncouple Cu_{a_3} from cytochrome $\underline{a}_3$. For example, if the ligand bridging between Cu_{a_3} and cytochrome $\underline{a}_3$ is a weak field ligand, then coordination of a strong field ligand, such as NO, to Cu_{a_3} can reorient the crystal field such that the copper $3d_{x^2-y^2}$ orbital (the orbital containing the unpaired electron for tetragonal copper) no longer is directed toward the bridging ligand (see Figure 1). In this case, NO would uncouple Cu_{a_3} from cytochrome $\underline{a}_3$. However,

if the bridging ligand is itself a reasonably strong field ligand, then the coordination of NO to Cu_{a_3} would still leave the $3d_{x^2-y^2}$ orbital of Cu_{a_3} directed toward the bridging ligand, although NO may alter the crystal field of Cu_{a_3} substantially. In this case, NO may not uncouple Cu_{a_3} from cytochrome $\underline{a}_3$.

Cyanide slowly binds to cytochrome $\underline{a}_3$ in the "g12" conformation and, once bound, the g' = 12 EPR signal is eliminated. However, no other EPR signals are observed from the cytochrome $\underline{a}_3$-Cu_{a_3} site in the presence of cyanide. This result suggests that cyanide facilitates an antiferromagnetic coupling between Cu_{a_3} and cytochrome $\underline{a}_3$ when bound. In this regard, magnetic susceptibility measurements[14] indicate that Cu_{a_3} and cytochrome $\underline{a}_3$ are antiferromagnetically coupled in the oxidized cyanide-bound enzyme with an exchange interaction of 40 cm^{-1}. The interesting observation, though, is that NO readily uncouples Cu_{a_3} from cytochrome $\underline{a}_3$ once cyanide has bound to cytochrome $\underline{a}_3$.

Consider the following situation. When cyanide binds to cytochrome $\underline{a}_3$ it replaces the ligand bridging between cytochrome $\underline{a}_3$ and Cu_{a_3} (L in Figure 1). In this configuration, the $3d_{x^2-y^2}$ orbital of Cu_{a_3} is directed toward the bridging cyanide ligand and an antiferromagnetic exchange interaction of 40 cm^{-1} is facilitated by cyanide between the two metals. Then NO coordinates to the free axial position on Cu_{a_3} and rearranges the crystal field about Cu_{a_3} such that one lobe of the $3d_{x^2-y^2}$ orbital of Cu_{a_3} now is directed toward the coordinated NO. The question then is:

which of the remaining ligands do the lobes of the Cu_{a_3} $3d_{x^2-y^2}$ orbital point toward? This will be determined by the crystal field strength of R_1 and R_3 relative to that of R_2 and the bridging cyanide (Figure 1). In the absence of exogenous ligands the $3d_{x^2-y^2}$ orbital is directed toward R_1, R_2, and R_3. Thus, these three ligands must provide a reasonably strong crystal field. However, Fe(III)-CN^- is not a particularly strong field ligand; and, hence, it is quite reasonable that the coordination of NO to the axial position of Cu_{a_3} would rearrange the crystal field about Cu_{a_3} such that the $3d_{x^2-y^2}$ orbital no longer points toward the ligand bridging between the two metals, even when the bridging ligand is cyanide. In this manner, the mechanism by which NO uncouples Cu_{a_3} from cytochrome $\underline{a}_3$ in the presence of cyanide may be understood.

The above considerations also suggest that the difference between the "g12" conformation and the "resting" conformation (Figure 1) may lie in the nature of the ligand that bridges between the two metals. For example, if the bridging ligand in the "g12" conformation: (i) is a strong field ligand of Cu_{a_3}, (ii) mediates a strong antiferromagnetic exchange interaction between the two metals, and (iii) is strongly bound to cytochrome $\underline{a}_3$ and Cu_{a_3}; whereas the bridging ligand in the "resting" conformation: (i) is a weak field ligand of Cu_{a_3} and (ii) is weakly bound to cytochrome $\underline{a}_3$, then the differences between these two conformations could be explained by a change in the ligand bridging between the two metals.

It has been suggested that a reasonable structure in which

Cu_{a_3} and cytochrome $\underline{a}_3$ can be strongly antiferromagnetically coupled with $-J > 200\ cm^{-1}$ is one in which Cu_{a_3} and cytochrome $\underline{a}_3$ are bridged by a μ-oxo ligand.[20] Such a structure is attractive because such a bridge may easily be formed upon the four electron reduction of O_2.

In view of the above considerations, we propose the model for the "g12" conformation of the oxidized enzyme shown in Figure 8. Cytochrome $\underline{a}_3$ has both axial positions occupied by strongly bound ligands in the model; and, hence, would not be expected to readily bind exogenous ligands. Furthermore, a strong antiferromagnetic exchange interaction between Cu_{a_3} and cytochrome $\underline{a}_3$ could be mediated through the μ-oxo bridge.[20]

4.5 Nature of the Fluorocytochrome $\underline{a}_3$-Cu_{a_3} EPR Signal.

When fluoride is added to the 'oxygenated' conformation, an unusual EPR signal is induced with resonances at g = 8.5, 6, 5, 4.3, and 3.2 which we have referred to as the fluorocytochrome $\underline{a}_3$-Cu_{a_3} EPR signal. This signal must arise from a state in which both cytochrome $\underline{a}_3$ and Cu_{a_3} are oxidized, since no reductant was added to the enzyme; and, moreover, the signal was immediately eliminated by NO without the appearance of any EPR signals characteristic of the partially reduced NO-bound enzyme (see chapter II, Table 2).

When two paramagnetic sites are in close proximity, it is expected that both exchange and dipolar interactions will greatly modify the EPR spectra of both sites.[21] In fact a strong exchange interaction can completely eliminate the EPR signals from either site, such as occurs when two S = 1/2

FIGURE 8

Proposed structure for the "g12" conformation. For Cu(II) in a tetragonal crystal field, as shown, the unpaired electron resides in a $3d_{x^2-y^2}$ orbital which is depicted by the lobes pointing toward the ligands in the square plane. R_1, R_2, R_3, and R_4 denote endogenous ligands.

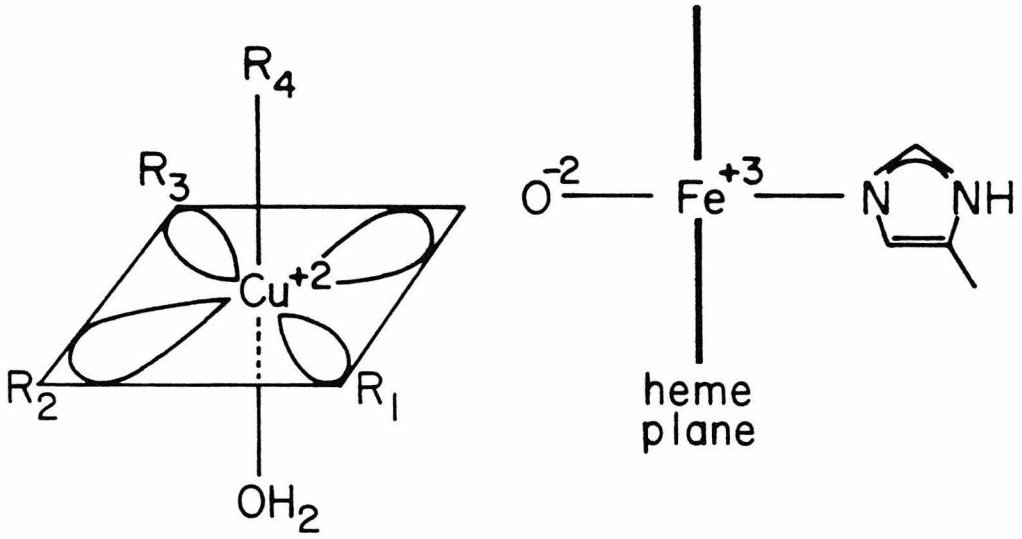

No Rapid Binding of Ligands

to Cytochrome $\underline{a}_3$

"g12" CONFORMATION

sites are strongly antiferromagnetically coupled. For cytochrome c oxidase, we have an S = 5/2 heme interacting with an S = 1/2 copper. As we described in section 4.3, Griffith[15] and Morse[17] have shown that multiple EPR resonances are not expected at X-band for a strongly antiferromagnetically coupled heme and copper. We can, therefore, conclude that the fluorocytochrome a_3-Cu_{a_3} EPR signal arises from a state in which Cu_{a_3} and cytochrome a_3 are weakly exchange and/or dipolar coupled. Thus, fluoride must largely eliminate the exchange interaction between Cu_{a_3} and cytochrome a_3 upon binding to cytochrome a_3 in the 'oxygenated' conformation.

A number of features of the fluorocytochrome a_3-Cu_{a_3} EPR signal suggest that this signal arises from a dipolar coupled S = 5/2 heme and S = 1/2 copper. The dipolar Hamiltonian is dependent on the angle between the applied magnetic field and the internuclear vector. For a powder spectrum all angles are possible. Hence, some molecules will be at the "magic" angle at which the dipolar interaction is zero. In the fluorocytochrome a_3-Cu_{a_3} EPR signal, a resonance at g = 6 was observed that was identical to the high-spin fluorocytochrome a_3 EPR signal induced by NO. This resonance could be due to those molecules near the "magic" angle. In addition, the fluorocytochrome a_3-Cu_{a_3} EPR signal has resonances at g = 8.5 and g = 5, each equally split from the g = 6 resonance, suggestive of a dipolar splitting of the fluorocytochrome a_3 EPR signal by an S = 1/2 site.

4.6 Sequence of Conformations Formed Upon Reoxidation of the Reduced Enzyme with O_2. When reduced cytochrome c oxidase is reoxidized with O_2, three conformations are sequentially formed: first, the "g5" conformation; second, the 'oxygenated' conformation; and third, the "g12" conformation. The structure that we have proposed for the "g12" conformation suggests a sequence by which these conformations can be formed upon the reaction of the reduced enzyme with O_2.

In chapter II, we proposed a mechanism for the reaction of O_2 with reduced cytochrome c oxidase. This mechanism included a Fe(IV)-oxide state when the enzyme had transferred three electrons to the coordinated O_2. The transfer of the fourth electron to this Fe(IV)-oxide site converted the enzyme into the fully oxidized enzyme. If our mechanism for the reaction of O_2 with the reduced enzyme is correct, then a series of transient states should be formed when the Fe(IV)-oxide state is reduced with another electron. 1) Initially an Fe(III)-oxide state would be formed. 2) The Fe(III)-oxide would be rapidly protonated to form an Fe(III)-hydroxyl. 3) Then a ligand, presumably water, would have to be displaced from Cu_{a_3} in forming a hydroxyl bridge between Cu_{a_3} and cytochrome a_3. 4) Finally, Cu_{a_3} and cytochrome a_3 would have to move closer together, probably mediated by the protein matrix, to form a μ-oxo bridge.

In Figure 9, we propose that the "g5", 'oxygenated', and "g12" conformations can be identified as three of the intermediates formed in sequence upon reoxidation of the reduced enzyme by O_2. An interesting point that we did not previously

FIGURE 9

Proposed sequence of states formed upon reoxidation of reduced cytochrome c oxidase by O_2. In all cases, Cu_{a_3} is proposed to have a tetragonal structure. For a tetragonal Cu(II), the unpaired electron resides in a $3d_{x^2-y^2}$ orbital which is depicted by the lobes pointing toward the ligands in the square plane. R_1, R_2, R_3, and R_4 denote endogenous ligands.

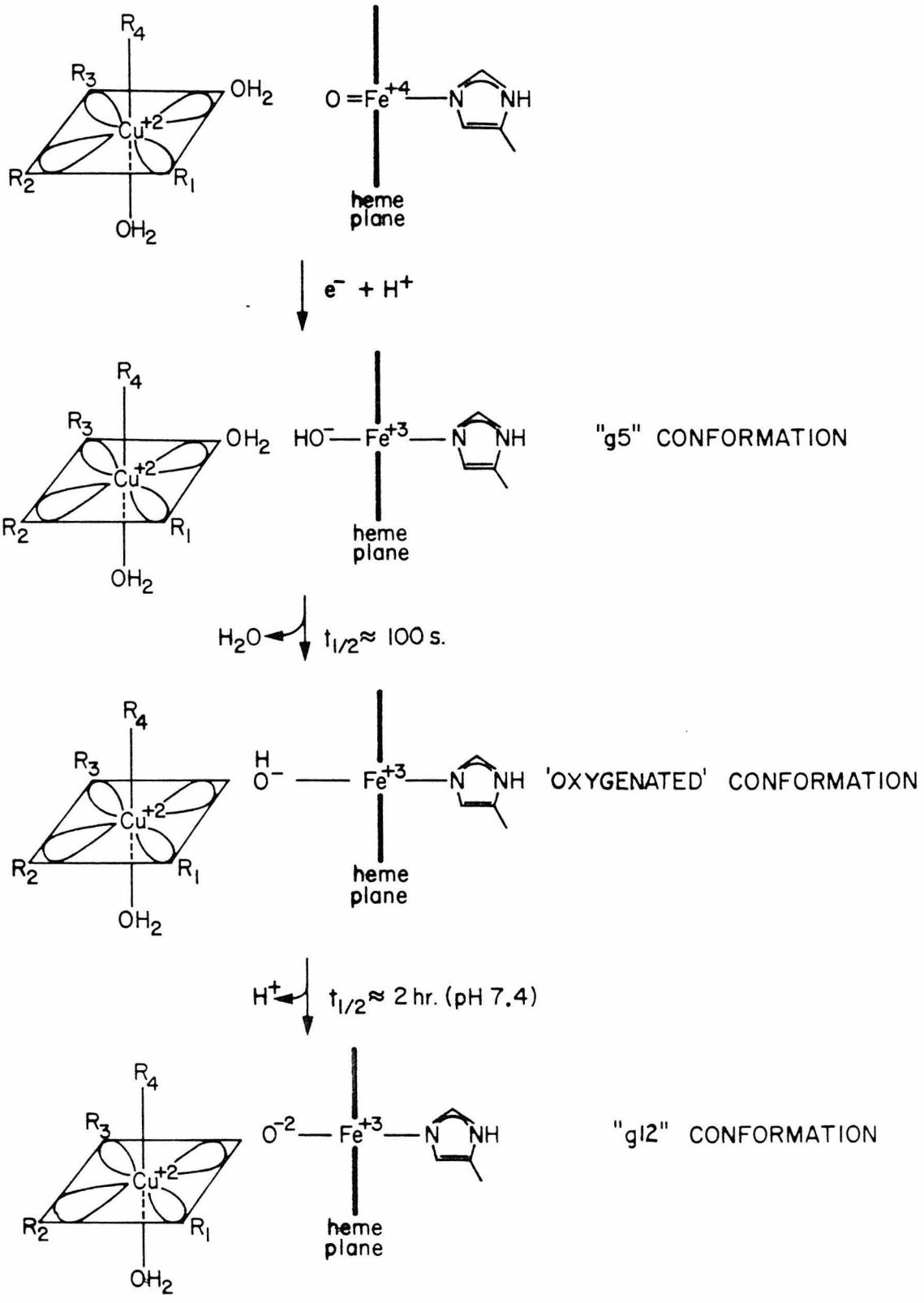
R4
R3
OH2
Cu+2
R2
R1
OH2
O=Fe+4
N
NH
heme plane
e⁻ + H⁺
HO⁻
Fe+3
"g5" CONFORMATION
H2O
t1/2≈ 100 s.
H
O⁻
'OXYGENATED' CONFORMATION
H⁺
t1/2≈ 2 hr. (pH 7.4)
O⁻²
"g12" CONFORMATION

comment on is that reoxidation of the reduced enzyme by ferricyanide rapidly formed the "g12" conformation, a result expected if intermediates in the reduction of O_2 to water are not blocking the rapid formation of a μ-oxo bridge between the metal ions.

As a final point, it is apparent that the conformations of the oxidized enzyme are different with respect to ligand binding properties and exchange coupling. It may be possible to prepare homogeneous samples of each conformation and investigate the optical spectra, MCD, and magnetic susceptibility of each conformation. In the least, the results of previous studies of these types may require reinterpretation consistent with the possibility of conformational heterogeneity within the samples.

References

1. Stevens, T.H., G.W. Brudvig, D.F. Bocian and S.I. Chan (1979), Proc. Natl. Acad. Sci. USA 76, 3320.
2. Chan, S.I., T.H. Stevens, G.W. Brudvig and D.F. Bocian, in "Proceedings of the International Symposium on Frontiers in Protein Chemistry", (T. Liu, K.T. Yasunobu and G. Mamiya, eds.), Elsevier, Amsterdam, in press.
3. Hartzell, C.R. and H. Beinert (1974), Biochim. Biophys. Acta 368, 318.
4. Yu, C., L. Yu and T.E. King (1975), J. Biol. Chem. 250, 1383.
5. Muijsers, A.O., R.H. Tiesjema and B.F. Van Gelder (1971), Biochim. Biophys. Acta 234, 481.
6. Aasa, R., S.P.J. Albracht, K.E. Falk, B. Lanne and T. Vänngård (1976), Biochim. Biophys. Acta 422, 260.
7. Aasa, R. and T. Vänngård (1975), J. Magn. Reson. 19, 308.
8. DeVries, S. and S.P.J. Albracht (1979), Biochim. Biophys. Acta 546, 334.
9. Greenaway, F.T., S.H.P. Chan and G. Vincow (1977), Biochim. Biophys. Acta 490, 62.
10. Scholes, C.P., R.A. Isacson and G. Feher (1971), Biochim. Biophys. Acta 244, 206.
11. Shaw, R.W., R.E. Hansen and H. Beinert (1978), J. Biol. Chem. 253, 6637.
12. Rosén, S., R. Brändén, T. Vänngård and B.G. Malmström (1977), FEBS Lett. 74, 25.

13. Antonini, E., M. Brunori, A. Colosimo, C. Greenwood and M.T. Wilson (1977), Proc. Natl. Acad. Sci. USA 74, 3128.

14. Tweedle, M.F., L.J. Wilson, L. Garćia-Iñiguez, G.T. Babcock and G. Palmer (1978), J. Biol. Chem. 253, 8065.

15. Griffith, J.S. (1971), J. Mol. Phys. 21, 141.

16. Wertz, J.E. and J.R. Bolton (1972), "Electron Spin Resonance", McGraw-Hill, N.Y., p. 242.

17. Morse, R.H., personal communication.

18. Leigh, J.S., Jr., personal communication.

19. Blumberg, W.E. (1979), International Conference on Copper-Containing Proteins, Villa Giulia, Manziana, Italy.

20. Blumberg, W.E. and J. Peisach (1979), in "Cytochrome Oxidase", (T.E. King, Y. Orii, B. Chance and K. Okunuki, eds.), Elsevier, Amsterdam, p. 153.

21. Smith, T.D. and J.R. Pilbrow (1974), Coord. Chem. Rev. 13, 173.

CHAPTER IV: NATURE OF Cu_a

1. INTRODUCTION

When EPR spectra were first recorded from cytochrome c oxidase, it was recognized that only one of the two coppers in the enzyme exhibited an EPR signal.[1,2] The observed EPR spectrum was not like those normally observed for Cu(II), however, and a number of explanations were forwarded. These included the proposal of an interaction between the two copper atoms in the enzyme rendering a site with unusual EPR characteristics and only one-half the expected EPR intensity of two coppers.[1] Subsequently it was shown[3,4] that the EPR "visible" copper was an isolated S = 1/2 site. Thus, the unusual EPR spectrum of the EPR "visible" copper (which will be referred to as the Cu_a center) should be explained on the basis of the geometry and/or ligation of an isolated copper ion. A considerable interest in the structure of the Cu_a center has derived from efforts to explain the unusual EPR properties of this site.

The EPR signal from the Cu_a center is atypical of Cu(II) in that no copper hyperfine splittings are clearly resolved and the g-values are quite small; in fact one g-value is below that of the free electron. Only two mechanisms, consistent with an isolated copper site, can be invoked to explain the unusual EPR properties. One possibility is that the unpaired electron spin resides primarily on an associated ligand.[5-8] This mechanism calls for extensive charge delocalization from the involved associated ligand onto the copper ion. The g-values

for the Cu_a center are, in fact, typical of those in thiyl radicals and it has been suggested that the Cu_a center EPR signal might be due to a disulfide interacting with a copper ion[8] or due to a sulfur radical.[5] A second possibility is that the orbital containing the unpaired electron is a hybrid 3d copper orbital with strong admixtures of 4s and 4p character.[9,10] In this case, the unpaired electron would reside primarily on the copper. The unusual EPR properties would result from distorting the copper into a near tetrahedral geometry which allows mixing of copper 4s and 4p orbitals with the 3d ground state. These points will be discussed further in section 3.2.

With regard to the second possibility, a class of copper proteins is known in which the copper ion is forced into a distorted tetrahedral geometry. These copper sites are referred to as type 1 or "blue" coppers and have been extensively studied because these coppers also exhibit unusual properties.[11] In particular, the EPR spectra of type 1 coppers are unusual in that the copper hyperfine interaction is considerably reduced from that normally observed from Cu(II) complexes, although the g-values are normal. The optical spectrum, from which the name "blue" copper originated, also is unusual in that a very strong charge transfer absorption ($\varepsilon \approx 5000\ \underline{M}^{-1}cm^{-1}$) is observed near 600 nm. Normally Cu(II) has only very weak optical bands in the visible spectrum.

The Cu_a center in cytochrome *c* oxidase has been associated with the type 1 coppers for two reasons. First, the EPR

spectrum of the Cu_a center superficially resembles that of type 1 coppers; secondly, cytochrome c oxidase has a very intense absorption near 600 nm part of which part has been believed to be due to copper.[12,13] Therefore, if the unusual EPR properties of the Cu_a center result from a distortion of the copper ion into a near tetrahedral geometry that allows mixing of 3d, 4s, and 4p orbitals, then type 1 coppers may be appropriate models for the Cu_a center.

A number of studies have been carried out in which the Cu_a center has been compared to type 1 coppers. The EPR parameters of the Cu_a center were compared to those of the type 1 coppers.[5] It was found that the type 1 coppers fell within a well defined region in a plot of A_{11} versus g_{11}, whereas the Cu_a parameters were markedly different.

X-ray absorption studies[14,15] indicate that one of the coppers in oxidized cytochrome c oxidase is in a highly covalent environment. The use of mixed valence states of the enzyme has allowed the highly covalent copper to be assigned to the Cu_a center.[15] Comparison of the x-ray absorption data on the Cu_a center with that from the type 1 coppers plastocyanin[14] and stellacyanin[15] has shown that the type 1 coppers do not closely resemble the Cu_a center. In particular, the x-ray absorption edge studies indicate that the type 1 copper in plastocyanin is in the cupric oxidation state when oxidized and in the cuprous oxidation state when reduced. However, the x-ray absorption edge of the Cu_a center does not change substantially upon reduction; in both the oxidized and reduced

states the Cu_a center appears as either a highly covalent Cu(II) or a Cu(I).

These results indicate that the Cu_a center does not closely resemble the type 1 coppers. Hence, the unusual EPR properties of the Cu_a center may not necessarily derive from merely forcing a copper ion into a near tetrahedral geometry as required for mixing of copper 3d, 4s, and 4p orbitals. Furthermore, the x-ray absorption results are supportive of the model in which the unusual EPR properties of the Cu_a center arise from delocalization of unpaired electron spin density onto an associated ligand. In this case the copper should appear to be cuprous in both the oxidized and reduced states, as was observed.

We have undertaken further experiments to distinguish whether or not the unusual EPR properties of the Cu_a center arise from delocalization of unpaired electron spin density onto an associated ligand. The EPR spectrum of the Cu_a center is similar to that of sulfur radicals. On this basis, it may be expected that sulfhydryl binding reagents such as Ag^+ and Hg^{+2} would disrupt the Cu_a center. In section 3.1, we investigate the effect of Ag^+, Hg^{+2}, and p-HMB on the EPR and optical spectra of cytochrome c oxidase and also the type 1 copper in plastocyanin.

The available data on the g-values and the magnitude of the copper hyperfine parameters of the Cu_a center are discussed in section 3.2 and used to calculate the relative amounts of 3d and 4p character in the orbital containing the unpaired

electron necessary to obtain the observed EPR properties of the Cu_a center. These calculations and the results of the Ag^+ binding experiments are used to formulate a model for the Cu_a center which is presented in section 4. Finally, the available physical data on the Cu_a center are interpreted in terms of this model.

2. MATERIALS AND METHODS

Cytochrome c oxidase was isolated by the method of Hartzell and Beinert[16] and was dissolved in 50 mM Tris/HNO_3, 0.5% Tween 20, pH 7.4. French bean plastocyanin was a gift of Professor H.B. Gray and was dissolved in 50 mM Tris/HNO_3, pH 7.4. The enzyme samples were dialyzed three times against one liter of 50 mM Tris/HNO_3, pH 7.4 to remove ions or molecules that bind Ag^+ or Hg^{+2} such as halides, phosphate, or cholate. The concentration of cytochrome c oxidase was determined by the pyridine hemochromagen assay [17] and that of plastocyanin was determined optically[18] at 597 nm using $\varepsilon = 4500\ \underline{M}^{-1}cm^{-1}$.

Two types of Ag^+ binding experiments were performed: (i) the direct addition of a solution of Ag^+ or Hg^{+2} to the enzyme sample followed by the monitoring of optical changes with time of incubation; and (ii) the addition of Ag^+ to the enzyme sample by dialysis followed by measurement of the EPR spectrum or activity.

In the first experiment, solutions of $AgNO_3$ or $HgCl_2$ were added to the enzyme samples to yield a final Ag^+ or Hg^{+2} concentration that was 10-fold greater than the enzyme concentration.

For cytochrome c oxidase and plastocyanin the enzyme concentration was based on 2 heme a/enzyme and 1 copper/enzyme, respectively. The entire optical spectrum was immediately recorded and, thereafter, the absorbance change at 598 nm was monitored with time. After six hours, the entire optical spectrum was recorded and the samples were placed in EPR tubes and frozen at -80°C.

For the addition of Ag^+ by dialysis, 0.2 ml samples of cytochrome c oxidase were placed in a dialysis bag and dialyzed against a solution of $AgNO_3$ dissolved in the same buffer as the protein. Ag^+ was added by dialysis to assure that a constant concentration of Ag^+ was maintained and to avoid precipitation of the enzyme which occurred when $AgNO_3$ was directly added to concentrated samples of cytochrome c oxidase. Control samples were prepared as above except KNO_3 was substituted for $AgNO_3$. Individual samples of cytochrome c oxidase were removed at various times and their activity was measured immediately. An aliquot of the sample was then removed for a protein assay and the remainder of the sample was placed in an EPR tube and frozen at -80°C.

EPR spectra were recorded on a Varian E-line century series X-band spectrometer equipped with an Air Products Heli-Trans low temperature system. The method of Aasa and Vänngård[19] was used to integrate the overlapping copper EPR signals. Optical spectra were recorded at room temperature on a Beckman Acta CIII or a Cary 17 spectrometer.

3. RESULTS

3.1 Ag^+ Titrations. The direct addition of 0.25 mM Ag^+ or 0.25 mM Hg^{+2} to 0.025 mM oxidized cytochrome c oxidase[21] did not cause the 598 nm band of the enzyme to be significantly reduced in intensity (Figure 1). We observed a slight decrease in A_{598} of 0.006 upon the addition of Ag^+ and 0.018 upon the addition of Hg^{+2} to the enzyme. However, small changes also occurred throughout the spectrum from 450-750 nm (Figure 2), and these small optical changes are most likely due to a perturbation of the hemes by Ag^+ and Hg^{+2}. Optical measurements could not be made at times longer than ~6 hrs. because cytochrome c oxidase began aggregating and the sample became increasingly cloudy.

We also repeated the experiments of Katoh and Takamiya[20] on the effect of Ag^+ and Hg^{+2} on plastocyanin (a type 1 copper protein). Our results confirm that Ag^+ and Hg^{+2} do bleach the absorption at 597 nm in this enzyme (Figure 1).

These experiments demonstrate that Cu_a either is not a type 1 copper or is not accessible to Ag^+ or Hg^{+2} during the 6 hr. incubation of the enzyme. A further conclusion is that Cu_{a_3} cannot be a type 1 copper, as has been suggested.[15] Since Cu_{a_3} is known to bind exogenous ligands[22] and is presumably directly accessible to the solvent, we should have observed a large decrease in A_{598} when Ag^+ or Hg^{+2} were added to cytochrome c oxidase, if Cu_{a_3} were a type 1 copper ($\Delta A = 0.12$ for $\Delta\varepsilon = 4500\ \underline{M}^{-1}cm^{-1}$).

FIGURE 1

Changes in absorbance at 598 nm with time upon incubation of cytochrome c oxidase and plastocyanin with Ag^{+}, Hg^{+2}, or alone. The concentration of cytochrome c oxidase in these experiments was 2.5×10^{-5} M (based on 2 heme a/enzyme) and that of French bean plastocyanin was 8.3×10^{-5} M.

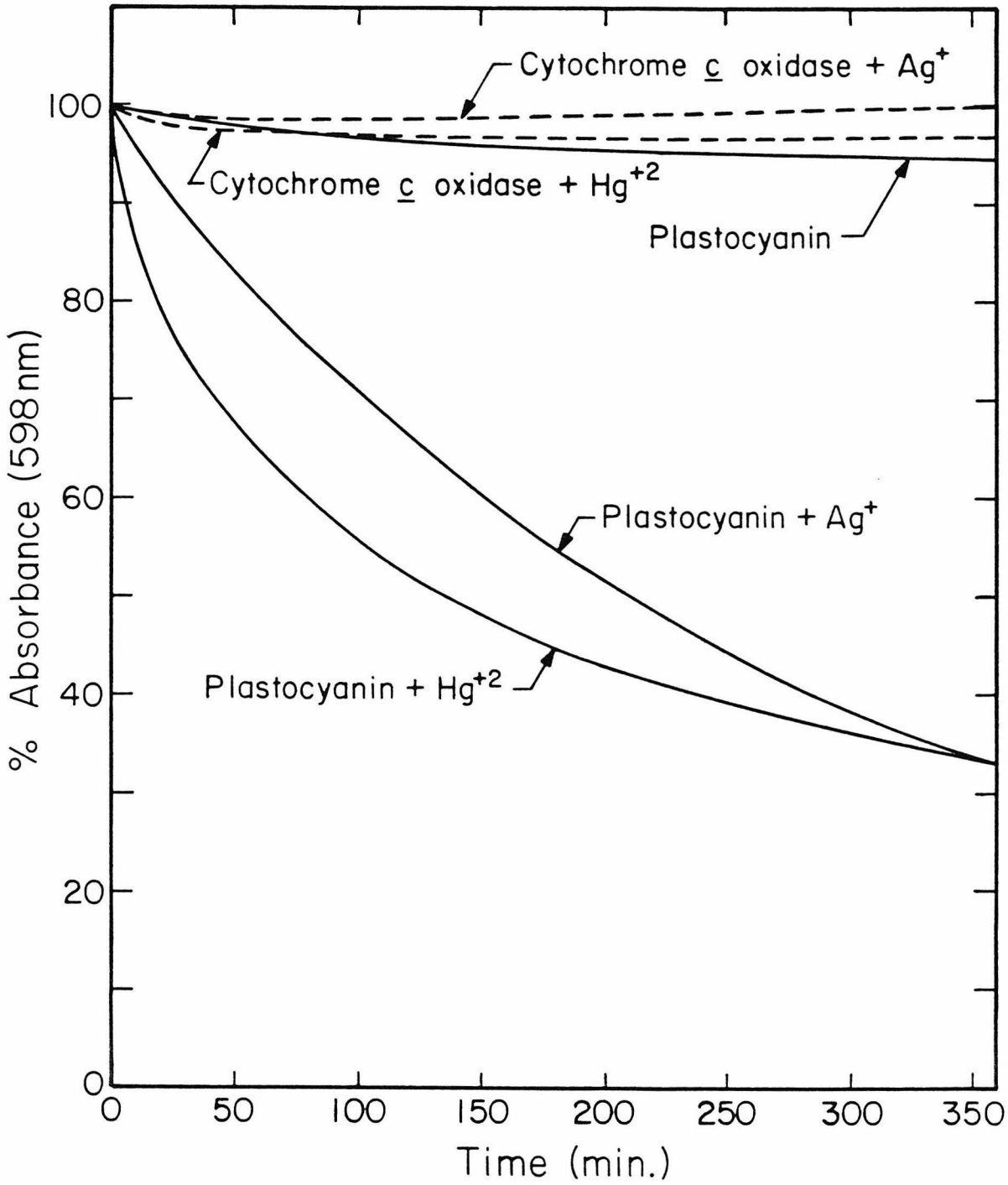
Cytochrome c oxidase + Ag+
Cytochrome c oxidase + Hg+2
Plastocyanin
Plastocyanin + Ag+
Plastocyanin + Hg+2
% Absorbance (598nm)
Time (min.)
0
20
40
60
80
100
0
50
100
150
200
250
300
350

FIGURE 2

Absorption spectra of oxidized cytochrome c oxidase before (——) and after (----) incubation of the enzyme for 6 hr. with $HgCl_2$.

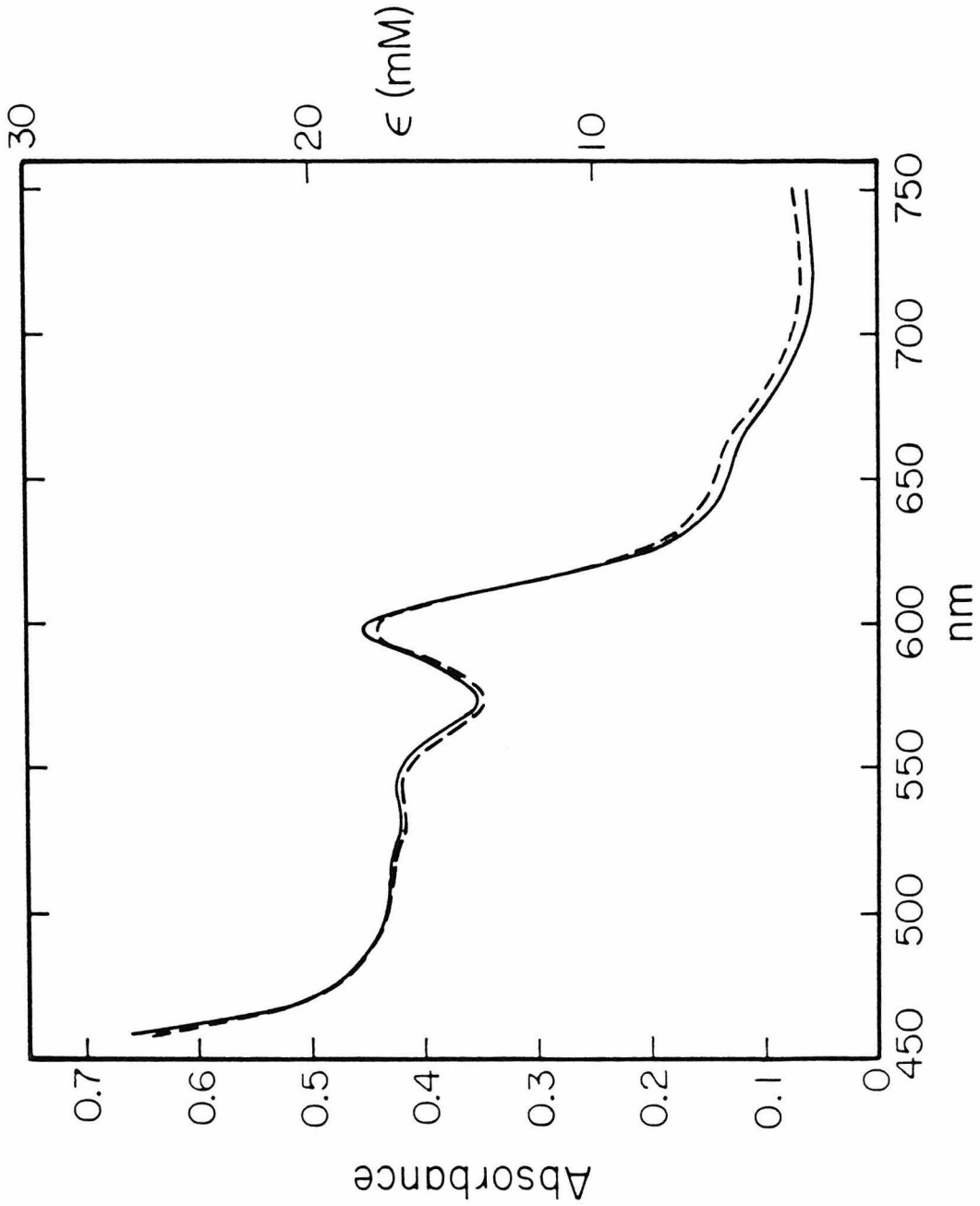
30
20
10
ε (mM)
0.7
0.6
0.5
0.4
0.3
0.2
0.1
0
Absorbance
450
500
550
600
650
700
750
nm

Cu_a does not bind exogenous ligands, so the question remains as to whether Ag^+ or Hg^{+2} could reach the Cu_a center during the 6 hr. incubation of the enzyme. To investigate this possibility we examined the EPR spectra of samples of 0.07 mM cytochrome c oxidase to which 0.07 or 0.7 mM Ag^+ was added by dialysis. We found that dialysis of the enzyme against Ag^+ for several days resulted in the appearance of a normal Cu(II) EPR signal (Figure 3), and a concomitant decrease in the activity of the enzyme (Figure 4). In contrast, the addition of p-HMB to the enzyme produced no change in the EPR spectrum of the Cu_a center or in the enzymatic activity, even after long exposure. This suggests that Ag^+ binds a sulfhydryl group which is inaccessible to p-HMB, and is essential to the integrity of the Cu_a center.

The dialysis of cytochrome c oxidase against Ag^+ resulted in a biphasic decrease in the enzyme's activity which can be fitted to the sum of two exponentials. A scheme such as that shown below will result in the observed activity decrease.

$$A \xrightarrow{K_1} B \xrightarrow{K_2} C$$

Here A represents native cytochrome c oxidase; B, a less active state of the enzyme which is rapidly formed upon the addition of Ag^+; and C, an inactive state which is formed very slowly.

The initial rapid loss of activity is dependent on the Ag^+ concentration and probably is due to a Ag^+ induced aggregation of the protein. Indeed, it has been observed that the activity of cytochrome c oxidase is dependent on the state of

FIGURE 3

EPR spectra of native cytochrome c oxidase (top), cytochrome c oxidase dialyzed against a 10-fold excess of Ag^+ for 7 days at 4°C (middle), and the hyperfine structure in the $g_\perp$ region of the Ag^+-transformed species (bottom). Conditions: temperature, 10K; microwave power, 0.2 mW; modulation amplitude, 8G; and microwave frequency, 9.16 GHz.

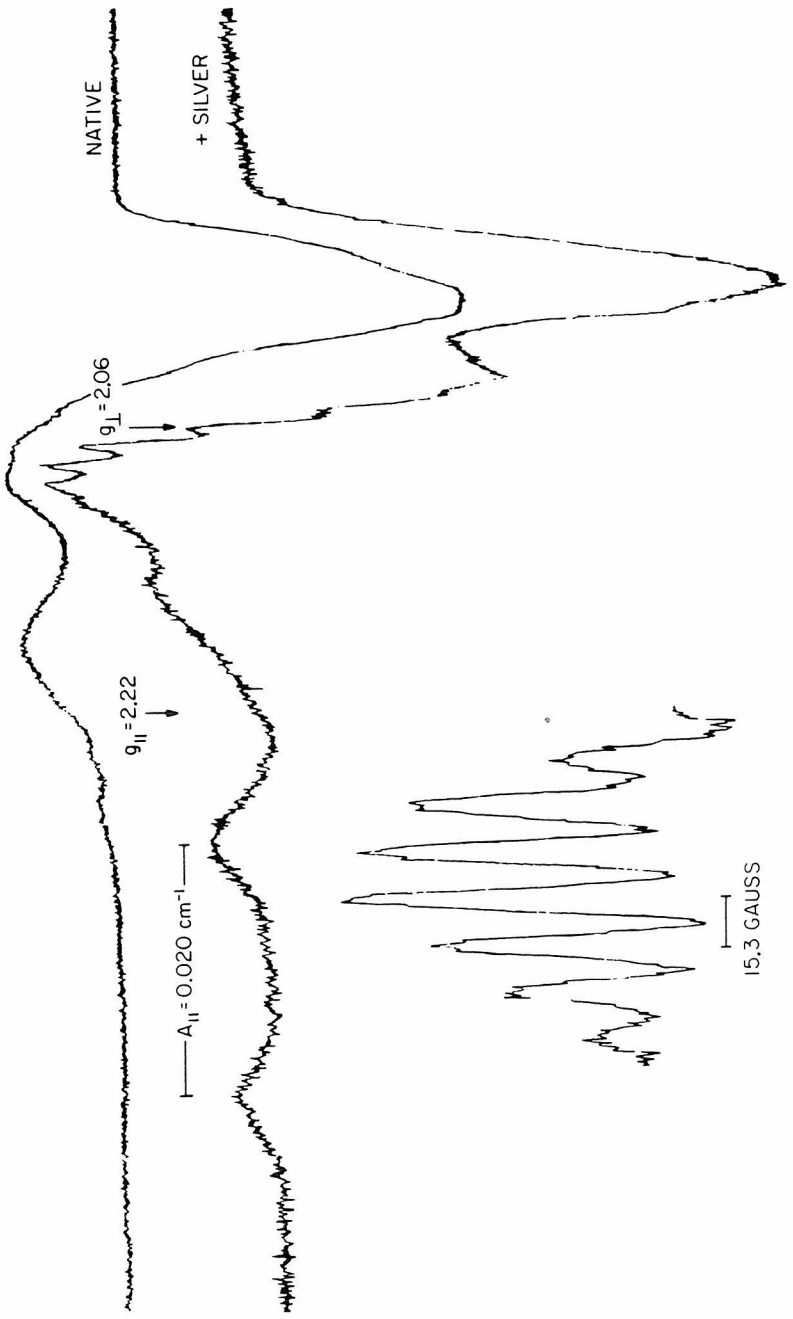

CYTOCHROME OXIDASE

FIGURE 4

The activity of cytochrome c oxidase and the EPR intensity of the native Cu_a center during dialysis against Ag^+. The concentration of the enzyme was 7.2×10^{-5} M (assuming 2 heme a/enzyme). The activity points are the average of three measurements and the error is estimated to be ±20%. The EPR intensity points are the average of two samples and the error is estimated to be ±10%. Conditions for activity assay: temperature, 30.0°C; reaction medium, 50 mM phosphate, 0.2 mg/ml cytochrome c, 3 mM ascorbate, pH 7.4. Conditions for EPR: temperature, 10K; microwave power, 0.2 mW; modulation amplitude, 10G; microwave frequency, 9.16 GHz.

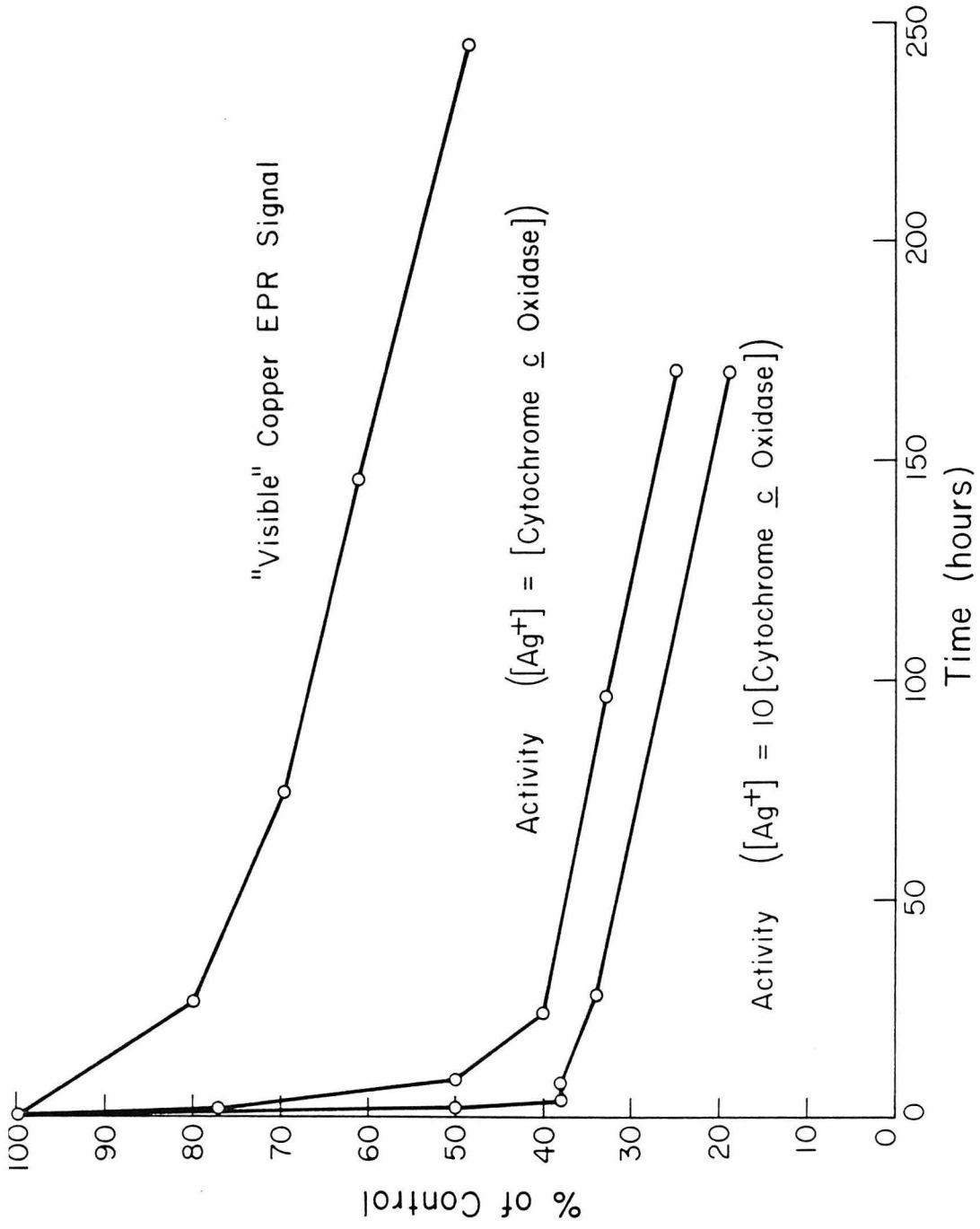
"Visible" Copper EPR Signal
Activity ([Ag+] = [Cytochrome c Oxidase])
Activity ([Ag+] = 10[Cytochrome c Oxidase])
% of Control
Time (hours)
100
90
80
70
60
50
40
30
20
10
0
0
50
100
150
200
250

aggregation of the enzyme;[23] the enzyme is much less active when not well dispersed. However, the rate of protein aggregation in our experiments depends on a number of factors including the rate at which Ag^+ diffuses across the dialysis membrane as well as the number of binding sites on the protein. Thus the kinetics of the initial rapid loss of activity are complex.

Cytochrome c oxidase has a pI of 4-5 which indicates that an excess of negatively charged groups was present under the conditions of our experiments[24] (pH 7.4). The binding of Ag^+ to these negatively charged groups (carboxyl and histidinyl amino acid functional groups and phosphate from associated phospholipids) would reduce the electrostatic repulsion between protein molecules and lead to protein aggregation. Over the range of Ag^+ concentrations examined (0.7-0.07 mM), the binding of Ag^+ to carboxyl and phosphate groups would be concentration dependent. At the higher Ag^+ concentrations more Ag^+ ions would be bound per protein molecule and consequently larger protein aggregates would be formed. Thus we expect the activity of state B to depend on the Ag^+ concentration, and this was observed.

The slow loss of activity observed at long times when cytochrome c oxidase was dialyzed against Ag^+ occurred at a rate which was equal to the rate of disappearance of the Cu_a center EPR signal (Figure 4). This step occurred at a rate which was independent of the Ag^+ concentration over the range of 0.7-0.07 mM with a first-order rate constant $K_2 = 0.003\ hr^{-1}$. Since the EPR signal of the Cu_a center disappeared at the same rate as the loss of activity, it appears that this slow step

was a disruption of the Cu_a center by Ag^+ which produced an inactive enzyme.

As the native Cu_a center EPR signal disappeared, a normal Cu(II) EPR signal appeared with no change in the total EPR intensity of the copper signals. This normal Cu(II) EPR signal exhibited superhyperfine structure in the $g_\perp$ region due to three nitrogens (Figure 3, bottom). This result suggests that in the native enzyme Cu_a is ligated to one or more nitrogens.

The effect of Ag^+ on the Cu_a center EPR signal can be compared to the effect of Ag^+ on the EPR signal from the type 1 copper in plastocyanin. We found that the type 1 copper EPR signal was also disrupted by Ag^+ and was transformed into a normal Cu(II) EPR signal (Figure 5). The Ag^+-transformed EPR signal from plastocyanin is very similar to the Ag^+-transformed signal from Cu_a. The EPR parameters for the two Ag^+-transformed species were: $g_{11}=2.22$, $g_\perp \approx 2.06$, $A_{11}=0.020$ cm^{-1} for the Cu_a center and $g_{11}=2.22$, $g_\perp \approx 2.04$, $A_{11}=0.019$ cm^{-1} for plastocyanin. On this basis, it may be argued that the binding site of Cu_a bears some resemblance to the type 1 copper binding site in plastocyanin.

Returning now to our optical experiments, it appears that Ag^+ could not have significantly disrupted the Cu_a center within the 6 hr. optical measurement. Therefore, the question of whether or not the Cu_a center contributes to the optical spectrum of cytochrome c oxidase cannot be answered from our Ag^+ binding experiments. However, recent resonance Raman results[25] indicate that neither copper in cytochrome c oxidase contributes

FIGURE 5

EPR spectra of native plastocyanin (top) and plastocyanin incubated with 8.3×10^{-4} M Ag^{+} for 6 hr. at 20°C (bottom). The concentration of plastocyanin was 0.5 mM (top) and 8.3×10^{-5} M (bottom). Conditions: temperature, 77K; microwave power, 10 mW; modulation amplitude, 10G; microwave frequency, 9.24 GHz. The peak labeled with an asterisk in the bottom spectrum is from native plastocyanin.

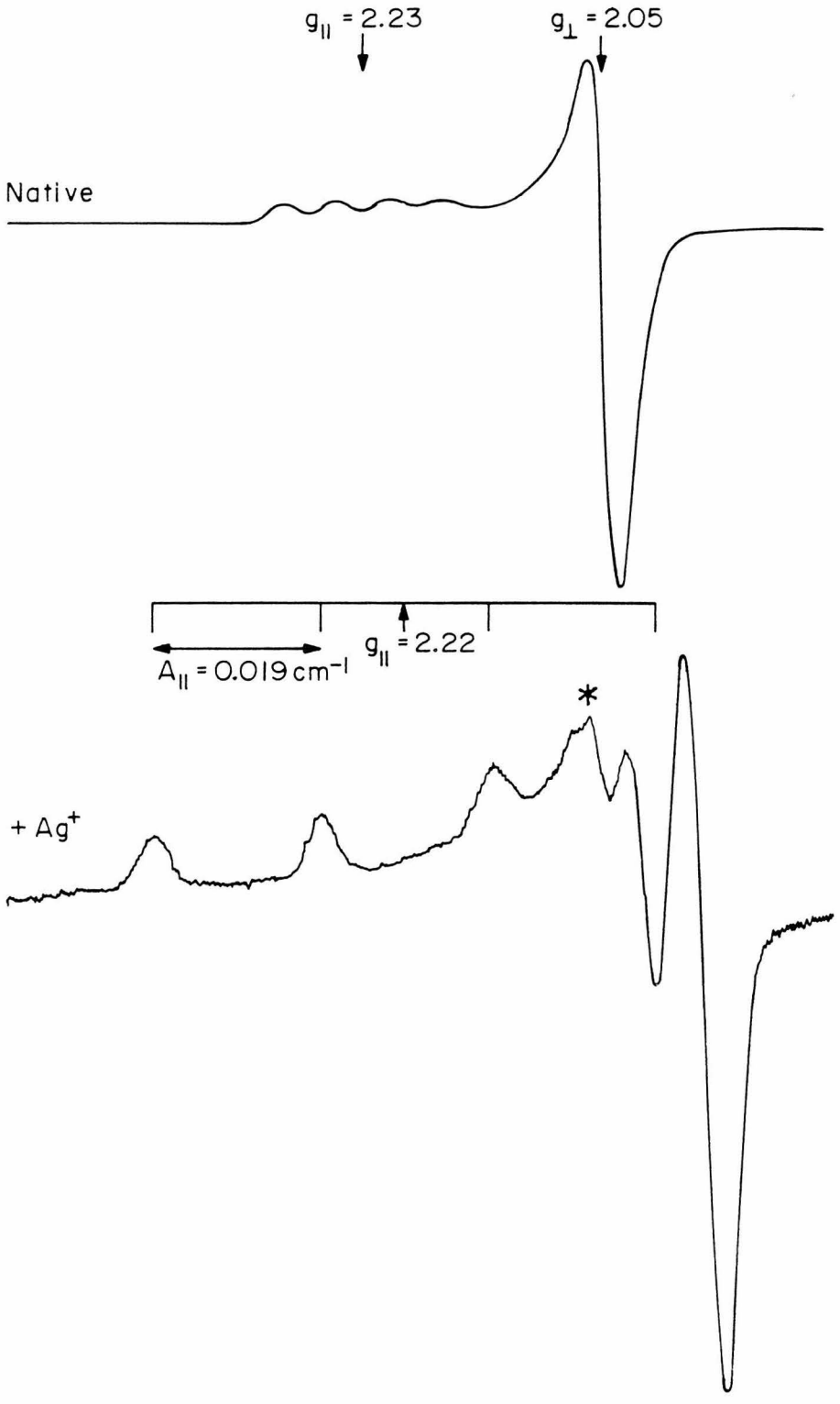

Plastocyanin

a significant amount to the absorbance at 600 nm. This result demonstrates that Cu_a cannot be a type 1 copper, although our Ag^+ binding experiments indicate that the Cu_a binding site bears some resemblance to the type 1 copper binding site.

3.2 Analysis of the Cu_a Center EPR Signal. (1) g-values. Among copper proteins two types of EPR signals have been observed. Type 2 coppers exhibit EPR signals similar to those of tetragonal inorganic Cu(II) complexes. Type 1 coppers, on the other hand, exhibit EPR signals with normal g-values but with a reduced copper hyperfine splitting. The Cu_a center exhibits an EPR signal unlike either type 1 or type 2 copper in that both the g-values and copper hyperfine splitting are reduced from those normally observed for Cu(II).

It is possible to calculate the g-values for Cu(II) in either a tetragonal or a tetragonally distorted tetrahedral geometry.[26] The calculated g-values are:

tetragonal (elongation along z)

$$g_{11} = g_e - \frac{8\lambda}{\Delta_1} \quad (1)$$

$$g_{\perp} = g_e - \frac{2\lambda}{\Delta_2} \quad (2)$$

tetragonal (compressed along z)

$$g_{11} = g_e \quad (3)$$

$$g_{\perp} = g_e - \frac{6\lambda}{\Delta_3} \quad (4)$$

tetrahedral (compressed along z)

$$\begin{cases} g_{11} = g_e - \frac{8\lambda}{\Delta_4} & (5) \\ g_\perp = g_e - \frac{2\lambda}{\Delta_5} & (6) \end{cases}$$

where Δ_1, Δ_2, Δ_3, Δ_4, and Δ_5 are the crystal field splittings defined in Figure 6, and λ is the spin-orbit coupling parameter. For the free Cu(II) ion $\lambda = -830\ cm^{-1}$. However, in cases where the crystal field splittings of inorganic Cu(II) complexes have been measured, calculation of the g-values based on the spin-orbit coupling parameter from the free ion leads to too large a g-anisotropy.[27] The conclusion is that covalency leads to delocalization of some unpaired spin density onto the ligands. Such covalency reduces the effective spin-orbit coupling parameter of copper, since nitrogen or oxygen ligands do not contribute significantly to the spin-orbit coupling. Provided that the value of λ is adjusted to account for covalency effects, good agreement is obtained between the g-values predicted from crystal field splittings and the g-values observed for a wide range of Cu(II) complexes coordinated to nitrogen and/or oxygen ligands.

For complexes in which Cu(II) is ligated to sulfur, formulas (1)-(6) do not necessarily allow a good fit to the observed g-values when the crystal field splitting are known and the spin-orbit coupling is decreased appropriately. For example, the EPR spectrum[11] and the crystal field splittings[28]

FIGURE 6

Energy levels of $3d^9$ states. The energy increases toward the top of the page, but the separation of the states is not drawn to scale.

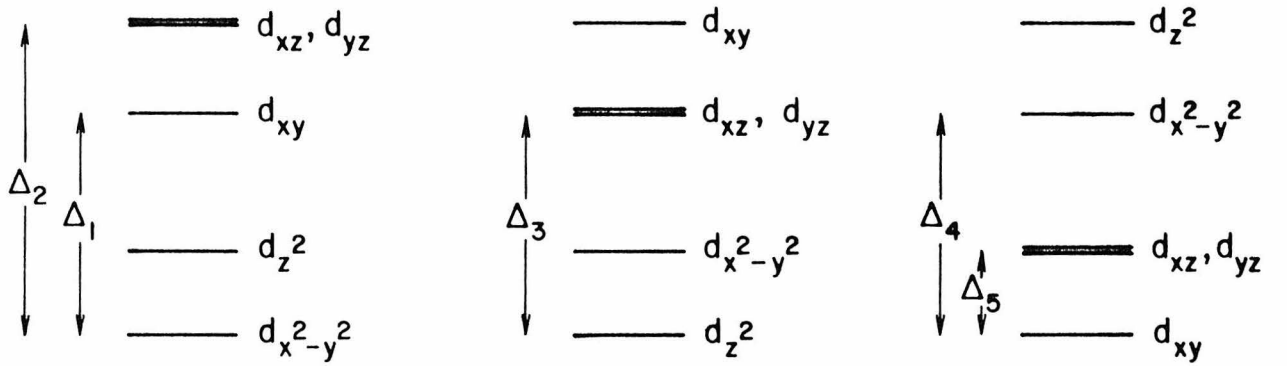
d_{xz}, d_{yz}
d_{xy}
Δ_2
Δ_1
d_z^2
$d_{x^2-y^2}$
tetragonal
(elongation along z)
d_{xy}
d_{xz}, d_{yz}
Δ_3
$d_{x^2-y^2}$
d_z^2
tetragonal
(compression along z)
d_z^2
$d_{x^2-y^2}$
Δ_4
Δ_5
d_{xz}, d_{yz}
d_{xy}
tetrahedral
(compression along z)

for the type 1 copper in plastocyanin have been measured. In this case Cu(II) is ligated to one cysteine sulfur, one methione sulfur, and two histidine nitrogens in a flattened tetrahedral geometry.[29] For such a geometry, either formulas (1) and (2) or (5) and (6) are appropriate, depending on the degree of distortion from a tetrahedral geometry. According to Solomon et al.,[28] the ground state of the Cu(II) in plastocyanin is $d_{x^2-y^2}$ and, hence, formulas (1) and (2) will be used to calculate the g-values. Using[28] Δ_1=10,300 cm^{-1}, Δ_2 = 5500 cm^{-1}, and λ = -290 cm^{-1} (λ was chosen to fit g_{11}), the g-values are predicted to be g_{11} = 2.23 and $g_\perp$ = 2.11. These can be compared to the observed g-values of g_{11} = 2.23 and $g_\perp$ = 2.05. The discrepancy in $g_\perp$ can be attributed to the delocalization of some unpaired spin density onto a sulfur.

Since sulfur itself has a significant spin-orbit coupling, new terms involving the spin-orbit coupling of sulfur must be added to formulas (1) and (2) to provide a good fit between the observed and calculated g-values of Cu(II) ligated to sulfur. The corrections to formulas (1) and (2) are:

tetragonal (elongation along z) (with sulfur ligands)

$$g_{11} = g_e - \frac{8\lambda}{\Delta_1} + f(\lambda_s) \qquad (7)$$

$$g_\perp = g_e - \frac{2\lambda}{\Delta_2} + f'(\lambda_s) \qquad (8)$$

where λ is the spin-orbit coupling of copper, λ_s is the spin-orbit coupling of sulfur and Δ_1 and Δ_2 are the same as in

equations (1) and (2). Analogous correction terms also should be added to equations (3) - (6). When a large fraction of the unpaired electron is localized on a sulfur ligand, as may be the case for the Cu_a center, the $f(\lambda_s)$ term can become larger than the copper spin-orbit coupling term. In this case it is most appropriate to describe the system as a Cu(I)-sulfur radical site.

A point which we wish to emphasize here is that Cu(II) complexes always exhibit g-values greater than or equal to the free electron g-value because λ is negative for a $3d^9$ system. In order to observe g-values less than the free electron g-value, such as is observed for the Cu_a center, it is necessary to mix an orbital with a positive spin-orbit coupling with the 3d orbital containing the unpaired electron. There are only two reasonable possibilities; either the 3d orbital is mixed with the 4p orbital of copper,[9,10] or the 3d orbital is mixed with an orbital from an associated sulfur ligand.[5-8]

(2) Copper hyperfine coupling. It is possible to determine the relative amounts of 3d and 4p character in a hybrid copper orbital from the magnitude of the copper hyperfine interaction. Recent ENDOR studies have revealed a small copper hyperfine interaction associated with the Cu_a center, but this copper hyperfine interaction is nearly isotropic[10] ($|A_x|$ = 68 MHz, $|A_y|$ = 98 MHz, $|A_z|$ = 90 MHz). These values for the Cu_a center can be compared to those from the type 1 copper proteins

plastocyanin[11] ($|A_x| \approx |A_y| \approx 60$ MHz, $|A_z| = 189$ MHz) or stellacyanin[10] ($A_x = |167|$ MHz, $A_y = |87|$ MHz, $A_z = |96|$ MHz) and from the square planar copper phthalocyanine complex[30] ($|A_x| = |A_y| = 90$ MHz, $|A_z| = 656$ MHz). The copper hyperfine interaction for the Cu_a center indicates that both the isotropic hyperfine interaction and the distributed dipole interaction between the unpaired electron and the copper nucleus are small. The implication is that either the unpaired electron spin density resides on an associated ligand sufficiently removed from the copper ion, or the unpaired electron is localized on a copper ion with cubic (or higher symmetry) coordination. With respect to the second interpretation, forcing the copper ion into a tetrahedral crystal field, for example, places the $3d^9$ electron configuration in one of the triply degenerate T_2 states, which in combination will lead to a vanishingly small distributed dipole interaction. However, one expects Jahn-Teller distortion to stabilize one of the T_2 states so that the distributed dipole interaction should, in fact, be quite significant for the resultant distorted tetrahedral complex. In any case, this possibility can be excluded on the basis of the g-anisotropy observed for the Cu_a center as discussed in the previous section.

Another way to reduce the distributed dipole interaction between the unpaired electron and the copper nucleus without delocalizing the spin onto an associated ligand would be to mix the 3d orbital, in which the unpaired electron principally resides, with an appropriate 4p orbital. A number of investiga-

tors have invoked such 3d-4p mixing to account for the unusual EPR properties observed for the Cu_a center.[9,10] However, recent ENDOR results, i.e., the small anisotropy in the copper hyperfine interaction, places limits of the extent of this d-p mixing. We have ascertained the relative amounts of 3d and 4p character in a hybrid orbital necessary to eliminate the anisotropic copper hyperfine interaction by calculating the distributed dipole interaction of an electron in a 3d or 4p orbital with the copper nucleus. From Table 1 it is evident that a $3d_{x^2-y^2}$ or $3d_{xy}$ orbital (the orbitals which contain the unpaired electron in square-planar or flattened tetrahedral geometry, respectively) can be mixed with a $4p_z$ orbital to eliminate the anisotropic copper hyperfine interaction. However, it is necessary to include about three times as much $4p_z$ character as $3d_{x^2-y^2}$ or $3d_{xy}$ character to obtain an isotropic copper hyperfine interaction. This is a consequence of the larger value of $\langle\frac{1}{r^3}\rangle$ for a 3d orbital compared to a 4p orbital. We feel such a large mixing is unreasonable in view of the fact that the $3d^8 4p$ configuration lies about 125,000 cm^{-1} above the $3d^9$ configuration for divalent copper.[14] Thus, although mixing of copper 3d and 4p orbitals could, in principle, account for the observed EPR properties of the Cu_a center, this possibility is unreasonable from the standpoint of energetics.

Our view is that the EPR properties of the Cu_a center are best accounted for by delocalization of the unpaired electron spin onto an associated ligand. If the spin resides in a

Table 1: Distributed Dipole Interactions of an Electron with the Copper Nucleus

	Orientation		
Orbital	X	Y	Z
$3d_{x^2-y^2}$	-B	-B	2B
$3d_{xy}$	-B	-B	2B
$3d_{xz}$	-B	2B	-B
$3d_{yz}$	2B	-B	-B
$3d_{z^2-r^2}$	B	B	-2B
$4p_z$	B'	B'	-2B'
$4p_x$	-2B'	B'	B'
$4p_y$	B'	-2B'	B'

B = 329 MHz ($^{63}Cu^{+2}$) (30)

B' ≅ 130 MHz ($^{63}Cu^{+2}$), extrapolated from data in reference 30.

ligand orbital, the observed isotropic copper hyperfine coupling could arise from a small admixture of the copper 4s orbital with the ligand orbital containing the unpaired electron (see the discussion in section 4.2). The question remains as to what ligands among the various amino acid residues can render to Cu_a the unusual EPR properties manifested by this metal center. As we discussed in the previous section, the unpaired electron must be delocalized onto an atom with a substantial spin-orbit coupling. Among the possible ligands in proteins, sulfur appears to be the only candidate onto which the unpaired electron could be delocalized. It is likely, then, that at least one of the ligands of Cu_a is a sulfur. This conclusion is consistent with the Ag^+ binding results which implicated that a sulfhydryl is associated with Cu_a.

4. DISCUSSION

4.1 Model for the Cu_a Center. Our Ag^+ binding experiments have suggested that at least one sulfhydryl is associated with the Cu_a center and that the Cu_a center is relatively inaccessible to hydrophilic species such as Ag^+. Since cytochrome c oxidase is an integral membrane-bound protein, this suggests that the Cu_a center lies in a region of low dielectric constant. It, therefore, seems likely that the charge balance for Cu(II) in the oxidized enzyme must be provided by anionic groups in close proximity to the metal itself, presumably those ligated to Cu_a. However, this results in the separation of two -1 charges from a +2 charge which is an inherently unstable situation in a medium of low dielectric constant. The electrostatic potential

energy could be lowered by approximately 30 kcal/mole by delocalization of one negative charge from an associated ligand onto the copper atom, rendering it effectively a Cu(I)-ligand radical site. Cysteine sulfur is the most likely anionic ligand to donate an electron to a Cu(II), since other potential anionic ligands contain nitrogen or oxygen which are much poorer electron donors than cysteine sulfur.

It is now useful to consider what the possible ligands to Cu_a may be. The type 1 copper in plastocyanin is known[29] to be ligated to one cysteine, one methionine, and two histidine amino acid residues. In addition the copper in plastocyanin is in a reasonably hydrophobic environment, being about 10 Å from the closest approach of water.[29] Therefore, we can conclude that the ligation of one sulfhydryl to Cu(II) in a hydrophobic environment does not allow a sufficient charge delocalization onto copper to account for the unusual EPR properties of the Cu_a center (see the example discussed in section 3.2). However, it is known that the addition of an excess of cysteine to Cu(II) in solution causes a spontaneous reduction of the copper to Cu(I) with a concomitant oxidation of cysteine to cystine.[8] Thus, we would expect that ligation of two cysteines to Cu(II) in a hydrophobic environment would cause nearly complete delocalization of one electron from sulfur onto copper, the second cysteine being necessary to facilitate the redox reaction.

The EPR properties of the Cu_a center are best accounted for by a Cu(I)-sulfur radical site (section 3.2). On the basis of

the above argument, such a Cu(I)-sulfur radical complex would be expected to be formed if two cysteines are ligated to Cu(II) in a hydrophobic environment. Thus we assign two of the ligands of Cu_a to cysteine, one a cysteinate and the other a thiyl radical.

We assign the remaining two ligands of Cu_a to nitrogens from histidine residues and propose a model for the Cu_a center shown in Figure 7. The assignment of two ligands to nitrogens is consistent with ENDOR[31] and the nuclear modulation of the electron spin echo[32] results from the Cu_a center, in which nitrogen hyperfine coupling was observed. Furthermore, the EPR signal observed after dialysis of cytochrome c oxidase against Ag^+ resembles that observed from Ag^+ treated plastocyanin. The analogy of the Cu_a binding site with that of the type 1 copper, plastocyanin, suggests that the nitrogen ligands of Cu_a may derive from histidine.

It is also interesting that the mitochondrially synthesized subunit II of cytochrome c oxidase exhibits a sequence homology with members of the plastocyanin/azurin family.[33] Subunit II has been proposed to be the copper binding subunit in cytochrome c oxidase.[34] We note that the single substitution of a cysteine for a methionine as ligands to copper buried in a hydrophobic environment may be all that is necessary to transform a type 1 copper center into the Cu_a center.

4.2 Comparison of the Proposed Model for the Cu_a Center with the Available Physical Data. Four types of experiments have provided information on the Cu_a center: (i) EPR (particularly

FIGURE 7

Proposed structure for the Cu_a center in cytochrome c oxidase.

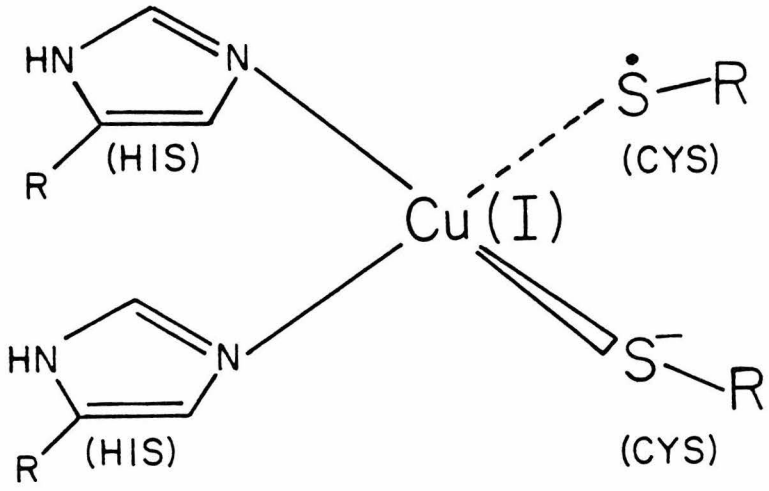
HN
N
(HIS)
R
S
R
(CYS)
Cu(I)
HN
N
(HIS)
R
S⁻
R
(CYS)

S-band EPR); (ii) ENDOR; (iii) nuclear modulation of the electron spin echo; and (iv) x-ray absorption spectroscopy. We will discuss in turn how the data from each of these experiments apply to the model of the Cu_a center (Figure 7).

X-ray absorption edge data from the Cu_a center[14,15] provided strong evidence that Cu_a was unlike other coppers found in proteins. The position of the bound state transitions are sensitive to the oxidation state and/or covalency of the copper ion. The "1s-4s" transition observed from Cu_a in the oxidized enzyme falls within the range for Cu(I) complexes but also at the extreme of the range for covalent Cu(II) complexes.[15] Therefore, the x-ray absorption edge studies only indicate that Cu_a is either a Cu(I) or a very covalent Cu(II) in the oxidized enzyme. An important point, however, is that the energy of the "1s-4s" transition of Cu_a does not change substantially when the enzyme is reduced. This result is supportive of our model in which an associated ligand is the actual electron acceptor.

Recently EXAFS experiments have been undertaken on the copper x-ray absorption edge of cytochrome c oxidase. The preliminary results[35] indicate that one sulfur atom, two nitrogen atoms, and a fourth ligand with a longer bond are associated with Cu_a. In the oxidized enzyme the sulfur is 2.26 Å from copper and the nitrogens are 2.0 Å from copper. When the enzyme is reduced the bond lengths are 2.31 Å and 2.0 Å for the Cu-S and Cu-N bonds, respectively. The Cu-S bond length for Cu_a in both oxidized and reduced cytochrome c oxidase

is close to the Cu-S_{cys} bond length in reduced plastocyanin[29] (2.26 Å and 2.31 Å for oxidized and reduced cytochrome c oxidase versus 2.1 Å and 2.25 Å for oxidized and reduced plastocyanin). This similarity between the Cu-S bond length in oxidized cytochrome c oxidase and reduced plastocyanin, as well as the lack of change of the Cu-S bond length upon reduction of cytochrome c oxidase is strong evidence that Cu_a is formally Cu(I) in the oxidized enzyme and is liganded to one cysteinate sulfur, in excellent agreement with our model. The fourth ligand of Cu_a, that with a longer bond, can be assigned to a cysteine thiyl radical, since a longer Cu-S bond is expected for a thiyl radical ligated to Cu(I).

ENDOR experiments[10,31] have revealed that copper, protons, and nitrogen(s) are coupled to the Cu_a center EPR signal. It is useful to compare the magnitudes of these hyperfine couplings observed from the Cu_a center EPR signal with those observed from the type 1 copper stellacyanin[36,37] (Table 2). From Table 2 it can be seen that both the copper and nitrogen hyperfine interactions associated with the Cu_a center are significantly smaller than those associated with the type 1 copper in stellacyanin. However, if the unpaired electron resides entirely on a sulfur associated with a Cu(I), then the copper and nitrogen hyperfine interactions are expected to be close to zero if the mechanism of hyperfine coupling is purely dipolar.

In order to explain the origin of the copper and nitrogen hyperfine coupling, it is necessary to discuss the polarization of inner shell paired electrons and also bonding electrons by

Table 2: Hyperfine Interactions* Associated with the Cu_a Center and Stellacyanin

Nuclei	Magnitude of Hyperfine Coupling (MHz)					
	Cu_a Center			Stellacyanin		
	X	Y	Z	X	Y	Z
Copper	68	98	90	167	87	96
Proton						
a) weakly coupled	-	2.3	2.0	At least 5 weakly		
	-	1.2	1.3	coupled protons		
	-	0.8	1.3	(anisotropic		
	-	0.3	0.4	coupling)		
b) strongly coupled	12,19 (isotropic)			20 (isotropic)		
Nitrogen	17 (isotropic)			32	32	44
				44	32	32

*Data taken from references 10, 31, 36, and 37.

the outer shell unpaired electron.[38] The orbitals involved are depicted in Figure 8 for the limit where all the unpaired electron is placed in a sulfur $3p_z$ orbital.

Consider first the sulfur radical. The unpaired electron in the sulfur $3p_z$ orbital influences the inner shell electrons and the influences are not equivalent for each of two "paired" electrons. This is because the "paired" electron that is aligned parallel to the unpaired electron will be slightly more favored than the "paired" electron aligned antiparallel to the unpaired electron (a consequence of Hund's rule). The result is that the two electrons that are "paired" will have different orbitals and the net spin of the "paired" electrons will no longer be zero. There will be a net unpaired spin component aligned parallel to the unpaired electron. This effect is depicted for the $3p_x$ orbital of sulfur (Figure 8) as a slightly longer arrow denoting the spin aligned parallel to the unpaired electron.

The electron "pair" in the sulfur $3p_x$ orbital is donated to one of the copper $4sp^3$ orbitals in the formation of the Cu_a coordination complex. Thus, copper will possess a net fractional unpaired electron spin in a $4sp^3$ orbital and consequently a reasonable (and nearly isotropic) copper hyperfine coupling is expected for a Cu(I)-sulfur radical complex. Since the copper 4s orbital obtains some unpaired electron density by this mechanism, the magnitude of the copper hyperfine coupling can be fairly large because the 4s orbital has a finite probability of being at the nucleus.

FIGURE 8

Proposed model for spin polarization of the sulfur $3p_x$, copper $4sp^3$, and nitrogen $2sp^2$ orbitals by the unpaired electron in a sulfur $3p_z$ orbital.

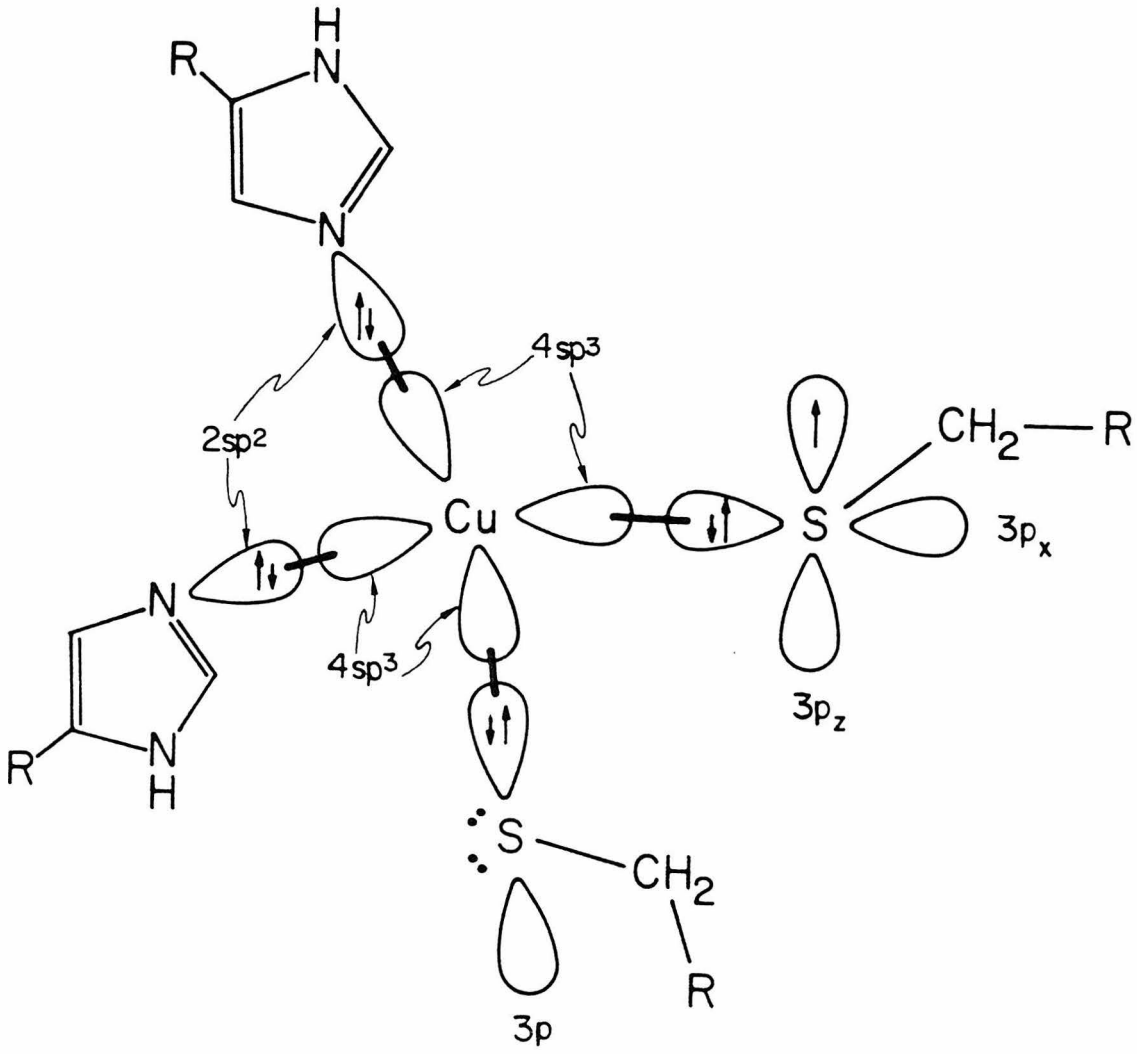
R
H
N
N
4sp3
2sp2
CH2
R
Cu
S
3px
N
4sp3
3pz
R
N
H
S
CH2
R
3p

It is possible to estimate the spin density in a given orbital from the ratio of the observed hyperfine coupling to the coupling calculated if one unpaired electron resides in this orbital. Symons[30] has tabulated the isotropic and anisotropic couplings for the valence s and p, d, or f orbitals of the naturally occurring elements. The contribution of each orbital to the orbital containing the unpaired electron can be calculated from:

$$\begin{aligned} F(\text{iso}) &= A(\text{obs})/A(\text{iso}) \\ F(\text{aniso}) &= 2B(\text{obs})/2B(\text{aniso}) \end{aligned} \qquad (9)$$

where F(iso) and F(aniso) are the fractions of one unpaired electron in the valence s and p, d, or f orbitals, respectively; A(obs) is the observed isotropic coupling; 2B(obs) is the observed anisotropic coupling for the parallel component; and A(iso) and 2B(aniso) are the calculated couplings[30] for unit populations of valence s and p, d, or f orbitals, respectively.

The observed[10] isotropic copper hyperfine coupling for the Cu_a center is 85 MHz (the average of the three principal hyperfine couplings assuming all have the same sign). This value implies that only 1.7% of one unpaired electron resides in a copper 4s orbital [equation (9)].

The observed[10] anisotropic copper hyperfine coupling is approximately $|2B| = 17$ MHz (obtained by making the copper hyperfine coupling tensor axial, e.g. A = 68, 94, and 94 MHz, and assuming that all the couplings have the same sign). This small anisotropy in the copper hyperfine coupling can arise from two mechanisms: (i) the dipolar interaction between the copper

nucleus and the sulfur 3p orbital containing the unpaired electron, and (ii) the donation of a spin polarized lone "pair" from the sulfur $3p_x$ orbital to the copper $4sp^3$ orbital in the formation of the Cu_a coordination complex. In the latter case, the anisotropy arises from the distributed dipole interaction between the copper nucleus and the copper 4p orbital.

The dipolar interaction between the copper nucleus and the sulfur 3p orbital can be calculated to be 0.24 MHz from the point dipole expression:

$$E_d = \mu_e \mu_n r^{-3} \qquad (10)$$

where μ_e and μ_n are the electron and nuclear magnetic moments, and r is the distance between the copper and sulfur atoms. In this case r was chosen to be 2.8 Å, the value suggested by EXAFS experiments.[35] Clearly this dipolar interaction is too small to account for the observed anisotropic hyperfine coupling of 17 MHz.

If the anisotropic copper hyperfine coupling arises from a fractional unpaired electron spin density in a copper $4sp^3$ orbital, then the observed value for $|2B|$ indicates that about 7% of one unpaired electron resides in a copper 4p orbital [equation (2) and Table 1]. Alternatively, the anisotropic copper hyperfine coupling could arise from unpaired electron spin density in a copper 3d orbital. However, in this case only 3% of one unpaired electron resides in a 3d orbital as calculated from equation (9). If the anisotropic copper hyperfine coupling derives from a mixed 3d-4p orbital, then the net unpaired electron spin density on copper can be larger since the aniso-

tropic contributions to the copper hyperfine are in opposite directions for the two orbitals (see Table 1). However, the observed small anisotropic copper hyperfine coupling requires that a hybrid 3d-4p orbital contains about three times more 4p character than 3d character, an energetically unfavorable mixing as discussed in section 3.2(2).

The estimates of the spin density in the copper 4s and 4p orbitals of 1.7% and 7%, respectively, agree very well with our suggestion that the copper obtains some unpaired electron spin density from the donation of a spin polarized sulfur lone "pair" into a copper $4sp^3$ hybrid orbital. Thus, the copper hyperfine interaction observed for the Cu_a center can be accounted for both qualitatively and quantitatively by our model for the Cu_a center. However, considerably more weight could be given to the above argument if the signs of the copper hyperfine couplings were to be measured.

It is possible to see how unpaired electron spin density could be found on the nitrogens ligated to Cu_a from our spin polarization model (Figure 8). Since a net unpaired electron spin is donated to the copper $4sp^3$ orbital from sulfur, the other "paired" electrons of copper will be polarized. However, this is a second order effect and consequently the magnitude of the nitrogen hyperfine coupling will be smaller than that of Cu(II) complexes, as is observed. The nitrogen hyperfine coupling to the Cu_a center is isotropic with a magnitude of 17 MHz. This implies that about 1% of one unpaired electron resides in a 2s orbital of nitrogen (twice this amount if two

equivalent nitrogens contribute to the ENDOR spectrum) as calculated from equation (9). However, the unpaired electron spin density on nitrogen should reside in a $2sp^2$ hybrid orbital, and consequently the nitrogen hyperfine should be somewhat anisotropic. Such anisotropy is observed for stellacyanin[37] (Table 2) and also for Cu(II) phthalocyanin.[39] In both cases the magnitude of the anisotropy agrees very well with that expected if a nitrogen $2sp^2$ hybrid orbital contains the fractional unpaired electron spin. It is possible that the resolution of the nitrogen couplings to the Cu_a center by ENDOR is not sufficient to detect a small anisotropy, since the resonances are broadened due to the quadropole splittings from ^{14}N, and possibly to the overlap of two similar nitrogen resonances. Therefore, a calculation of nitrogen orbital populations for the Cu_a center is not in order at this time. Incorporation of ^{15}N labeled histidine into yeast cytochrome c oxidase could allow much more information about the nitrogens coupled to the Cu_a center to be obtained by ENDOR.[40]

Cu(II) ligated to nitrogen, oxygen, or sulfur would not be expected to exhibit large proton hyperfine couplings. Yet isotropic proton hyperfine couplings of 12 and 19 MHz are observed for the Cu_a center. Such proton hyperfine couplings can be readily accounted for from a cysteine sulfur radical, though. The proton couplings arise from the methylene protons adjacent to sulfur. For sulfur radicals generated by x-irradiation of N-acetyl-L-cysteine fairly large isotropic proton hyperfine couplings are observed (62 and 82 MHz) from

the methylene protons.[41] Such hyperfine interactions are expected to arise from hyperconjugation.[42] In this case the magnitude of the hyperfine interaction depends on the dihedral angle, ϕ, between the sulfur $3p_z$ orbital containing the unpaired electron and the C-H bond (see Figure 9) by the relations[41]

$$A_1 = A_o \rho_s^{\pi} \cos^2\phi$$
$$A_2 = A_o \rho_s^{\pi} \cos^2(\phi - 125°) \qquad (11)$$

where A_1 and A_2 are the isotropic proton couplings observed, A_o is a constant (for the N-acetyl-L-cysteine neutral sulfur radical, A_o = 88 MHz), and ρ_s^{π} is the π-spin density on sulfur. The proton couplings from Cu_a of 12 and 19 MHz require that ϕ = 59.5° or ϕ = 141.0° (see Figure 9). Choosing ϕ = 59.5° gives $A_o\rho_s^{\pi} \approx$ 70 MHz and choosing ϕ = 141° gives $A_o\rho^{\pi} \approx$ 20 MHz. The solution where ϕ = 59.5° corresponds to a π-spin density on sulfur of approximately 80%, assuming the value of A_o for N-acetyl-L-cysteine pertains. This amount of π-spin density on sulfur is quite reasonable for a sulfur radical, being close to that observed for the N-acetyl-L-cysteine monosulfide radical.[41] The remaining unpaired electron spin density is delocalized through spin polarization onto protons, nitrogen, and copper. The proton hyperfine couplings for the Cu_a center, therefore, can also be quantitatively accounted for by our model.

A point of controversy is how a single large isotropic proton coupling can occur for the type 1 copper in stellacyanin (Table 2). This result can be easily explained by delocalization of ~30% of one unpaired electron into the $3p_z$ orbital of cysteine

FIGURE 9

Geometry of the sulfur $3p_z$ orbital with respect to the adjacent methylene group for the Cu_a center. Cases (A) and (B) correspond to the two solutions to equation 11 obtained from the isotropic proton hyperfine couplings observed for the Cu_a center (Table 2). The diagrams are drawn such that the methylene carbon lies directly behind sulfur.

A

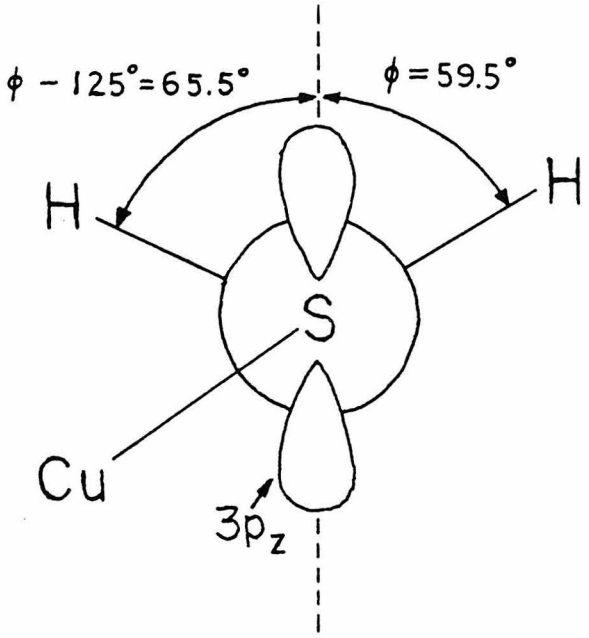

B

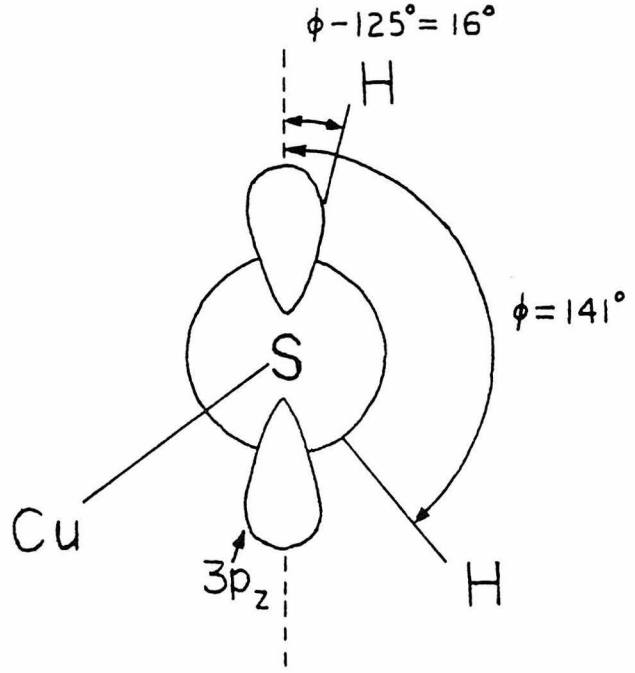

sulfur ligand. Then a geometry where $\phi \approx 35°$ would give proton couplings from the methylene protons of cysteine of 20 and 0 MHz. The delocalization of ~30% of one unpaired electron onto sulfur is quite reasonable in view of the g-values [see section 3.2(1)] and the reduced copper hyperfine coupling (due in part to covalency, see reference 5).

Overall the ENDOR results thus far obtained on the Cu_a center are at least consistent, and in many respects supportive, of our model for the Cu_a center. The same is true for the results on the nuclear modulation of the electron spin echo from the Cu_a center.[32] For Cu(II) complexes, the nuclear modulation produces a pattern which depends on the type, number, and distance of interacting nuclear spins. In particular, imidazole ligation to Cu(II) gives rise to a characteristic pattern.[43] For the Cu_a center this pattern was not observed implying either that imidazole is not ligated to Cu_a (unlikely in view of the ligations known for the copper proteins plastocyanin,[29] azurin,[44] and superoxide dismutase[45]) or that the unpaired electron resides on a ligand associated with Cu_a. The most prominent features in the nuclear modulation pattern arose from interactions of the Cu_a center with protons, as expected for a sulfur radical with a neighboring methylene group. Thus, the nuclear modulation of the electron spin echo from the Cu_a center is also entirely consistent with our model.

The EPR spectrum of the Cu_a center was discussed in section 3.2. It was concluded that the g-values and copper hyperfine coupling for the Cu_a center could only be reasonably explained

by a Cu(I)-sulfur radical complex. At X, K, or Q band the EPR spectrum of the Cu_a center exhibits a g-anisotropy but no resolved hyperfine splittings of any kind.[3] However, at S-band a number of hyperfine components are resolved.[46] These hyperfine interactions are consistent with a copper hyperfine coupling of ~10, 45, and $\leq$40 G in the X, Y, and Z directions, respectively. The magnitude of these copper couplings agree reasonably well with those determined by ENDOR;[10] the differences can be ascribed to inaccuracies expected in measurement of these couplings by ENDOR and S-band EPR. For example, the magnitude of the copper hyperfine coupling is least accurately determined for the Y orientation by ENDOR and for the X and Z orientations in the S-band EPR spectrum. One additional feature observed in the S-band EPR signal of the Cu_a center is a 25 G hyperfine coupling due to an S = 1/2 site that is apparent only at the Y orientation. A proton appears to be the most likely S = 1/2 center that could be involved, but a search for proton couplings by ENDOR did not reveal any resonances of this magnitude.[10] Another possible S = 1/2 site is oxidized cytochrome *a*. At low temperatures the electron relaxation rate of cytochrome *a* would be sufficiently slow that a dipolar splitting could be observed in the Cu_a center EPR spectrum provided cytochrome *a* is sufficiently close to the Cu_a center. This dipolar splitting should be orientation dependent and also only observable when the relaxation rate of cytochrome *a* is long with respect to the dipolar interaction, e.g., at low temperature. Both of these characteristics are

observed for the 25 G hyperfine interaction at S-band. Thus, we feel that the 25G hyperfine coupling due to an S = 1/2 site observed in the S-band EPR spectrum of the Cu_a center may be due to a dipolar interaction with cytochrome a. This point will be elaborated on in chapter V.

In conclusion, all of the physical data that we and others have been able to muster on the Cu_a center are consistent with our proposal that the Cu_a center consists of a Cu(I) ligated by two nitrogens of neutral imidazoles and two cysteine sulfurs, one a cysteinate and the other a thiyl radical as shown in Figure 7.

4.3 Role of the Cu_a Center. The role of cytochrome c oxidase is to conserve a portion of the energy released in the four electron reduction of O_2 to water. Recent evidence suggests that energy is conserved in mitochondria by coupling the generation of an electrochemical gradient to the transfer of electrons. This electrochemical gradient is proposed to consist of both a pH and a potential gradient.[47] In the case of cytochrome c oxidase, the transfer of electrons is proposed to be coupled to the translocation of protons across the inner mitochondria membrane.[48] The Cu_a center may be involved in such a proton pumping mechanism.

Reduction of the Cu_a center results in an isolated negative charge within a region of low dielectric constant. This situation should result in a large increase in potential energy of the Cu_a center which could be coupled to the conservation of energy in cytochrome c oxidase. One scheme for the utilization

of the increase in potential energy upon reduction of the Cu_a center involves a proton pumping mechanism which is depicted in Figure 10. In this scheme, the increased potential energy which is generated by reduction of the Cu_a center is utilized by pulling a proton from the matrix solution to balance the charge. Upon transfer of an electron away from the Cu_a center, this proton would leave an isolated positive charge buried in a hydrophobic environment, which could be expelled from the Cu_a center to the opposite side of the mitochondrial membrane. Through a mechanism such as this the Cu_a center could be intimately involved in a proton pumping mechanism. It may well be that the unusual nature of the Cu_a center is directly related to its role of coupling electron transfer to proton pumping in cytochrome c oxidase.

FIGURE 10

A possible proton pumping mechanism in cytochrome c oxidase.

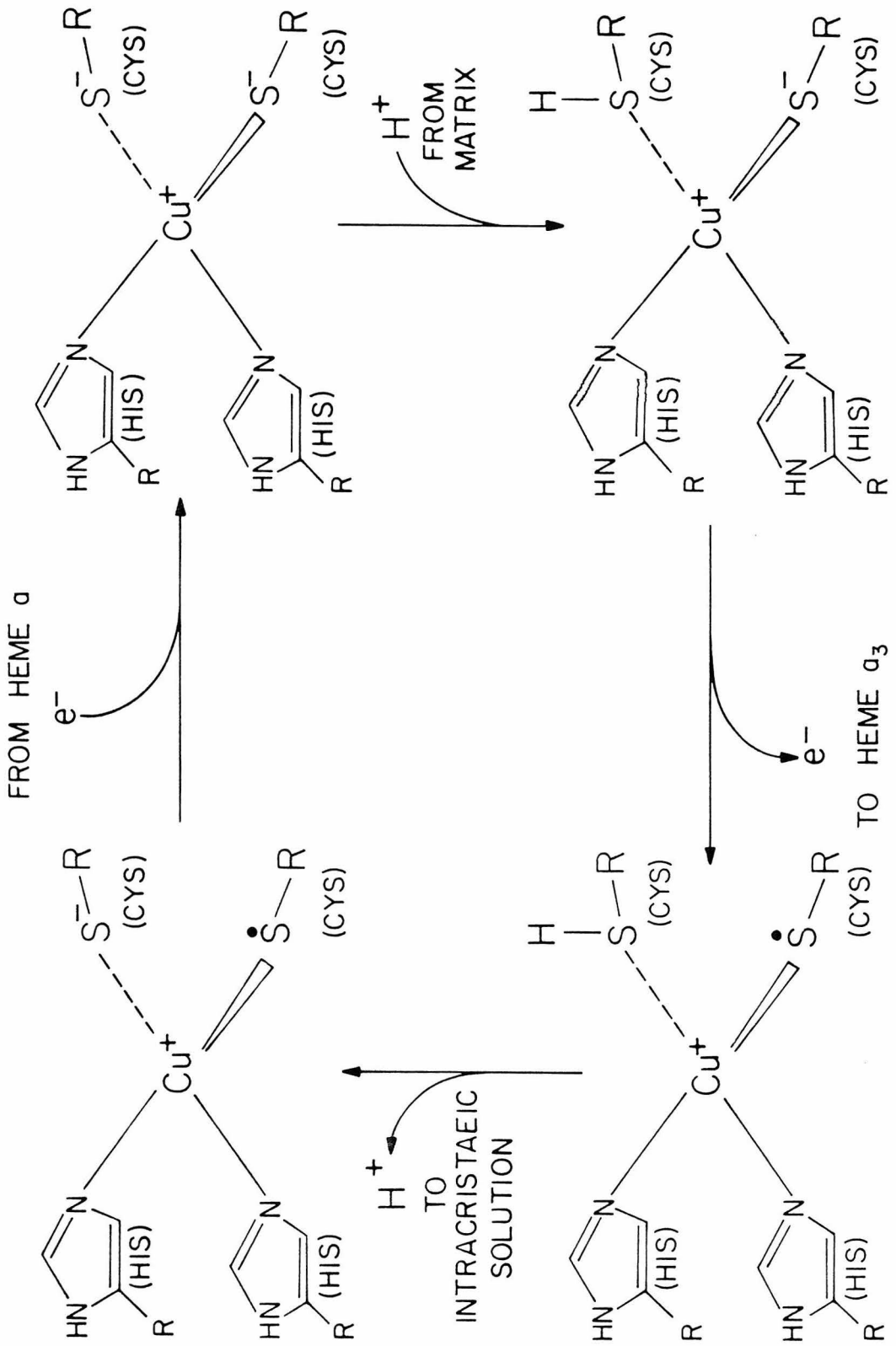
FROM HEME a
e⁻
H⁺
FROM
MATRIX
e⁻
TO HEME a₃
H⁺
TO
INTRACRISTAEIC
SOLUTION
Cu⁺
(CYS)
(HIS)
HN
R
H
N

References

1. Beinert, H., D.E. Griffiths, D.C. Wharton and R.H. Sands (1962), J. Biol. Chem. 237, 2337.
2. Beinert, H. and G. Palmer (1964), J. Biol. Chem. 239, 1221.
3. Aasa, R., S.P.J. Albracht, K.E. Falk, B. Lanne and T. Vänngård (1976), Biochim. Biophys. Acta 422, 260.
4. Tweedle, M.F., L.J. Wilson, L. Garćia-Iñiguez, G.T. Babcock and G. Palmer (1978), J. Biol. Chem. 253, 8065.
5. Peisach, J. and W.E. Blumberg (1974), Arch. Biochem. Biophys. 165, 691.
6. Chan, S.I., D.F. Bocian, G.W. Brudvig, R.H. Morse and T.H. Stevens (1978), in "Frontiers of Biological Energetics", vol. 2 (P.L. Dutton, J.S. Leigh, Jr. and A. Scarpa, eds.), Academic Press, N.Y., p. 883.
7. Chan, S.I., D.F. Bocian, G.W. Brudvig, R.H. Morse and T.H. Stevens (1979), in "Cytochrome Oxidase", (T.E. King, Y. Orii, B. Chance and K. Okunuki, eds.), Elsevier, Amsterdam, p. 177.
8. Hemmerich, P. (1966), in "The Biochemistry of Copper", (J. Peisach, P. Aisen and W.E. Blumberg, eds.), Academic Press, N.Y., p. 15.
9. Greenaway, F.T., S.H.P. Chan and G. Vincow (1977), Biochim. Biophys. Acta 490, 62.
10. Hoffman, B.M., J.E. Roberts, M. Swanson, S.H. Speck and E. Margoliash (1980), Proc. Natl. Acad. Sci. USA 77, 1452.
11. Fee, J.A. (1975), Struct. Bonding (Berlin) 23, 1.

12. Wharton, D.C. (1974), Metal Ions Biol. Systems 3, 157.

13. Gibson, Q.H. and C. Greenwood (1965), J. Biol. Chem. 240, 2694.

14. Hu, V.W., S.I. Chan and G.S. Brown (1977), Proc. Natl. Acad. Sci. USA 74, 3821.

15. Powers, L., W.E. Blumberg, B. Chance, C.H. Barlow, J.S. Leigh, Jr., J. Smith, T. Yonetani, S. Vik and J. Peisach (1979), Biochim. Biophys. Acta 546, 520.

16. Hartzell, C.R. and H. Beinert (1974), Biochim. Biophys. Acta 368, 318.

17. Takemori, S. and T.E. King (1965), J. Biol. Chem. 240, 504.

18. Milne, P.R. and J.R.E. Wells (1970), J. Biol. Chem. 245, 1566.

19. Aasa, R. and T. Vänngård (1975), J. Mag. Res. 19, 308.

20. Katoh, S. and A. Takamiya (1964), J. Biochem. 55, 378.

21. Brudvig, G.W. and S.I. Chan (1979), FEBS Lett. 106, 139.

22. Stevens, T.H., G.W. Brudvig, D.F. Bocian and S.I. Chan (1979), Proc. Natl. Acad. Sci. USA 76, 3320.

23. Robinson, N.C. and R.A. Capaldi (1977), Biochemistry 16, 375.

24. Capaldi, R.A. and M. Briggs (1976), in "The Enzymes of Biological Membranes", vol. 4 (A. Martinosi, ed.), Plenum Press, N.Y., p. 87.

25. Bocian, D.F., A.T. Lemley, N.O. Petersen, G.W. Brudvig and S.I. Chan (1979), Biochemistry 18, 4396.

26. Abragam, A. and B. Bleaney (1970), "Electron Paramagnetic Resonance of Transition Ions", Oxford, London, p. 456.

27. Abragam, A. and B. Bleaney (1970), "Electron Paramagnetic Resonance of Transition Ions", Oxford, London, p. 457.

28. Solomon, E.I., J.W. Hare and H.B. Gray (1976), Proc. Natl. Acad. Sci. USA 73, 1389.

29. Colman, P.M., H.C. Freeman, J.M. Guss, M. Murata, V.A. Noris, J.A.M. Ramshaw and M.P. Venkatappa (1978), Nature 272, 319.

30. Symons, M. (1978), "Chemical and Biochemical Applications of Electron Spin Resonance Spectroscopy", Wiley, N.Y., p. 176.

31. Van Camp, H.L., Y.H. Wei, C.P. Scholes and T.E. King (1978), Biochim. Biophys. Acta 537, 238.

32. Blumberg, W.E. and J. Peisach (1979), in "Cytochrome Oxidase", (T.E. King, Y. Orii, B. Chance and K. Okunuki, eds.), Elsevier, Amsterdam, p. 153.

33. Steffens, G.J. and G. Buse (1979), in "Cytochrome Oxidase", (T.E. King, Y. Orii, B. Chance and K. Okunuki, eds.), Elsevier, Amsterdam, p. 79.

34. Yu, C. and L. Yu (1977), Biochim. Biophys. Acta 495, 248.

35. Scott, R.A., personal communication.

36. Rist, G.H., J.S. Hyde and T. Vänngård (1970), Proc. Natl. Acad. Sci. USA 67, 79.

37. Roberts, J.E., T.G. Brown, B.M. Hoffman and J. Peisach (1980), J. Amer. Chem. Soc. 102, 825.

38. Watson, R.E. and A.J. Freeman (1961), Phys. Rev. 123, 2027.

39. Symons, M. (1978), "Chemical and Biochemical Applications of Electron Spin Resonance Spectroscopy", Wiley, N.Y., p. 138.

40. Stevens, T.H., work in progress.

41. Hadley, J.H., Jr. and W. Gordy (1977), Proc. Natl. Acad. Sci. USA 74, 216.

42. Wertz, J.E. and J.R. Bolton (1972), "Electron Spin Resonance", McGraw-Hill, N.Y., p. 124.

43. Mims, W.B., J. Peisach and J.L. Davis (1977), J. Chem. Phys. 66, 5536.

44. Adman, E.T., R.E. Stenkamp, L.C. Sieker and L.H. Jensen (1978), J. Mol. Biol. 123, 35.

45. Richardson, J.S., K.A. Thomas, B.H. Rubin and D.C. Richardson (1975), Proc. Natl. Acad. Sci. USA 72, 1349.

46. Froncisz, W., C.P. Scholes, J.S. Hyde, Y. Wei, T.E. King, R.W. Shaw and H. Beinert (1979), J. Biol. Chem. 254, 7482.

47. DePierre, J.W. and L. Ernster (1977), Ann. Rev. Biochem. 46, 201.

48. Wikström, M. and K. Krab (1979), Biochim. Biophys. Acta 549, 177.

CHAPTER V: DISTRIBUTION OF THE METAL CENTERS IN CYTOCHROME C OXIDASE

1. INTRODUCTION

1.1 Previous Studies on Cytochrome c Oxidase.

It is generally accepted that cytochrome c oxidase utilizes the electron potential energy drop from the transfer of electrons from cytochrome c to dioxygen to establish a pH and/or potential gradient across the inner mitochondrial membrane.[1] However, the proportion of the potential energy stored in a pH gradient versus that stored in a potential gradient is unresolved. A number of proposals[1,2] have been advanced to explain the existing data and these proposals differ because two questions about the structure and mechanism of cytochrome c oxidase remain unanswered: (1) Is the oxygen binding site on the same or opposite side of the membrane as the cytochrome c binding site? and (2) Does cytochrome c oxidase pump protons across the membrane? These points are interrelated, since if the cytochrome c and oxygen binding sites are on the same side of the membrane, then protons must be pumped across the membrane from the matrix to the cytosol-side to achieve the observed polarity of the pH gradient established by cytochrome c oxidase. In order to address these questions, it is important to know the relative proximity of the four metal centers in cytochrome c oxidase to one another.

At this time only one study[3] has addressed the question of the distances between the metal centers. In this experiment fluorescence quenching was used to determine the distances

between three sites: (i) a highly reactive sulfhydryl group on subunit II, which was alkylated by the 1,5 or 2,6 isomer of N-(iodoacetamidoethyl)-1-amino-naphthalene-5-sulfonate; (ii) cytochrome c, or its fluorescent porphyrin analog, covalently attached to subunit III by a disulfide bond; and (iii) endogenous heme a, either cytochrome a or cytochrome a_3. The fluorescence quenching is dominated by the distance between the fluorescent label and the closest paramagnetic heme site. Three such distances were measured in the labeled cytochrome c oxidase complex. The distance between the heme groups of cytochrome c and the closest endogenous heme a (presumably cytochrome a) was 25 Å, the distance between the heme group of cytochrome c and the sulfhydryl group on subunit II was 35 Å, and the distance between the sulfhydryl group on subunit II and the closest endogenous heme a was 52 Å. However, these experiments do not address the question of where the coppers are in cytochrome c oxidase. In addition, the use of fluorescent probes suffers from the problem that the probe may not be attached to the same site in all the enzyme molecules. In this regard cytochrome c oxidase has two cytochrome c binding sites[4] (one high affinity and one lower affinity) and six reactive sulfhydryl groups.[5]

1.2 Dipolar Electron Spin Relaxation. Electron spin relaxation measurements can also be used to calculate distances between paramagnetic centers within a protein.[6-8] In the case of proteins containing more than one metal center, the metal centers themselves can be used as probes. If two para-

magnetic centers are close to one another, then their respective electron spin relaxation rates will be increased due to the dipolar interaction between the two sites. This effect is particularly pronounced for a slowly relaxing electron spin close to a much more rapidly relaxing spin. Such a situation is realized at room temperature when a nitroxide spin label is adjacent to a transition metal ion such as Mn^{+2} or Cu^{+2}. Recently there has been considerable interest in using the "spin-probe-spin-label" method to determine distances in biological systems.[6,8] Thus far these studies have involved the use of extrinsic nitroxide spin-labels coordinated to specific sites on proteins, or other polymers, containing one or more bound transition metal ion. It is also possible to utilize two intrinsic paramagnetic sites within a protein. In enzymes containing multiple non-equivalent metal atoms which have greatly different intrinsic electron spin relaxation rates, such as cytochrome c oxidase, the "spin-probe-spin-label" method may allow distances between metal centers to be determined.

When two paramagnetic centers are close to one another, the magnetic field produced by the magnetic moment of one site will be felt by the second site. The classical dipolar interaction, $\mathcal{H}_d$, between the two magnetic moments $\bar{\mu}_1$ and $\bar{\mu}_2$ is:

$$\mathcal{H}_d = \frac{\bar{\mu}_1 \cdot \bar{\mu}_2}{r^3} - \frac{3(\bar{\mu}_1 \cdot \bar{r})(\bar{\mu}_2 \cdot \bar{r})}{r^5} \qquad (1)$$

where $\bar{r}$ is the radius vector from $\bar{\mu}_1$ to $\bar{\mu}_2$.[9] We will discuss the simple case of two paramagnetic S = 1/2 sites each with an

isotropic g-tensor that are interacting only through a dipolar mechanism. One of these sites, species 2, is assumed to have a much faster intrinsic electron spin relaxation rate than the other, species 1. In this case, the EPR properties of species 1 depend on the electron spin relaxation rate of species 2.

The relaxation of the magnetization of a paramagnetic species to its equilibrium value can be characterized by two parameters: longitudinal (T_1) and transverse (T_2) times. When a paramagnetic sample is placed in an external magnetic field the sample will attain a net magnetization parallel to the external field. The rate at which the magnetization parallel to the external field approaches equilibrium is characterized by T_1. This process <u>is</u> accompanied by a change in energy of the spin-system and T_1 can be identified with the time of spin-lattice relaxation. T_2 characterizes the relaxation of the component of magnetization which is perpendicular to the external magnetic field. Transverse relaxation <u>is not</u> accompanied by a change in energy of the spin-system and T_2 can be identified with the time of spin-spin relaxation.

For our example of two S = 1/2 spins interacting through a dipolar mechanism, the EPR spectrum of the more slowly relaxing site, species 1, will be affected in two ways by the more rapidly relaxing site, species 2. First, if T_1^{-1} for species 2 is less than the dipolar interaction, i.e.,

$$\frac{\bar{\mu}_1 \cdot \bar{\mu}_2}{r^3} > \frac{h}{T_1} \qquad (2)$$

then species 1 will "see" species 2 through a dipolar mechanism in one of two orientations, either parallel to the external field or antiparallel to the external field, provided the external field is sufficiently strong.[10] In this static case the EPR signal of species 1 will be split into two resonances separated by $2\bar{\mu}_1 \cdot \bar{\mu}_2 \, r^{-3}$. The second case is when T_1^{-1} for the rapidly relaxing site is greater than the dipolar interaction, i.e.,

$$\frac{\bar{\mu}_1 \cdot \bar{\mu}_2}{r^3} < \frac{h}{T_1} \tag{3}$$

In this case species 1 will "see" species 2 as an average magnetization. Consequently, the EPR signal of species 1 will be slightly shifted depending on whether the magnetic field from species 2 adds or subtracts from the external magnetic field, but no splitting will be observed in the EPR signal of species 1.

The dipolar interaction between species 1 and 2 will also affect the electron spin relaxation rates of the two sites.[11] In the example that we have been discussing the relaxation rate of the more slowly relaxing site can be dramatically affected by the rapidly relaxing site. The general theory of spin relaxation has been given.[9,11] Using first order time dependent perturbation theory, the following expressions for the spin relaxation rates can be obtained:[8]

$$\frac{1}{T_1} = \frac{1}{T_1^\circ} + J(J+1)\left[\frac{b^2 T_{2k}}{1+(\omega_k-\omega_j)^2 T_{2k}^2} + \frac{c^2 T_{1k}}{1+\omega_j^2 T_{1k}^2} + \frac{e^2 T_{2k}}{1+(\omega_k+\omega_j)^2 T_{2k}^2}\right] \tag{4}$$

where: $b^2 = 1/6\gamma_k^2\gamma_j^2\hbar^2 r_{jk}^{-6} \quad (1-3\cos^2\theta)^2$

$c^2 = 3/4\gamma_k^2\gamma_j^2\hbar^2 r_{jk}^{-6} \quad \sin^2 2\theta$

$e^2 = 3/2\gamma_k^2\gamma_j^2\hbar^2 r_{jk}^{-6} \quad \sin^4\theta$

$$\frac{1}{T_2} = \frac{1}{T_2^\circ} + J(J+1)\left[A^2 T_{1k} + \frac{B^2 T_{2k}}{1+\omega_k^2 T_{2k}^2} + \frac{C^2 T_{2k}}{1+(\omega_k-\omega_j)^2 T_{2k}^2} + \frac{D^2 T_{1k}}{1+\omega_j^2 T_{1k}^2} + \frac{E^2 T_{2k}}{1+(\omega_k+\omega_j)^2 T_{2k}^2}\right] \tag{5}$$

where: $A^2 = 1/3\gamma_k^2\gamma_j^2\hbar^2 r_{jk}^{-6} \quad (1-3\cos^2\theta)^2$

$B^2 = 3/4\gamma_k^2\gamma_j^2\hbar^2 r_{jk}^{-6} \quad \sin^2 2\theta$

$C^2 = 1/12\gamma_k^2\gamma_j^2\hbar^2 r_{jk}^{-6} \quad (1-3\cos^2\theta)^2$

$D^2 = 3/8\gamma_k^2\gamma_j^2\hbar^2 r_{jk}^{-6} \quad \sin^2 2\theta$

$E^2 = 3/4\gamma_k^2\gamma_j^2\hbar^2 r_{jk}^{-6} \quad \sin^4\theta$

The subscripts j and k refer to the slowly relaxing site, species 1, and the rapidly relaxing site, species 2, respectively; θ is the angle between the radial vector $\bar{r}_{jk}$ and the external magnetic field; J is the total angular momentum of species 2; the γ's are the magnetogyric ratios, the ω's are the resonance frequencies in the magnetic field used to observe the resonance of species 1; T_{1k} and T_{2k} are the spin-lattice and spin-spin relaxation times of species 2; T_1° and T_2° are the spin-lattice and spin-spin relaxation times of species 1 in the absence of a dipolar interaction with species 2; and T_1 and T_2 are the spin-lattice and spin-spin relaxation times of species 1 in the presence of a dipolar interaction with species 2. Hyperfine interactions and g-anisotropy have been neglected in these formulas. These formulas are valid if: (i) first-order time dependent theory is adequate, i.e., if equation (3) pertains, and (ii) the dipolar field from species 2 is a random function in time. Both of these conditions are expected to be fulfilled if the spin-lattice relaxation time of species 2 is sufficiently short. In fact, equations (4) and (5) have been used to obtain reasonable estimates of the distance between a nitroxide spin label and a transition metal at room temperature.[8]

For the situation where equation (2) pertains, formulas (4) and (5) cannot be used to estimate the effect of a dipolar interaction on the electron spin relaxation rate of species 1 because the first-order perturbation calculation is not adequate. At the present time the theory of dipolar relaxation has not

been worked out sufficiently to allow the distance between two interacting sites to be obtained from spin relaxation measurements when equation (2) pertains. Nonetheless, the spin relaxation of species 1 is expected to be influenced to some extent by species 2, even when the spin relaxation rate of species 2 is slow. However, if the static dipolar splitting can be observed in the EPR signal from species 1, then the distance between species 1 and 2 still can be calculated in the limit where equation (2) pertains.

1.3 EPR Saturation. There are a number of methods available for measuring the spin relaxation rates.[12,13] Pulse methods (pulse saturation and spin-echo) permit the direct measurement of T_1 and T_2. However, specialized instrumentation is required for these measurements. Measurement by the method of continuous saturation can be carried out on the ordinary commercial EPR spectrometers. In order to obtain information on T_1 and T_2 by the method of continuous saturation, it is necessary to determine what mechanism determines the linewidth of the EPR signal in question.[14,15]

The linewidth of EPR signals is determined by two mechanisms: (i) homogeneous broadening and (ii) inhomogenous broadening. Homogeneous broadening reflects the lifetime of the excited state and leads to a Lorentzian lineshape. In this case the half-width at half-height, $\Delta H_{1/2}$, is a measure of T_2:

$$\Delta H_{1/2} = (\gamma T_2)^{-1} \qquad (6)$$

Inhomogeneous broadening arises from a number of mechanisms

including: unresolved hyperfine, dipolar interactions between spins with different Larmor frequencies, g-anisotropy, and 'g-strain' or heterogeneous populations of spin centers. In general proteins exhibit inhomogeneous broadened EPR signals. For proteins 'g-strain' is usually the largest factor in the inhomogeneous linewidth. Castner[16] has shown that the EPR absorption amplitude, Y, for inhomogeneously broadened lines is given by:

$$Y = \frac{Y_o \, P^{1/2}}{(1+\alpha P)^{1/2}} \exp(a^2 \alpha P)\{\frac{1-\phi[a(1+\alpha P)^{1/2}]}{1+\phi(a)}\} \qquad (7)$$

where $\phi(x)$ is the error function

$$\phi(x) = \frac{2}{\sqrt{\pi}} \int_o^x \exp(-u^2)\, du \qquad (8)$$

Y_o is a constant proportional to the number of spins in the resonant field, P is the incident microwave power, α is a saturation parameter proportional to the product of T_1 and T_2, and a is a parameter which measures the degree of inhomogeneous broadening (a is the ratio of the homogeneous linewidth and the inhomogeneous linewidth). Equation (7) can be reduced in the limit where a = 0 (inhomogeneous limit) and where a>>1 (homogeneous limit) to equations (9) and (10).

$$Y = \frac{Y_o \, P^{1/2}}{(1+\alpha P)^{1/2}} \qquad (a = 0) \qquad (9)$$

$$Y = \frac{Y_o P^{1/2}}{(1+\alpha P)} \qquad (a>>1) \tag{10}$$

For situations intermediate between the inhomogeneous and homogeneous limits, the EPR absorption amplitude can be empirically fit[17,18] to the following function:

$$Y = \frac{Y_o P^{1/2}}{(1+\alpha P)^{b/2}} \tag{11}$$

where b is the 'inhomogeneity parameter' which can vary from 1.0 for the inhomogeneous to 2.0 for the homogeneous limit.

The saturation of an EPR signal occurs when the rate at which energy is absorbed from a powerful microwave field cannot be matched by the rate at which the system returns to equilibrium. Hence, as the microwave field is increased a point will be reached when a paramagnetic species no longer can continue to absorb microwaves at an increasing rate. This is the point where the rate of microwave absorption equals the rate at which the system returns to equilibrium. This phenomenon is implicit in equations (7) and (9)-(11) and is represented graphically in Figure 1. Two domains exist in Figure 1: one in which the EPR signal height is proportional to the microwave field (or to the square root of the microwave power) and another in which the EPR signal height increases at a progressively slower rate as the microwave field is increased. The first domain is where the EPR signal intensity is limited by the microwave field intensity and the second domain is where the EPR signal

FIGURE 1

EPR signal amplitude observed with increasing microwave power. The inhomogeneous limit refers to equation (9) and the homogeneous limit refers to equation (10). Y_o and α were taken to be 0.5 and 0.3, respectively, in both cases.

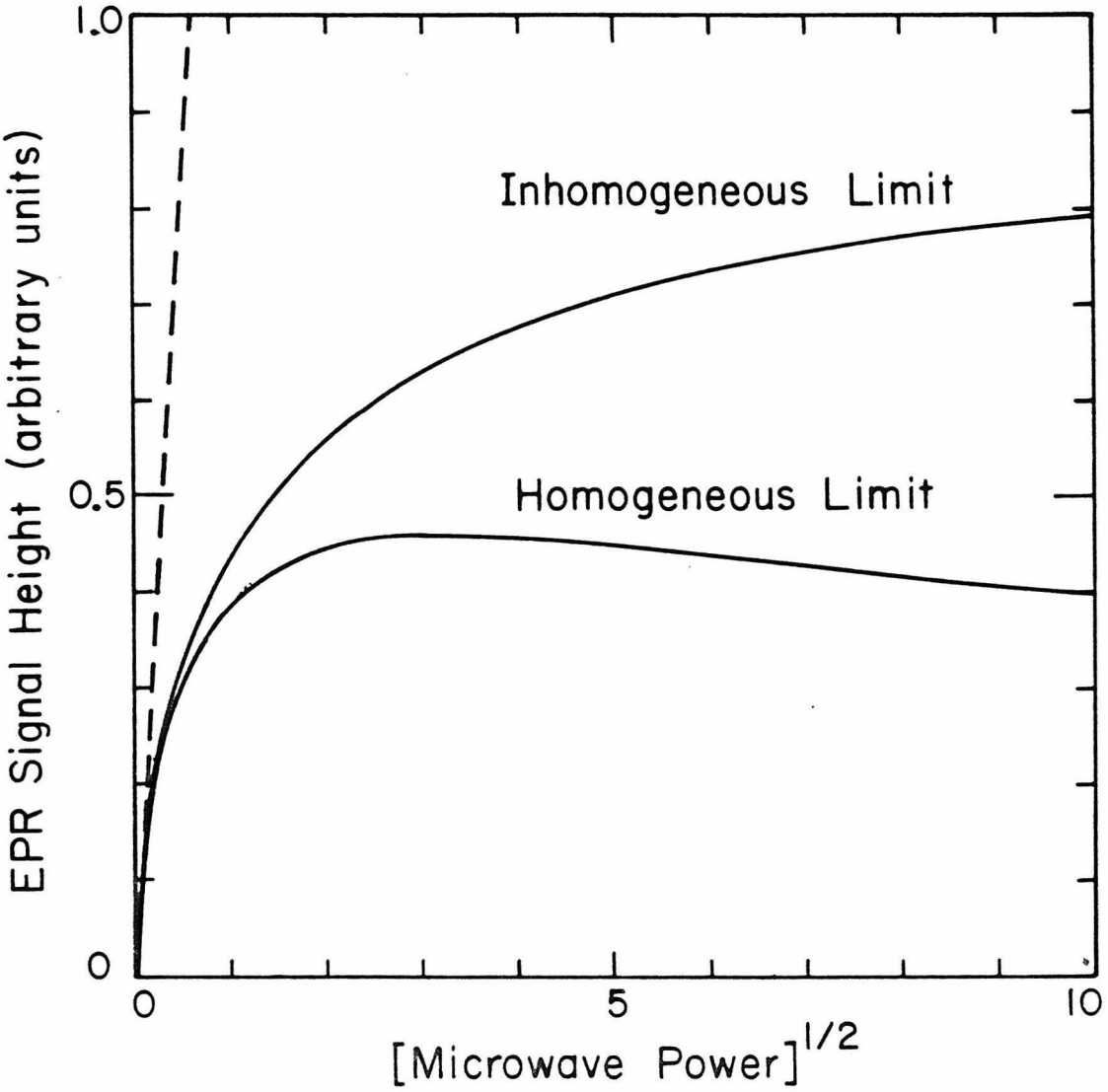
1.0
0.5
0
EPR Signal Height (arbitrary units)
Inhomogeneous Limit
Homogeneous Limit
0
5
10
[Microwave Power]^1/2

intensity is limited by the spin relaxation rates, T_1 and T_2. Consequently, measurement of the EPR signal intensity as a function of microwave power provides information on the product of T_1 and T_2.

1.4 Temperature Dependence of T_1. All of the complexes for which EPR saturation was measured in this work were sufficiently dilute that spin-spin interactions between equivalent sites could be ignored and all centers observed had a single unpaired electron. For these samples the dominant spin-lattice relaxation mechanism is expected to arise either from the crystal field Stark effect as outlined by Van Vleck[19,20] and Kronig[21], the Orbach[22] process in which spin-lattice relaxation proceeds via a low-lying excited state, or the dipolar mechanism described in the section 1.2 (this mechanism can occur for dilute samples only if two distinct paramagnetic sites within the same protein are in close proximity).

The Van Vleck process of spin-lattice relaxation occurs when lattice vibrations induce periodic variations in the crystalline electric field of a paramagnetic ion.[23] These changes react on the spin through the spin-orbit interaction, and thereby alter the spin's orientation in the magnetic field. This process is dependent on the number of phonons (lattice vibrations) with a frequency near the Larmor frequency of the spin (direct process) and on the total number of phonons (Raman process). These processes are shown in Figure 2. The direct process predominates at low temperature ($T \lesssim 10K$) when a larger fraction of the phonons have an energy equal to $h\nu$ and

FIGURE 2

Mechanisms of spin-phonon interaction. The straight lines represent phonon induced EPR transitions. The wavy lines represent phonons. The direct process involves relaxation of the spin from the $M_s = 1/2$ to $M_s = -1/2$ levels with the creation of a phonon equal in energy to the splitting of the two levels. The Raman process involves the inelastic scattering of a phonon. In this case E_1 can be any value. The Orbach process involves the excitation of the spin from the $M_s = 1/2$ level to a low-lying excited state by a phonon. This excited state is more strongly coupled to the $M_s = -1/2$ level than the $M_s = 1/2$ level, thus providing an efficient relaxation mechanism. Here $E_2 = \Delta_c - h\nu/2$.

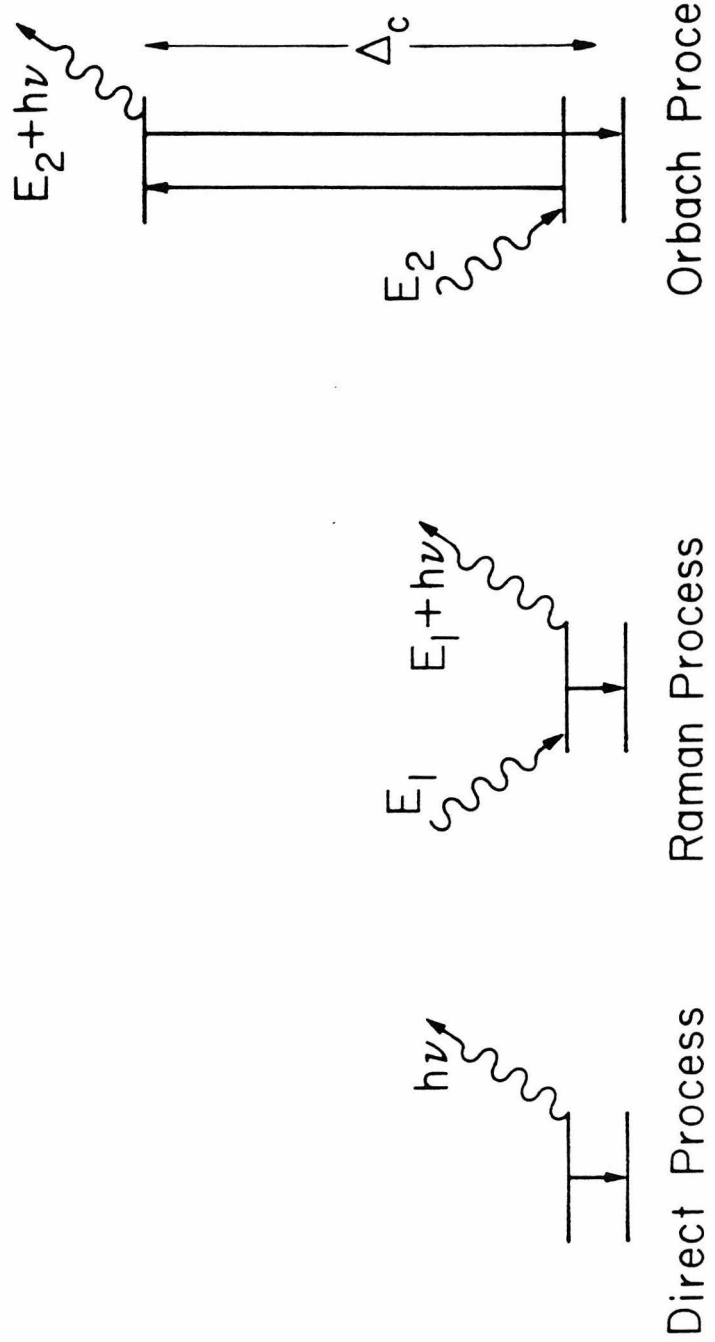
$E_2+h\nu$
Δ_c
E_2
Orbach Process
E_1
$E_1+h\nu$
Raman Process
$h\nu$
Direct Process

the Raman process predominates at higher temperature when very few of the phonons have an energy equal to $h\nu$. Because the phonon distribution curve is temperature dependent, the spin-lattice relaxation rate induced by the Van Vleck process increases with temperature as:

$$\frac{1}{T_1} = NT \qquad \text{(direct process)} \qquad (12)$$

$$\frac{1}{T_1} = N'T^n J_{n-1}(\theta_D/T) \qquad \text{(Raman process)} \qquad (13)$$

where N and N' are temperature-independent constants, T is the temperature, θ_D is the Debye temperature and $J_{n-1}(\theta_D/T)$ is the transport integral defined as

$$J_n(x) = \int_o^x \frac{e^z Z^n}{(e^z-1)^2}\, dz \qquad (14)$$

Consequently the Van Vleck process leads to a temperature dependence of T_1 that is proportional to T below ~10K due to the predominance of the direct process, T^n for $10 \lesssim T << \theta_D$ due to the predominance of the Raman process and the temperature independence of the transport integral ($J_n(x) = n!$ if $T << \theta_D$), and T^2 for $T >> \theta_D$ due to the predominance of the Raman process and the transport integral contributing a T^{2-n} dependence when $T >> \theta_D$. When $T \approx \theta_D$ the temperature dependence of T_1 will not be constant, but will vary from T^n when $T \lesssim \theta_D$ to T^2 when $T \gtrsim \theta_D$. Theoretical calculations[23] predict that n is either 7 or 9. However, experimentally values of n between 5 and 11

have been measured.[24,25]

The Orbach process (see Figure 2) leads to a temperature dependence of T_1 of:

$$\frac{1}{T_1} = N''[\exp(\Delta_c/kT)-1]^{-1} \qquad (15)$$

where Δ_c is the separation between the ground state and a low lying excited state that can be thermally populated, and N'' is a coefficient which depends on the phonon-spin coupling.[22] For paramagnetic ions with a low lying excited state (within about 50 cm^{-1} of the ground state for temperatures less than 50K), the Orbach process will dominate the spin-lattice relaxation.

When the spin-lattice relaxation is influenced by a dipolar interaction the temperature dependence of T_1 can become quite complicated. For example, consider equation (4) for a case where $T_1^{o-1} = KT^2$, $T_{1k} >> T_{2k}$, and $T_{1k}^{-1} = K'T^2$. These conditions may well apply at room temperature. In this case $T_1^{-1} = KT^2 + J(J+1)K'C^2T^2/(1+\omega_j^2 K'^2 T^4)$. If $K'C^2 >> K$, then T_1^{-1} may <u>decrease</u> with increasing temperature before finally becoming proportional to T^2 at high temperature. Such a temperature dependence for T_1 is a strong indication of a dipolar interaction. However, in general the temperature dependence of T_1 will not positively implicate a dipolar mechanism. In order to really prove that a dipolar interaction contributes to the spin relaxation of a particular species, it is necessary to observe a change in the spin relaxation rate in the presence and absence of the neighboring paramagnetic

site. For the case of nitroxide spin labels adjacent to a transition ion, the relaxation rate in the absence of the paramagnetic ion can be easily obtained by replacing the paramagnetic ion with an equivalent diamagnetic one, such as the replacement of Mg^{+2} for Mn^{+2}. For the case of a protein containing multiple non-equivalent metal centers, it may be possible to selectively remove or reduce one or more metal centers. It may also be possible to eliminate the paramagnetism from a paramagnetic site by inducing a transition from a high to low spin state. Such is the case for the cytochrome $\underline{a}_3$-Cu_{a_3} site in cytochrome $\underline{c}$ oxidase. This site is S = 2 in the native oxidized enzyme but becomes diamagnetic when cyanide is bound.[26]

1.5 EPR Saturation of the Cu_a Center. The Cu_a center in cytochrome $\underline{c}$ oxidase has been observed to have unusual EPR saturation characteristics. At 77K the EPR signal from the Cu_a center is very difficult to saturate,[27] while at 10K the EPR signal is easily saturated[28,29] relative to other Cu(II) complexes. The origin of this unusual saturation behavior has not been explained and may be an indication that Cu_a is close to one of the hemes in cytochrome $\underline{c}$ oxidase.

In chapter IV the nature of the Cu_a center was discussed. It was concluded that the Cu_a center is best described as a Cu(I)-sulfur radical center. We have investigated the temperature dependence of the EPR saturation of the Cu_a center in this chapter. These data are compared to the EPR saturation of a number of copper proteins and inorganic copper complexes,

several sulfur radicals, and also several low spin hemes, including cytochrome a. We also examined the effect of changing the spin state of the cytochrome a_3-Cu_{a_3} site and of partially reducing cytochrome a on the EPR saturation of the Cu_a center. From these studies an estimate of the relative proximity of Cu_a to each of the two hemes in cytochrome c oxidase is presented.

2. MATERIALS AND METHODS

2.1 Sample Preparation. Beef heart cytochrome c oxidase was isolated by the procedure af Hartzell and Beinert.[30] The purified protein was dissolved in 50 mM Tris/acetate buffer, 0.5% Tween 20, pH 7.4 and stored at -85°C until use. The preparation used in this work contained 9 nmoles heme a/mg protein and the concentration was 0.25 mM aa_3.

French bean plastocyanin, Pseudomonas aeruginosa azurin, Rhus vernicifera stellacyanin, and Rhus vernicifera laccase were the generous gift of Professor Harry B. Gray. The protein concentrations were 0.5 mM, 0.5 mM, 0.5 mM, and 0.2 mM respectively.

Bis(N-t-butylsalicylaldiminato) Cu(II) (b-tbs Cu) was synthesized by the method of Sacconi and Ciampolini[31] and was recrystallized from cyclohexane twice before use. The sample used to record EPR spectra was dissolved in anhydrous methanol to a concentration of 0.8 mM. Cu(II) EDTA was prepared by the addition of $CuCl_2$ to a 0.1 M solution of EDTA, pH 7.4 to give a final copper concentration of 1 mM.

The sulfur radicals were prepared by UV irradiation of cysteine. Two types of samples were used: (i) polycrystalline cysteine-HCl and (ii) a saturated solution of cysteine-HCl in a 2:1 mixture of ethylene glycol-H_2O (the frozen solution formed a glass). Both types of samples were placed under an Ar atmosphere and irradiated at 77K with a 200 W Hg-Xe arc lamp. EPR spectra were recorded without warming the samples. A variety of sulfur radicals are formed by the UV irradiation.[32,33] These radicals exhibit a range of g-anisotropy and the g_{max} components of the EPR spectra of two separate sulfur radicals were resolved well enough to measure the EPR saturation of each radical independently.

All EPR spectra were recorded on anaerobic samples. The samples were made anaerobic by three cycles of evacuation and flushing with argon and, thereafter, were stored under an atmosphere of argon. The cyanide complex of oxidized cytochrome c oxidase was prepared by first making the sample anaerobic, then adding a 1:2 mole ratio mixture of KCN and KH_2PO_4 to give a KCN concentration of 100 mM from a sidearm on the EPR tube, and finally incubating the sample for four hours at 4°C. The actual concentration of dissolved HCN (most of the KCN bubbled off as HCN) was estimated to be about 2 mM from the partial pressure of HCN over the sample and the solubility of HCN in water.

2.2 EPR Spectroscopy. The EPR spectra were recorded in the absorption mode on a Varian E-line century series X-band spectrometer employing 100 KHz field modulation. Incident

microwave power was read on the E-109 leveled attenuator scale and was calibrated by measurement of both a non-saturating Varian "strong pitch" sample and solid DPPH at room temperature. Temperature regulation was achieved with an Air Products Heli-Trans low temperature system. The temperature was measured immediately before and immediately after recording the EPR spectra with a Au(0.07% Fe)-chromel thermocouple which was placed in an oil filled EPR tube. The thermocouple was calibrated at 4.6K (boiling point of He) and 77.2K (boiling point of N_2). A linear variation in the thermocouple output with temperature was assumed between 4.6 and 77.2K. The temperature was found to be stable to within 0.5K for all spectra obtained.

The samples were in 5 mm outer diameter and 3.4 mm inner diameter quartz EPR tubes. In most cases sufficient sample was placed in the EPR tubes to completely fill the TE 102 microwave cavity (only for the Rhus laccase sample was the amount insufficient to fill the cavity). Correction for the distribution of the microwave magnetic field, H_1, within the sample was neglected.

2.3 Data Analysis. The EPR saturation in this work were fit to equation (11) by a non-linear least squares routine (share program No. 3094, Albert Chang, Caltech, IBM 370 FORTRAN library). Initially Y_o, α, and b were allowed to simultaneously vary. For a given paramagnetic compound, b is expected to increase monotonically with temperature from $b(T\rightarrow 0) \approx 1$ to $b(\text{high } T) = 2$. This is because the homogeneous linewidth

($\Delta H_L = \frac{1}{\gamma T_2}$) becomes small at low temperature as T_2 becomes long, and large at high temperature when T_2 becomes short, whereas the inhomogeneous linewidth remains constant. In some cases a least squares fit of the saturation data to equation (11) gave a value of b outside the limit $1 \leq b \leq 2$ and in other cases b did not vary smoothly with temperature. Therefore, a second least squares fit of the saturation data to equation (11) was performed in which only Y_o and α were allowed to vary; in each case b was specified to give $1 \leq b \leq 2$ and to ensure that b varied smoothly with temperature for each sample; the values of b were chosen on the basis of the initial least squares fit.

The product of T_1 and T_2 was obtained from the parameter α by the use of DPPH as a standard. At room temperature $T_1 = T_2 = 2 \times 10^{-8}$ s for solid DPPH.[34] On this basis, the proportionality between T_1T_2 and α was determined to be:

$$T_1T_2 = 2.1\alpha \qquad (\text{in } \mu\text{sec.}^2) \tag{16}$$

3. RESULTS

3.1 General Comments on the EPR Saturation Data. The EPR saturation for several type 1 copper proteins, the type 2 copper in laccase,[35] several inorganic Cu(II) complexes, several sulfur radicals, several low-spin heme proteins, and the Cu_a center and cytochrome a in both the native and cyanide-bound oxidized enzyme was examined between 8 and 60K (Figures 3-8). Before we discuss the observations on each particular group, we

FIGURE 3

EPR relaxation of type 1 coppers. The size of the points reflect the estimated error in T and $(T_1T_2)^{-1}$. The circles denote stellacyanin; the diamonds denote azurin; and the crosses denote plastocyanin. The EPR saturation was measured by the peak height of the EPR signal at g_y in all cases.

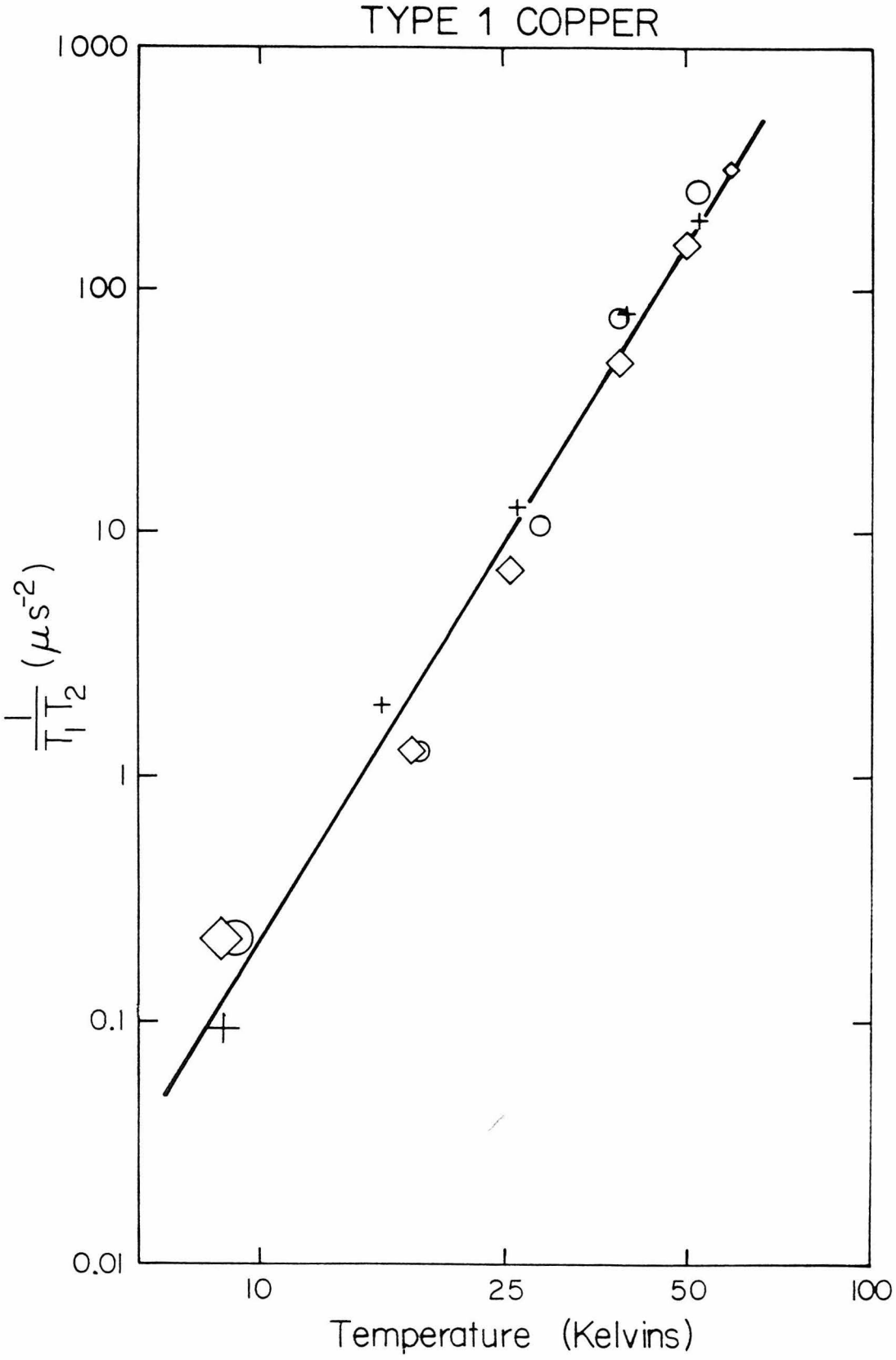
TYPE 1 COPPER
1000
100
10
1
0.1
0.01
$\frac{1}{T_1 T_2}$ (μs^{-2})
10
25
50
100
Temperature (Kelvins)

FIGURE 4

EPR relaxation of the type 2 copper in laccase and the inorganic Cu(II) complexes. The size of the points reflect the estimated error in T and $(T_1T_2)^{-1}$. The hexagons denote the type 2 copper in laccase; the diamonds denote Cu-EDTA #1; the squares denote Cu-EDTA #2; and the circles denote b-tbs Cu. Cu-EDTA #1 had g_{11} = 2.32 and A_{11} = 0.0147 cm^{-1}, while Cu-EDTA #2 had g_{11} = 2.28 and A_{11} = 0.0160 cm^{-1}. The difference in these two complexes probably was due to the protonation of two of the carboxyl groups of EDTA in Cu-EDTA #1 and only one of the carboxyl groups in Cu-EDTA #2. The EPR saturation was measured by the peak height of the EPR signal at g_{max} for all the above complexes except b-tbs Cu which was monitored at g_y.

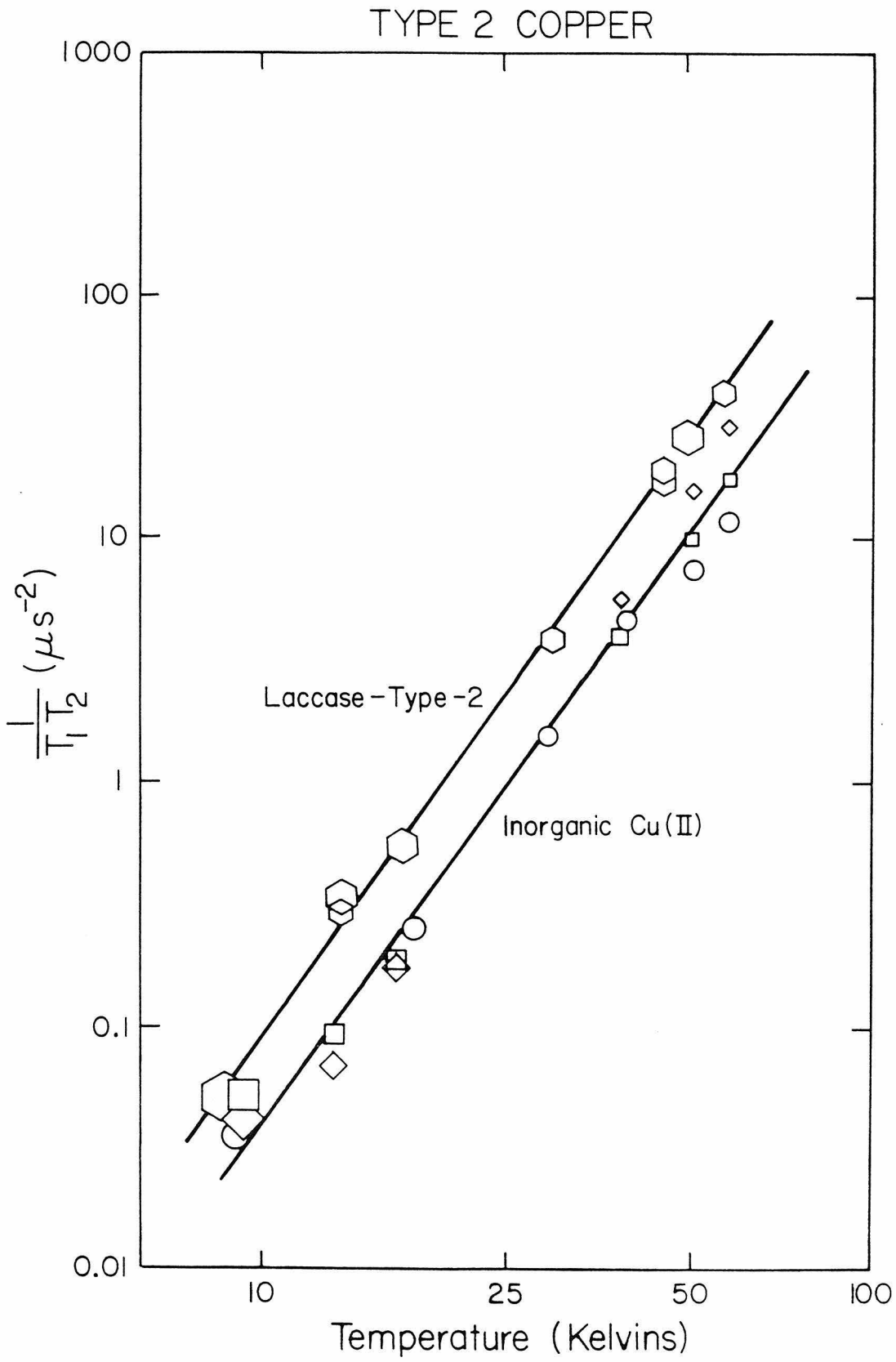
TYPE 2 COPPER
1000
100
10
1
0.1
0.01
$\frac{1}{T_1 T_2}$ (μs^{-2})
Laccase - Type -2
Inorganic Cu(II)
10
25
50
100
Temperature (Kelvins)

FIGURE 5

EPR relaxation of sulfur radicals. The size of the points reflect the estimated error in T and $(T_1T_2)^{-1}$. The EPR saturation was measured by the peak height of the EPR signal at g_{max} in all cases.

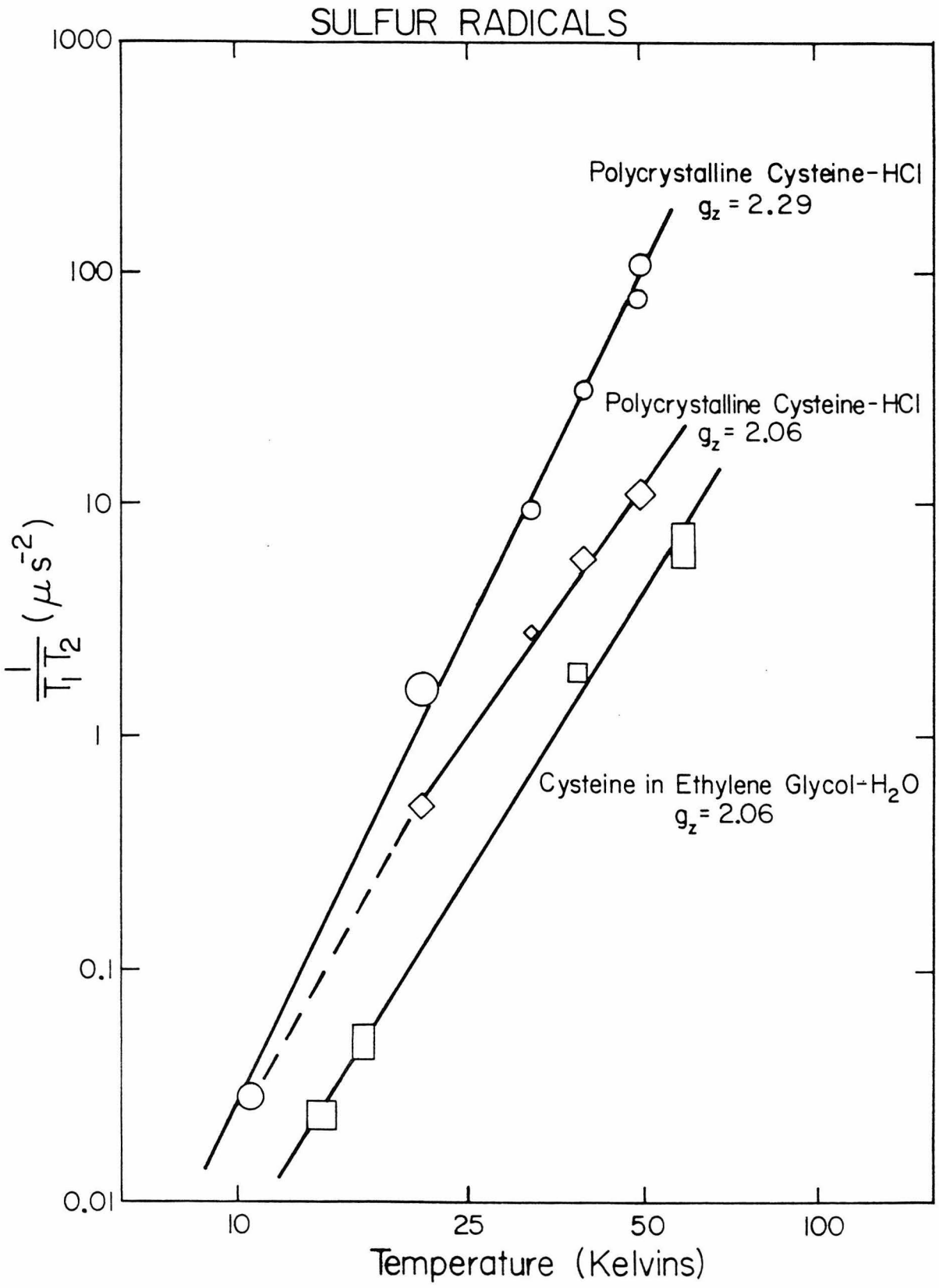
SULFUR RADICALS
1000
100
10
1
0.1
0.01
$\frac{1}{T_1 T_2}$ (μs^{-2})
Polycrystalline Cysteine-HCl
g_z = 2.29
Polycrystalline Cysteine-HCl
g_z = 2.06
Cysteine in Ethylene Glycol-H_2O
g_z = 2.06
10
25
50
100
Temperature (Kelvins)

FIGURE 6

EPR relaxation of the Cu_a center in cytochrome c oxidase. The size of the points reflect the estimated error in T and $(T_1T_2)^{-1}$. The circles denote the values obtained from the native oxidized enzyme and the diamonds denote the values obtained from the cyanide-bound oxidized enzyme. For comparison the lines drawn through the type 1 copper, cysteine-HCl (g_z = 2.29), and the type 2 copper in laccase data from Figures 3-5 are shown. The EPR saturation was measured by the peak height of the EPR signal at g_y.

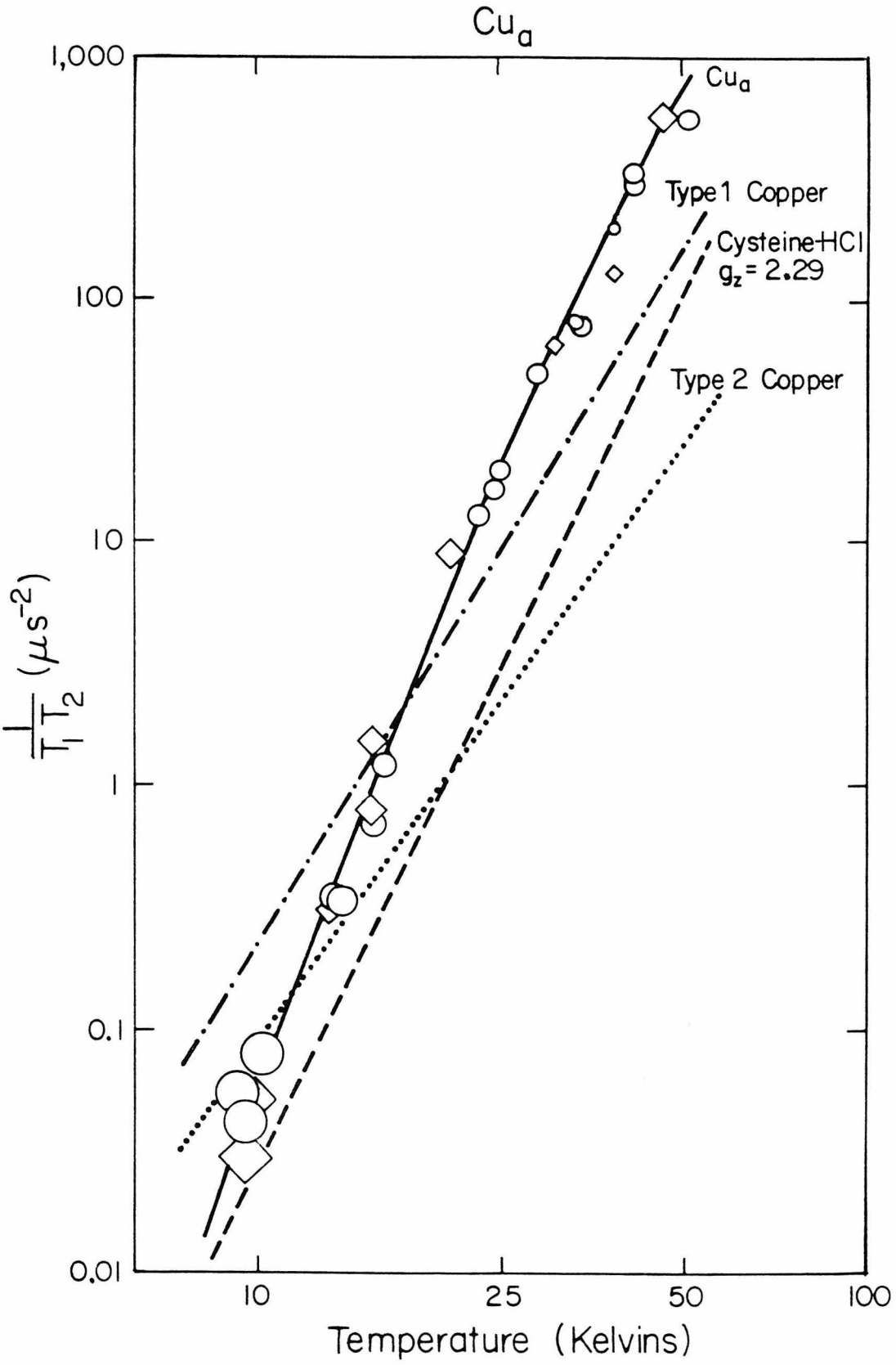
Cu$_a$
1,000
100
10
1
0.1
0.01
$\frac{1}{T_1 T_2}$ (μs^{-2})
Cu$_a$
Type 1 Copper
Cysteine-HCl
g_z = 2.29
Type 2 Copper
10
25
50
100
Temperature (Kelvins)

FIGURE 7

EPR relaxation of low-spin hemes. The size of the points reflect the estimated error in T and $(T_1T_2)^{-1}$. The dotted lines drawn below 12K are to emphasize that the temperature dependence of the low-spin hemes has a break at about 12K. The EPR saturation was measured by the peak height of the EPR signal at g_{max}.

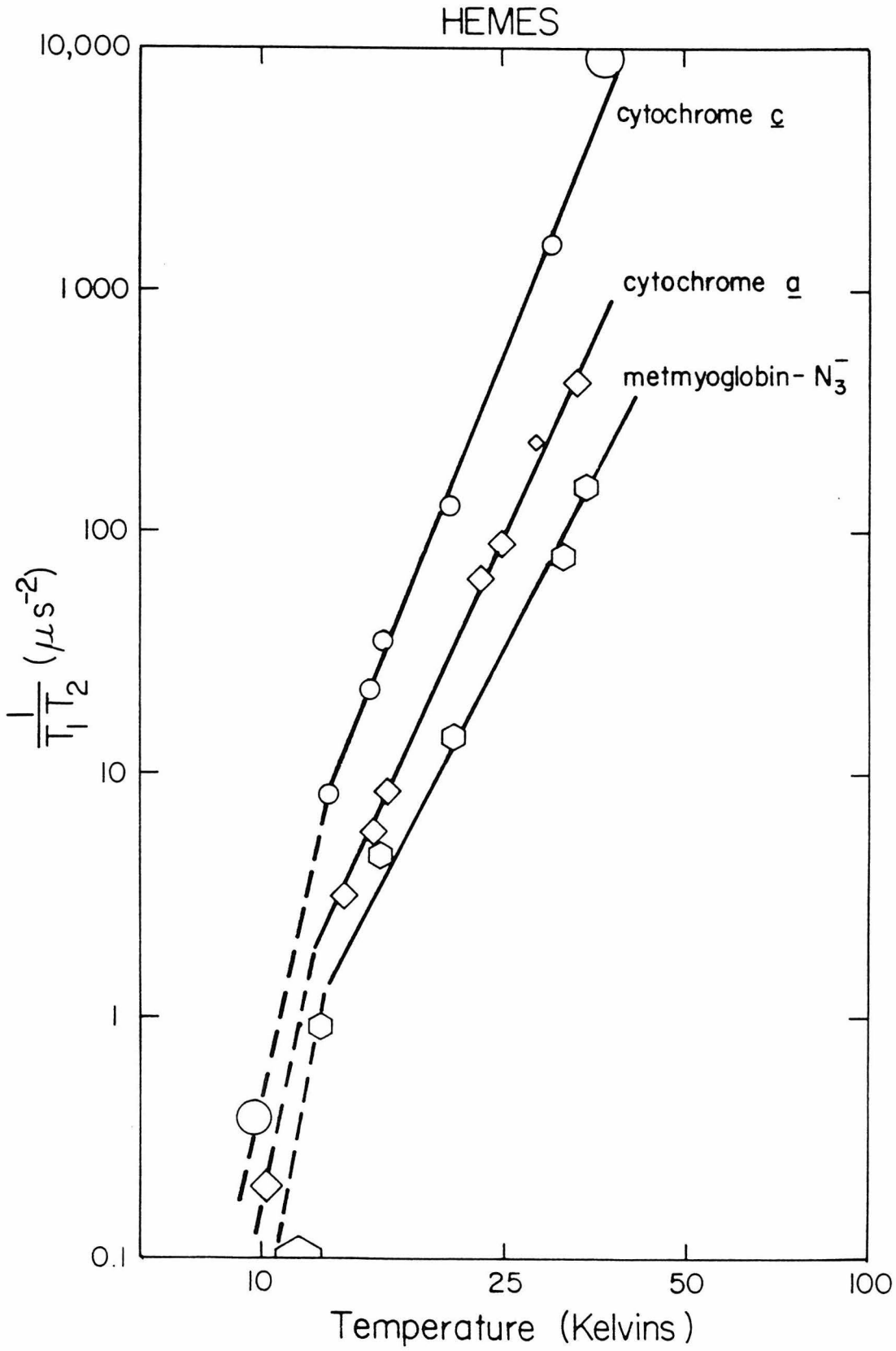
HEMES
10,000
1000
100
10
1
0.1
cytochrome c
cytochrome a
metmyoglobin- N_3^-
$\frac{1}{T_1 T_2}$ (μs^{-2})
10
25
50
100
Temperature (Kelvins)

FIGURE 8

EPR relaxation of the Cu_a center compared to that of cytochrome a. The size of the points reflect the estimated error in T $(T_1 T_2)^{-1}$.

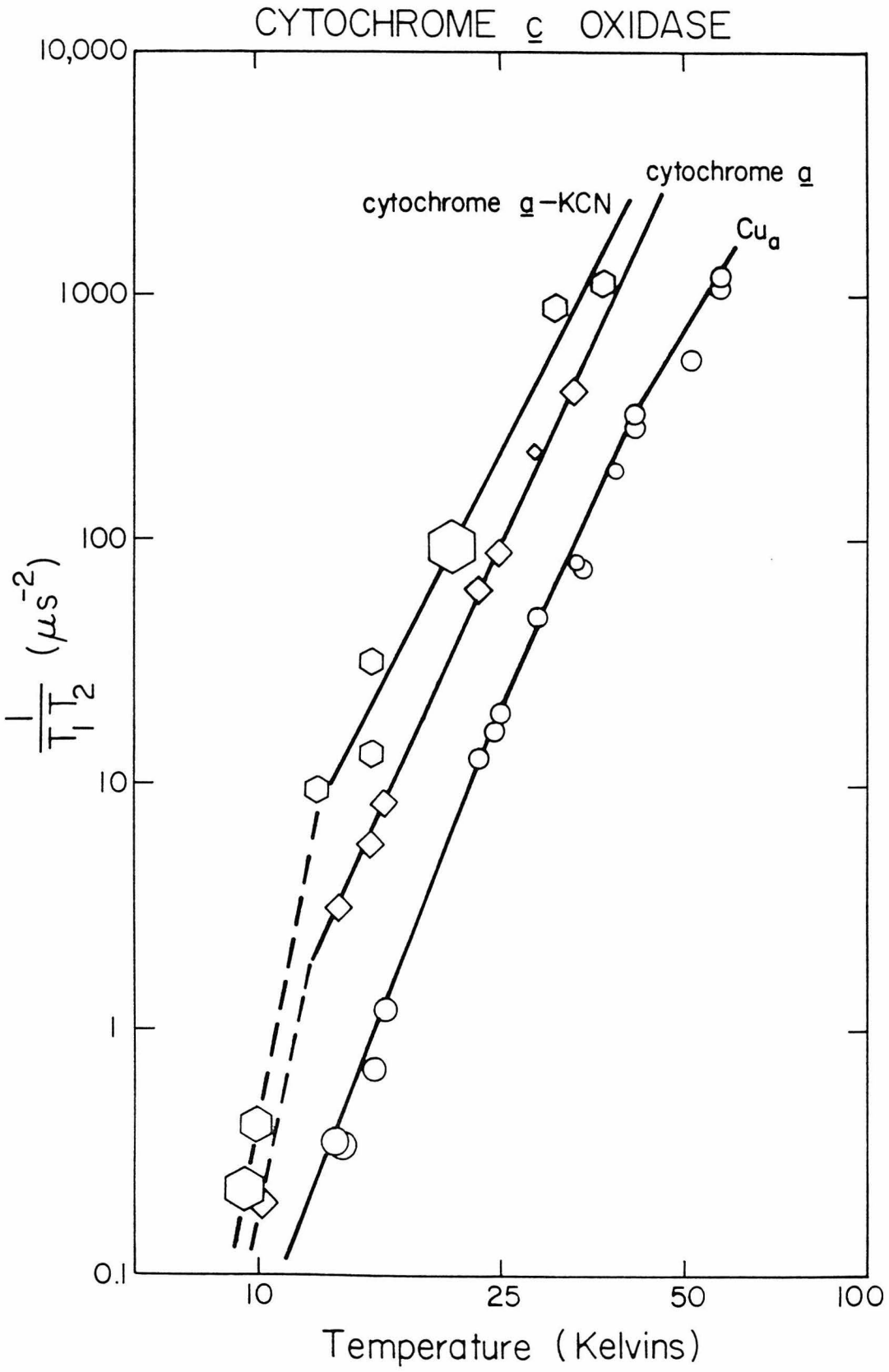
CYTOCHROME c OXIDASE
10,000
1000
100
10
1
0.1
$\frac{1}{T_1 T_2}$ (μs^{-2})
cytochrome a
cytochrome a–KCN
Cu_a
10
25
50
100
Temperature (Kelvins)

will discuss the relative differences between the different samples.

All of the species for which EPR saturation was measured had a spin of 1/2. However, the magnitude of the g-anisotropy varied considerably among the samples. In Figure 9 we have plotted log T_1T_2 observed at 10, 20, and 40K versus the g-anisotropy of the paramagnetic species. It appears that for cysteine radicals, type 2 Cu(II), inorganic Cu(II), and low-spin ferrihemes there is a nearly linear relation between log (T_1T_2) and the g-anisotropy. For $20 \leq T \leq 40K$ the proportionality between $\log(T_1T_2)$ and the g-anisotropy remained constant (note the parallel slopes in Figure 9B and C). At 10K the proportionality between $\log(T_1T_2)$ and the g-anisotropy had changed. The proportionality of $\log(T_1T_2)$ and the g-anisotropy indicates that the spin-lattice relaxation was dominated by the Van Vleck process (see section 1.4) for all the compounds examined except the type 1 coppers and the Cu_a center. The change in slope at 10K from the slope at 20 and 40K in Figure 9 may be an indication that a direct process was becoming important at 10K, but that the Raman process predominated at temperatures above 20K.

The type 1 coppers and the Cu_a center had relaxation rates greater than expected on the basis of their g-anisotropy. However, there is a distinct difference between the relaxation of the type 1 coppers and that of the Cu_a center. The type 1 coppers had had a relaxation rate faster than expected from the g-anisotropy, but at <u>all</u> the temperatures examined, the

FIGURE 9

EPR relaxation versus the g-anisotropy for all of the complexes studied at 10K, 20K, and 40K. The g-anisotropy was taken to be $[(g_x-2)^2 + (g_y-2)^2 + (g_z-2)^2]^{1/2}$. In addition to the abbreviations previously used, the following were used: Lac, laccase-type 2 copper; cys-H_2O, 2.06, cysteine sulfur radical in ethylene glycol/H_2O with g_z = 2.06; cys-HCl, 2.06, cysteine sulfur radical in polycrystalline cysteine-HCl with g_z = 2.06; cys-HCl, 2.29, cysteine sulfur radical in polycrystalline cysteine-HCl with g_z = 2.29; M, metmyoglobin-azide; a, cytochrome a; a-CN, cytochrome a in the cyanide-bound oxidized enzyme; c, cytochrome c.

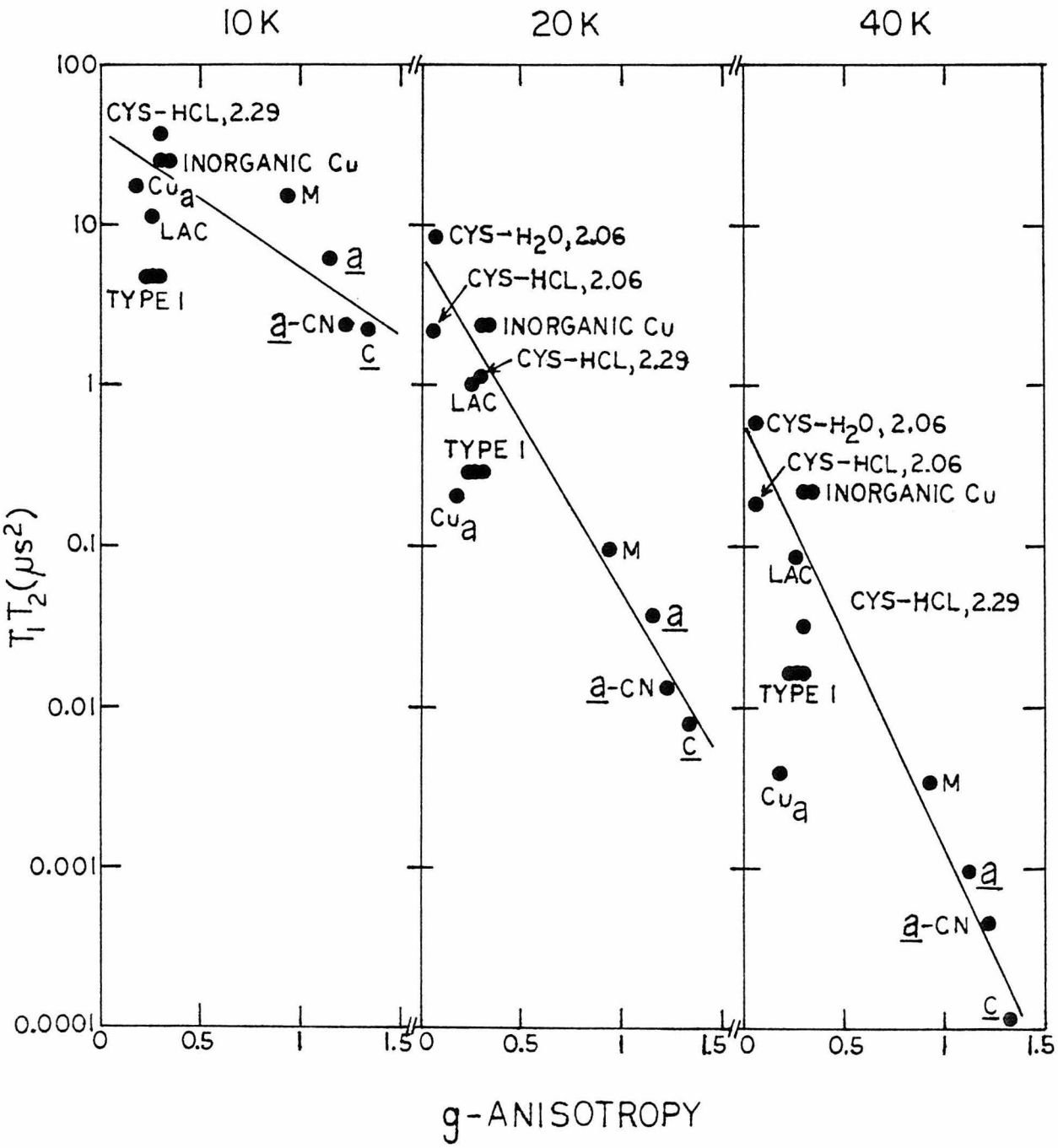
10 K
20 K
40 K
100
10
1
0.1
0.01
0.001
0.0001
$T_1T_2(\mu s^2)$
CYS-HCL, 2.29
INORGANIC Cu
Cu_a
M
LAC
a
TYPE I
a-CN
c
$CYS-H_2O$, 2.06
CYS-HCL, 2.06
0
0.5
1
1.5
g-ANISOTROPY

product of T_1 and T_2 was about 6-7 times shorter than expected. In contrast, at 10K the relaxation of the Cu_a center was close to that expected on the basis of the g-anisotropy, whereas, as the temperature was increased the relaxation of the Cu_a center became increasingly faster than expected. These observations will be discussed in section 4.

The temperature dependence of the product of T_1 and T_2 for all of the complexes examined is given in Table 1. In all cases the average temperature dependence of $-\log(T_1T_2)$ from 12 to 50K was between T^3 and T^7, although in most cases $-\log(T_1T_2)$ probably had a temperature dependence that steadily decreased with temperature. These results are also consistent with the temperature dependence expected if the spin-lattice relaxation is dominated by the Van Vleck mechanism [equation (13)] in the region where $T \approx \theta_D$. However, since all of our samples, except the polycrystalline cysteine-HCL sample, were amorphous, θ_D is not well defined and the calculated temperature dependence of the spin-lattice relaxation [equation (13)] does not necessarily apply to amorphous samples.

3.2 The Cu_a Center in Cytochrome c Oxidase. On the basis of our proposal that the Cu_a center is best described as a Cu(I)-sulfur radical complex (see chapter IV), it may be expected that the spin relaxation of the Cu_a center would be similar to a sulfur radical or possibly intermediate between a sulfur radical and a Cu(II). For this comparison the cysteine sulfur radical with g-values of 2.29, 1.99, and 1.99 is the most appropriate model for the Cu_a center. However, as can be seen from Figure 6,

Table 1: Temperature Dependence of $(T_1T_2)^{-1}$

Species	Temperature Dependence*
Plastocyanin	4.2
Azurin	3.9
Stellacyanin	4.2
Average of type 1 coppers	4.1
Laccase - type 2	3.4
bis(N-t-butylsalicylaldiminato)Cu(II)	3.2
Cu(II)-EDTA #1	3.7
Cu(II)-EDTA #2	3.2
Average of inorganic coppers	3.4
Cysteine-HCl (g_z = 2.29)	5.1
Cysteine-HCL (g_z = 2.06)	3.6
Cysteine in glass (g_z = 2.06)	4.1
Cu_a (native and cyanide derivative)	5.9
Cytochrome c	6.5 (T>12K)
Metmyoglobin-N_3^-	4.8 (T>12K)
Cytochrome a (native)	6.3 (T>12K)
Cytochrome a (cyanide derivative)	4.3 (T>12K)

*A linear least squares fit of the data to: $-\log T_1T_2 = A \log T + B$ was done to obtain the exponent of the temperature dependence, A, assuming $(T_1T_2)^{-1}$ has a T^A dependence.

the spin relaxation of the Cu_a center was not similar to either the sulfur radicals or any of the Cu(II) compounds examined, including the type 1 coppers. In particular, the Cu_a center has a more rapid spin relaxation than any of the sulfur radicals or Cu(II) compounds at temperatures above 20K. Below about 17K, T_1T_2 for the Cu_a center became longer than T_1T_2 for the type 1 coppers, and below about 11K T_1T_2 for the Cu_a center became longer than T_1T_2 for the type 2 and inorganic coppers. However, below 10K the spin relaxation of the Cu_a center was very similar to that of the cysteine sulfur radical with $g_z = 2.29$. This result is suggestive that the spin relaxation of the Cu_a center at low temperature ($T < 10K$) may be representative of the intrinsic relaxation rate which is similar to that of the sulfur radical. At higher temperature the spin relaxation of the Cu_a center could be increased due to a close proximity to one of the hemes in cytochrome c oxidase. Cytochrome a was measured to have a significantly faster relaxation rate than the Cu_a center (Figure 8). The cytochrome a_3-Cu_{a_3} site, being S = 2, is expected to have a much faster relaxation rate than any of the S = 1/2 species examined in this work. Thus, if the slowly relaxing Cu_a center were close to one of the hemes, then the hemes would be expected to substantially increase the relaxation rate of the Cu_a center as described in section 1.2.

It is possible to determine whether or not the Cu_a center is close to the cytochrome a_3-Cu_{a_3} site by examining the effect cyanide has on the spin relaxation of the Cu_a center.

In the oxidized enzyme cytochrome $\underline{a}_3$ and Cu_{a_3} together form a S = 2 site.[26] However, when cyanide binds to cytochrome $\underline{a}_3$ the high-spin heme becomes low-spin and the cytochrome $\underline{a}_3$-Cu_{a_3} site becomes diamagnetic.[26] The spin relaxation of the Cu_a center was unaffected by the formation of the cyanide complex (Figure 6). This result indicates that either the cytochrome $\underline{a}_3$-Cu_{a_3} site is sufficiently far from the Cu_a center so as to not significantly affect the relaxation rate of the Cu_a center, or that there is a compensating change in T_1 and T_2 of the Cu_a center such that the product of T_1 and T_2 remains unchanged. The saturation method only allows the product of T_1 and T_2 to be measured and, hence, these two possibilities cannot be distinguished at this time. Nevertheless, we feel that it is unlikely that a compensating change of T_1 and T_2 in the cyanide derivative from the values in the native enzyme could occur through a dipolar interaction. Moreover, if such a compensating change did occur, it would not be expected to persist over the entire range of temperature examined from 10-50K [see equations (4) and (5)].

An attempt was made to determine whether cytochrome $\underline{a}$ influences the relaxation of the Cu_a center by specifically reducing cytochrome $\underline{a}$. A sample was prepared in which cytochrome $\underline{a}$ was about 30% reduced and the Cu_a center was essentially fully oxidized. The degree of reduction was determined by comparison of the EPR signal intensities with those in the fully oxidized enzyme. However, it was found that the EPR saturation of the Cu_a center was unchanged in this sample.

Attempts to prepare a partially reduced sample in which all of cytochrome a was reduced and the Cu_a center was partially oxidized were unsuccessful. It appears that the reduction potentials of cytochrome a and the Cu_a center are sufficiently close that a sample cannot be prepared in which most of the oxidized Cu_a centers are in molecules in which cytochrome a is reduced. Hence, a direct proof that cytochrome a influences the EPR saturation of the Cu_a center was not obtained.

3.3 Cytochrome a. The EPR saturation of cytochrome a was typical of that expected for a low-spin heme with g-values of 3.00, 2.24, and 1.49. Both the temperature dependence of T_1T_2 (Figure 7) and the magnitude of T_1T_2 with respect to the g-anisotropy (Figure 9) observed for cytochrome a were in agreement with the values predicted by comparison with other low-spin ferrihemes. The EPR saturation properties of cytochrome a, therefore, indicate that T_1 and T_2 of cytochrome a are not significantly affected by any of the other metal centers in cytochrome c oxidase.

The effect of cyanide on the EPR saturation of cytochrome a also demonstrates that the cytochrome a_3-Cu_{a_3} site does not significantly shorten T_1 or T_2 of cytochrome a in the unliganded oxidized enzyme (Figure 8). If the cytochrome a_3-Cu_{a_3} site did decrease T_1 and T_2 of cytochrome a through a dipolar mechanism, then the addition of cyanide (making the cytochrome a_3-Cu_{a_3} site diamagnetic) should increase T_1 and T_2 of cytochrome a. However, the addition of cyanide was found to decrease the product of T_1 and T_2 of cytochrome a. This observation can be

explained by the shift of the g-values for cytochrome a that occurred when cyanide was added to oxidized cytochrome c oxidase (Figure 10). The observed decrease of T_1T_2 in the cyanide-bound enzyme correlates very well with the increased g-anisotropy induced when cyanide was present (Figure 9).

4. DISCUSSION

4.1 Mechanism of Spin Relaxation. The temperature dependence and the magnitude of T_1T_2 for all the complexes examined except the type 1 coppers and the Cu_a center can be reasonably accounted for if the Van Vleck Raman process dominated the spin-lattice relaxation (see Figure 9 and Table 1). It was previously concluded that the Van Vleck Raman process determines the spin-lattice relaxation for organosulfur radicals[32] and also for cytochrome c.[36,37] Our measurements extend these observations to include type 2 copper, inorganic Cu(II) coordinated to oxygen and nitrogen ligands, and low-spin ferrihemes.

The question remains as to why type 1 coppers and the Cu_a center do not exhibit the spin relaxation expected on the basis of their g-anisotropy (Figure 9). We will consider first the type 1 copper for which dipolar interactions are absent. The differences between the structure of type 1 copper and the inorganic Cu(II) complexes we examined are two-fold. First, type 1 copper is coordinated to at least one sulfur ligand;[38,39] the ligands to the type 1 coppers in both plastocyanin and azurin are one cysteine sulfur, one methionine sulfur, and two

FIGURE 10

EPR spectra of (top) native oxidized cytochrome c oxidase and (bottom) cyanide-bound oxidized cytochrome c oxidase. Conditions: temperature, 15K; microwave power, 20 mW; modulation amplitude, 16 G; microwave frequency, 9.25 GHz.

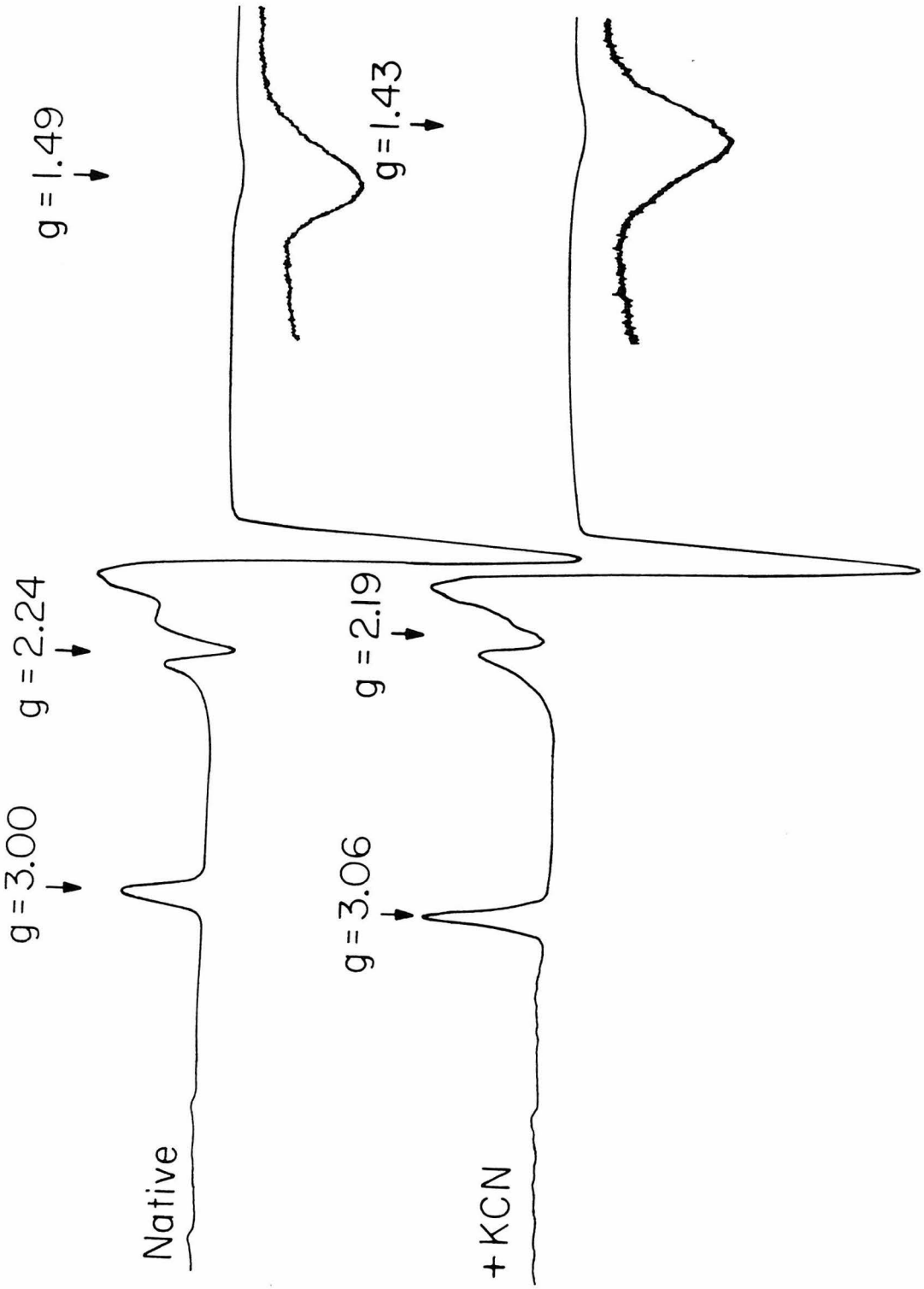
g = 1.49
g = 1.43
g = 2.24
g = 2.19
g = 3.00
g = 3.06
Native
+ KCN

histidine nitrogens, as opposed to only nitrogen and oxygen ligands in the inorganic Cu(II) complexes examined. Second, type 1 copper has a flattened tetrahedral geometry,[38] as opposed to a more nearly square-planar geometry for the inorganic Cu(II) complexes. The geometry does not seem to significantly affect the spin relaxation, though. For b-tbs-Cu the angle[31] between the two chelate ring planes is 54°. Hence, this complex has a quite distorted square planar structure. Nonetheless, the spin relaxation of b-tbs Cu was essentially the same as that of Cu-EDTA, which has a tetragonal geometry. However, it is possible that the presence of both sulfur and copper in the same spin center would lead to a faster spin relaxation than expected on the basis of the g-anisotropy. This is because both sulfur and copper have a fairly large spin-orbit coupling, but these couplings have opposite signs. Consequently, the g-values of Cu(II) coordinated to sulfur ligands may be reduced somewhat from those expected if sulfur were not coordinated to copper due to a cancellation of the copper and sulfur spin-orbit coupling terms (see chapter IV, section 3.2). Nonetheless, this effect is expected to be fairly small and it would seem that the unexpectedly rapid spin relaxation of the type 1 coppers is not due to the presence of sulfur ligands, since sulfur radicals alone were not anomalous.

In section 3.1 we pointed out that the product T_1 and T_2 for type 1 copper was about 6-7 times shorter than that expected on the basis of the g-anisotropy throughout the temperature range studied (10-50K). This result suggests that the spin-

lattice relaxation of the type 1 coppers does proceed via the Van Vleck mechanism, but that the coupling of the phonon bath to the spin center was more effective in the case of type 1 copper than the other Cu(II) complexes examined. The coupling of the phonon bath to the spin center depends on a number of variables. Most important is the lattice structure about the spin center. In this regard, it was found that the cysteine sulfur radical with $g_z = 2.06$ had a significantly slower relaxation rate when trapped in an ethylene glycol-H_2O matrix compared to the rate in crystalline cysteine-HCl (Figure 5). Moreover, we found that the temperature dependence of $(T_1T_2)^{-1}$ for the type 1 coppers could not be fit well at all with the temperature dependence expected if the spin-lattice relaxation was dominated by an Orbach process [equation (15)]. Thus, we conclude that the spin-lattice relaxation of the type 1 coppers is also dominated by the Van Vleck Raman process between 10 and 50K.

For the Cu_a center, the product of T_1 and T_2 was similar to that of the cysteine sulfur radical with $g_z = 2.29$ at 10K and this value was close to the value expected on the basis of the g-anisotropy of the Cu_a center. However, when the temperature was increased the relaxation rate of the Cu_a center became increasingly faster than that expected on the basis of g-anisotropy. This observation indicates that another relaxation mechanism was becoming important at temperatures greater than 10K. This new mechanism must have a strong temperature dependence. Only two possible mechanisms can be invoked to account

for this new relaxation pathway: a dipolar mechanism as described in section 1.2 or an Orbach mechanism as described in section 1.4. However, as was the case for type 1 coppers, the temperature dependence for the Cu_a center could not be fit well at all with the temperature dependence expected if the spin-lattice relaxation was dominated by an Orbach process [equation (15)]. Thus, the EPR saturation data from the Cu_a center appear to indicate that one of the hemes in cytochrome c oxidase influences the relaxation of the Cu_a center through a dipolar mechanism.

We ruled out the possibility that the cytochrome a_3-Cu_{a_3} site interacts with the Cu_a center through a dipolar mechanism by the comparison of the native and cyanide-bound oxidized enzyme. However, it is possible that cytochrome a is close enough to the Cu_a center to influence the relaxation rate of the Cu_a center.

In order to determine how a dipolar interaction between cytochrome a and the Cu_a center will affect the EPR properties of the Cu_a center, it is necessary to determine the magnitude of the spin-lattice relaxation of cytochrome a relative to the dipolar interaction between the two spin centers. We can use our EPR saturation data to estimate T_1 of cytochrome a. Assuming $T_1 = T_2$, our data indicate that T_1 of cytochrome a ranges from 3 μs (10K) to 0.01 μs (40K). Actually T_1 is expected[36] to be longer than these estimates, since over this temperature range $T_1 > T_2$. With this in mind, the estimates of T_1 for cytochrome a can be compared to the maximum dipolar

interaction between cytochrome a and the Cu_a center at various radial separations as calculated from equation (1). The maximum dipolar interaction is: 0.018 μs (r = 5 Å), 0.14 μs (r = 10 Å), 0.47 μs (r = 15 Å), and 1.1 μs (r = 20 Å). From these estimates it can be concluded that the spin-lattice relaxation rate of cytochrome a was sufficiently slow at 10K that, even if the radial separation of cytochrome a and Cu_a was as large as 20 Å, cytochrome a should induce a static dipolar splitting of the Cu_a center EPR signal. At temperatures greater than 10K this dipolar splitting should disappear; the temperature at which this occurs will depend on how large the dipolar splitting is. In addition the effect cytochrome a has on the Cu_a center relaxation rate should become increasingly more pronounced as the temperature is increased.

It has been observed at S-band that the Cu_a center EPR signal exhibits a 25 G splitting due to a S = 1/2 site only on the Y component.[40] We mentioned in chapter IV that this hyperfine coupling did not appear to be due to a proton.[41] Several observations suggest that this hyperfine coupling may be due to a static dipolar splitting of the Cu_a center EPR signal by cytochrome a. First, the splitting can only be observed at temperatures below about 30K. Above this temperature the splittings broaden and disappear. This result agrees very well with that predicted on the basis of our spin relaxation measurements. At about 30K the spin-lattice relaxation rate of cytochrome a becomes comparable to a 25 G dipolar interaction and, hence, the dipolar interaction will be averaged away by

the relaxation of cytochrome a above about 30K. Secondly, the 25 G hyperfine interaction is quite anisotropic, being unresolvable in the X and Z components of the EPR spectrum. A dipolar interaction is expected to be anisotropic. However, the dipolar interaction between a nuclear spin and the unpaired electron on the Cu_a center could not be large enough to produce a 25 G hyperfine interaction. In the case of protons, the nuclear spin would have to be within 1 Å to produce a sufficiently large dipolar field. If cytochrome a were the S = 1/2 species responsible for the 25 G hyperfine coupling, then the distance between cytochrome a and Cu_a is less than or equal to 13 Å. This maximum value was obtained by assuming the angle between the radial vector and the external magnetic field was 0° [equation (1)].

The S-band EPR result in addition to our EPR saturation data suggest that cytochrome a is within 13 Å of the Cu_a center. The question then arises of why the Cu_a center does not induce any observable splittings in the cytochrome a EPR signal and why the spin relaxation of cytochrome a is not altered by its proximity to the Cu_a center.

The manifestation of a dipolar splitting in the EPR spectrum is strongly dependent on the g-anisotropy of the paramagnetic site of interest. For example, dipolar interactions are much more evident in free radicals than in low-spin hemes[42] because the g-anisotropy of a free radical is small ($\Delta\omega_g < 1$ MHz) while that of a low-spin heme is large ($\Delta\omega_g > 1$ GHz) at X-band. In order for a dipolar interaction to significantly perturb the

EPR spectrum of a low-spin heme, the dipolar splitting, $\Delta\omega_d$, must be on the order of the g-anisotropy, i.e., $\Delta\omega_d \approx \Delta\omega_g$. For cytochrome a, $\Delta\omega_g$ = 6.6 GHz, while for the Cu_a center, $\Delta\omega_g$ = 810 MHz. Therefore, a dipolar interaction between cytochrome a and the Cu_a center will perturb the EPR signal from the Cu_a center to a greater degree than that of cytochrome a (see the example presented in reference 42).

The dipolar induced relaxation rates are given in equations (4) and (5). It is important to note that the dipolar contribution to $1/T_1$ adds to the intrinsic rate, $1/T_1^o$. The contribution of the dipolar mechanism of relaxation to the total relaxation rate will only be significant if the intrinsic relaxation rate is less than or approxomately equal to the dipolar relaxation rate. Hence, a rapidly relaxing site can strongly affect the relaxation of a nearby slowly relaxing site, while the reverse interaction is insignificant compared to the intrinsic relaxation rate of the rapidly relaxing site. Such is the case for the interaction between cytochrome a (rapid intrinsic relaxation) and the Cu_a center (slow intrinsic relaxation).

4.2 Distribution of the Metal Centers in Cytochrome c Oxidase. The anomalously short relaxation rate for the Cu_a center and the 25 G hyperfine coupling due to a S = 1/2 site discussed above together are consistent with the Cu_a center and cytochrome a being within 13 Å of each other. Furthermore, the lack of any effect by cyanide on the relaxation of the Cu_a center indicates that the cytochrome a_3-Cu_{a_3} site is sufficiently

far from the Cu_a center so as to not significantly affect the relaxation rate of the Cu_a center. From this result we can conclude that the cytochrome $\underline{a}_3$-Cu_{a_3} site must be more than 10 Å from the Cu_a center.

The relaxation of cytochrome $\underline{a}$ also was not significantly affected by the cytochrome $\underline{a}_3$-Cu_{a_3} site. However, the addition of cyanide to the enzyme altered the g-values of cytochrome $\underline{a}$, even though cyanide only binds to the cytochrome $\underline{a}_3$-Cu_{a_3} site. In view of the lack of effect of simply changing the ionic strength or the pH of the buffer on the cytochrome $\underline{a}$ EPR signal, this observation is an indication that the binding of cyanide to cytochrome $\underline{a}_3$ induces a conformational change of the protein that affects the crystal field of cytochrome $\underline{a}$. Interactions between the metal centers of this type have been proposed previously to explain the redox properties of the enzyme.[43] It appears that a conformational change of the protein can be propagated over a considerable distance within cytochrome $\underline{c}$ oxidase, allowing the crystal field of cytochrome $\underline{a}$ to be modified slightly in response to the transition of cytochrome $\underline{a}_3$ from high to low-spin.

The relative proximity of the metal centers in cytochrome $\underline{c}$ oxidase as suggested by this work is shown in Figure 11. Further work, in particular the measurement of T_1 as a function of temperature for both the Cu_a center and cytochrome $\underline{a}$, could allow the relative distances between the metal centers to be more accurately determined.

FIGURE 11

Proposed relative proximity of the metal centers in cytochrome c oxidase.

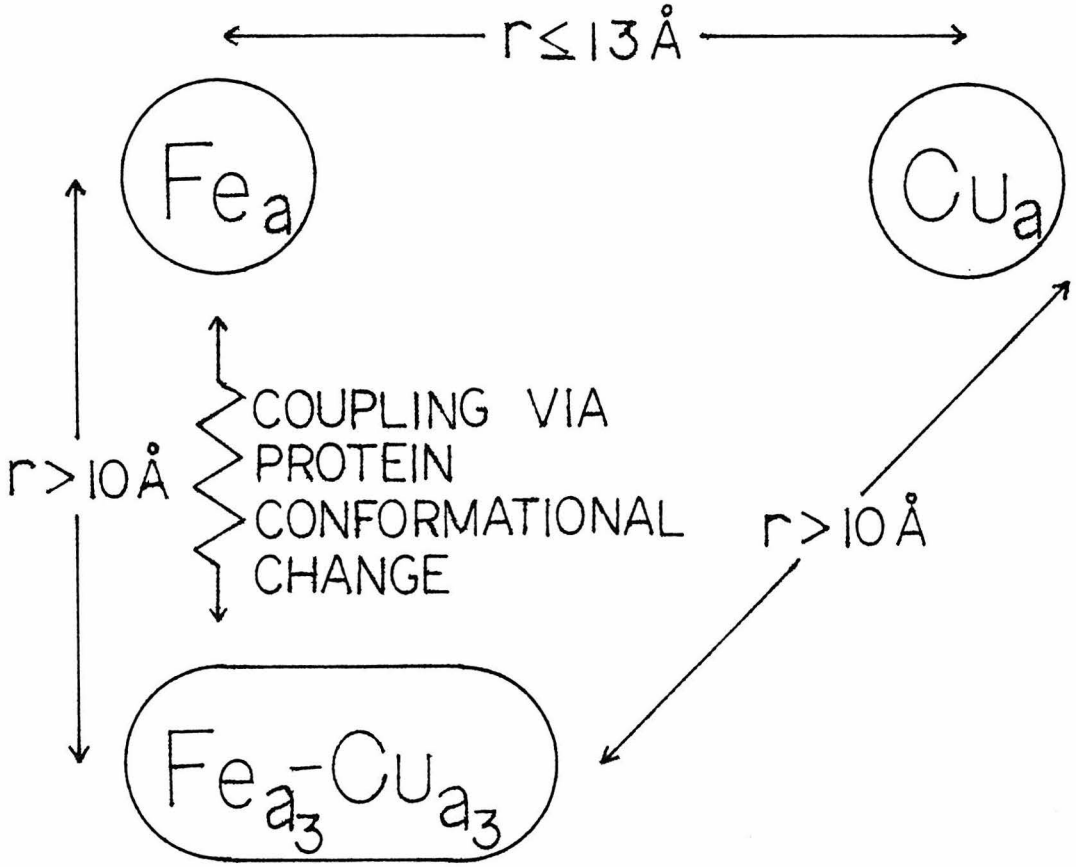
r≤13Å
Fe a
Cu a
r>10Å
COUPLING VIA
PROTEIN
CONFORMATIONAL
CHANGE
r>10Å
Fe a3 - Cu a3

References

1. Wikström, M. and K. Krab (1979), Biochim. Biophys. Acta 549, 177.
2. Mitchell, P. (1976), Biochem. Soc. Trans. 4, 399.
3. Dockter, M.E., A. Steinemann, G. Schatz (1978), J. Biol. Chem. 253, 311.
4. Ferguson-Miller, S., D.L. Brautigan and E. Margoliash (1978), J. Biol. Chem. 253, 149.
5. Mann, A.J. and H.E. Auer (1980), J. Biol. Chem. 255, 454.
6. Hyde, J.S., H.M. Swartz and W.E. Antholine (1979), in "Spin Labeling II", (L.J. Berliner, ed.), Academic Press, N.Y., 71.
7. Eaton, S.S. and G.R. Eaton (1978), Coord. Chem. Rev. 26, 207.
8. Kulikov, A.V. and G.I. Likhtenstein (1977), Adv. Molec. Relaxn. Int. Proc. 10, 47.
9. Abragam, A. (1961), "The Principles of Nuclear Magnetism", Oxford, London, chp. 8.
10. Pake, G.E. (1948), J. Chem. Phys. 16, 327.
11. Abragam, A. (1961), "The Principles of Nuclear Magnetism", Oxford, London, chp. 9.
12. Poole, C.P. and H.A. Farach (1971), "Relaxation in Magnetic Resonance", Academic Press, N.Y.
13. Kevan, L. and R.N. Schwartz, eds. (1979), "Time Domain Electron Spin Resonance", Wiley, N.Y.
14. Portis, A.M. (1953), Phys. Rev. 91, 1071.
15. Cullis, P.R. (1976), J. Magn. Res. 21, 397.

16. Castner, T.G., Jr. (1959) Phys. Rev. 115, 1506.

17. Rupp, H., K.K. Rao, D.O. Hall and R. Cammack (1978), Biochim. Biophys. Acta 537, 255.

18. Rupp, H. and A.L. Moore (1979), Biochim. Biophys. Acta 548, 16.

19. Van Vleck, J.H. (1939), J. Chem. Phys. 7, 72.

20. Van Vleck, J.H. (1940), Phys. Rev. 57, 426.

21. Kronig, R. de L. (1939), Physica (Utrecht) 6, 33.

22. Orbach, R. (1961), Proc. Roy. Soc. A264, 458.

23. for a discussion of spin-lattice relaxation see: Abragam, A. and B. Bleaney (1970), "Electron Paramagnetic Resonance of Transition Ions", Oxford, London, chp. 10.

24. Huang, C. (1965), Phys. Rev. 139, A241.

25. Kiel, A. and W.B. Mims (1967), Phys. Rev. 161, 386.

26. Tweedle, M.F., L.J. Wilson, L. Garćia-Iñiguez, G.T. Babcock and G. Palmer (1978), J. Biol. Chem. 253, 8065.

27. Beinert, H. and G. Palmer (1964), J. Biol. Chem. 239, 1221.

28. Chan, S.I., D.F. Bocian, G.W. Brudvig, R.H. Morse and T.H. Stevens (1978), in "Frontiers of Biological Energetics", vol. 2, (P.L. Dutton, J.S. Leigh, Jr. and A. Scarpa, eds.), Academic Press, N.Y., 883.

29. Chan, S.I., D.F. Bocian, G.W. Brudvig, R.H. Morse and T.H. Stevens (1979), in "Cytochrome Oxidase", (T.E. King, Y. Orii, B. Chance and K. Okunuki, eds.), Elsevier, Amsterdam, 177.

30. Hartzell, C.R. and H. Beinert (1974), Biochim. Biophys. Acta 368, 318.

31. Sacconi, L. and M. Ciampolini (1964), J. Chem. Soc. A, 276.

32. Akasaka, K. (1966), J. Chem. Phys. 45, 90.

33. Hadley, J.H., Jr. and W. Gordy (1977), Proc. Natl. Acad. Sci. USA 74, 216.

34. Lloyd, J.P. and G.E. Pake (1953), Phys. Rev. 92, 1576.

35. for a review of type 1 and type 2 copper proteins see: Fee, J. (1975), Struct. Bonding (Berlin) 23, 1.

36. Blum, H. and T. Ohnishi (1980), Biochim. Biophys. Acta 621, 9.

37. Mailer, C. and C.P.S. Taylor (1973), Biochim. Biophys. Acta 322, 195.

38. Colman, P.M., H.C. Freeman, J.M. Guss, M. Murata, V.A. Norris, J.A.M. Ramshaw and M.P. Venkatappa (1978), Nature 272, 319.

39. Adman, E.T., R.E. Stenkamp, L.C. Sieker and L.H. Jensen (1978), J. Mol. Biol. 123, 35.

40. Froncisz, W., C.P. Scholes, J.S. Hyde, Y. Wei, T.E. King, R.W. Shaw and H. Beinert (1979), J. Biol. Chem. 254, 7482.

41. Hoffman, B.M., J.E. Roberts, M. Swanson, S.H. Speck and E. Margoliash (1980), Proc. Natl. Acad. Sci. USA 77, 1452.

42. Palmer, G. (1979), Adv. Inorg. Bioch. 2, 153.

43. Lanne, B. and T. Vänngård (1978), Biochem. Biophys. Acta 501, 449.

CHAPTER VI: SUMMARY

Our objective in this work was two-fold. First to obtain information on the structure of the metal centers in cytochrome c oxidase; and, secondly, to determine the role each metal center plays in the overall function of the enzyme. For many enzyme molecules, x-ray crystallography has been the primary method used to obtain structural information. However, at the present time crystals of cytochrome c oxidase suitable for x-ray crystallography have not been obtained. Moreover, determining the structure of a large oligomeric complex, such as cytochrome c oxidase, by x-ray crystallography would be a monumental undertaking; perhaps it may not even be possible to refine the structure sufficiently to determine the geometry and ligation of the metal centers. In view of this, we have chosen to investigate the structure of the metal centers by other spectroscopic techniques, primarily EPR.

The work described in this thesis represents a continuation of the structural studies on cytochrome c oxidase that were initiated several years before I came to Caltech by Valerie Hu and Sunney Chan. Hu et al.[1,2] used the technique of x-ray absorption spectroscopy to investigate the oxidation state of the iron and copper atoms in the enzyme. One striking conclusion of Hu et al.[1] was that one of the copper atoms was in the +1 oxidation state in the oxidized enzyme. Subsequently, this work was brought into question by the claim that the enzyme was reduced by x-irradiation.[3] However, we have shown that x-

irradiation of oxidized cytochrome c oxidase did not cause any significant reduction of the metal centers under the conditions that x-ray absorption measurements are presently being made.[4] This work supports the conclusion of Hu et al.[1] that one of the copper atoms in the oxidized enzyme is formally Cu(I). We have undertaken further experiments to determine the nature of this unusual copper atom in cytochrome c oxidase. The Cu_a center in cytochrome c oxidase exhibits an unusual EPR signal that has been interpreted to arise either from delocalization of the unpaired electron spin onto an associated ligand[5] or from mixing of the copper 4p orbital with the 3d ground state.[6] We have found that Ag^+, a sulfhydryl binding agent, disrupts the Cu_a center.[7,8] This result, and an examination of the EPR properties of the native oxidized Cu_a center, suggests that the Cu_a center is best described as a Cu(I)-sulfur radical complex in the oxidized enzyme, in agreement with the earlier suggestion of Hu et al.[1] A model is proposed[7,8] for the structure of the Cu_a center in which a Cu(I), in a nearly tetrahedral geometry, is ligated to two nitrogens from neutral histidine residues, and two sulfurs, one a thiolate and one a thiyl radical from cysteine residues. This model is shown to be consistent with all the available data on the Cu_a center. It is suggested that the unusual structure for the Cu_a center may be a consequence of this center being involved in a proton pumping mechanism of cytochrome c oxidase.

Recently, Tom Stevens in our laboratory has initiated new work directed toward testing our model of the Cu_a center. Iso-

topically labeled histidine and cysteine has been incorporated into yeast cytochrome c oxidase. EPR studies of the enzyme containing isotopically labeled cysteine have already provided strong evidence in support of our model for the Cu_a center.[9] ENDOR studies on the isotopically labeled yeast enzymes should provide further information on the structure of the Cu_a center.

In contrast to the Cu_a center, the second copper in cytochrome c oxidase, Cu_{a_3}, has proven to be very difficult to study. In fact, other than x-ray absorption spectroscopy,[1-3] no direct observation of Cu_{a_3} had been possible until the work of Stevens et al..[10] Our most significant contribution in the present work has been the studies on the structure and function of the cytochrome a_3-Cu_{a_3} site.

In order to investigate the structure and function of the cytochrome a_3-Cu_{a_3} site by EPR, it is necessary to break the strong antiferromagnetic coupling that exists between these two metal centers in the oxidized enzyme. To do this, we have utilized NO as a spin probe. The function of NO is two-fold: to uncouple[10] cytochrome a_3 and Cu_{a_3}, and to induce a cycle of relatively slow reduction and reoxidation of the enzyme.[11] In combination, these two functions of NO allowed us to follow the reaction of NO with cytochrome c oxidase by EPR and, thereby, determine the states of enzyme formed during the catalytic cycle. These results were used to formulate a mechanism by which reduced cytochrome c oxidase reduces O_2 to water. This mechanism is shown to be consistent with the available data on the reaction of O_2 with the reduced enzyme.

When cytochrome c oxidase is reoxidized by O_2 several transient states of the enzyme are formed before the most stable oxidized conformation is obtained. We used NO as a probe to monitor the formation of these states by EPR. It was found that three conformations are formed in sequence. These conformations are interpreted to form when a $Cu_{a_3}(II)\text{-}OH_2$, $HO^-\text{-}Fe_{a_3}(III)$ state (the initial state formed when the reduced enzyme becomes fully oxidized by O_2) relaxes to a $Cu_{a_3}(II)\text{-}OH^-\text{-}Fe_{a_3}(III)$ state and finally to the most stable $Cu_{a_3}(II)\text{-}O^{-2}\text{-}Fe_{a_3}(III)$ state. The enzyme as isolated was found to be heterogeneous, containing a mixture of more than one of these conformations in various proportions depending on the method of preparation.

One of the most important questions on the structure of cytochrome c oxidase remains: where are the metal centers in the overall enzyme complex? In particular, it is not known at the present time whether cytochrome's a and a_3 are on the same or opposite sides of the inner mitochondrial membrane. Although this may seem like a simple question to answer, information on the position of the metal centers in cytochrome c oxidase has been indirect and difficult to obtain.

We have directed our effort toward determining the distances between the four metal centers. When two paramagnetic centers are in close proximity, the dipolar interaction between the two sites can modify both the EPR signals and electron relaxation rates of the interacting sites. We obtained a one-quarter reduced NO-bound state of cytochrome c oxidase by the specific reaction of NO and azide with the oxidized enzyme. In this

state, a triplet EPR signal was observed from nitrosylferro-cytochrome $\underline{a}_3$ and $Cu_{a_3}^{+2}$ due to the dipolar coupling of these two S = 1/2 sites. We estimated that the two metal centers that comprise the O_2 binding site, cytochrome $\underline{a}_3$ and Cu_{a_3}, are separated by about 5 Å on the basis of the magnitude of the dipolar coupling between them in the one-quarter reduced NO-bound enzyme.

The other two metal centers, cytochrome $\underline{a}$ and Cu_a, have generally been assumed to be isolated from each other and the O_2 binding site. However, we have found that the electron spin relaxation rate of the Cu_a center was more rapid than expected. On the basis of this result, and S-band EPR results, it is concluded that the Cu_a center is within 13 Å of cytochrome $\underline{a}$. In addition, the Cu_a center and cytochrome $\underline{a}$ are both sufficiently far from the cytochrome $\underline{a}_3$-Cu_{a_3} site that no dipolar interactions between either the Cu_a center or cytochrome $\underline{a}$ and the cytochrome $\underline{a}_3$-Cu_{a_3} site were detected.

This work has provided a rough picture of the distribution of the metal centers in cytochrome $\underline{c}$ oxidase. Further work is necessary to obtain more precise values for the distances between the metal centers. In addition, the location of each metal center within the cytochrome $\underline{c}$ oxidase complex still remains to be determined. However, our results on the distances between the metal centers, as well as the models we have proposed for the structures of the Cu_a center and the cytochrome $\underline{a}_3$-Cu_{a_3} site, provide a framework from which future studies on the structure and function of cytochrome $\underline{c}$ oxidase can be guided.

References

1. Hu, V.W., S.I. Chan and G.S. Brown (1977), Proc. Natl. Acad. Sci. USA 74, 3821.
2. Hu, V.W., S.I. Chan and G.S. Brown (1977), FEBS Lett. 84, 287.
3. Powers, L., W.E. Blumberg, B. Chance, C.H. Barlow, J.S. Leigh, Jr., T. Yonetani, S. Vik and J. Peisach (1979), Biochim. Biophys. Acta 546, 520.
4. Brudvig, G.W., D.F. Bocian, R.C. Gamble and S.I. Chan (1980), Biochim. Biophys. Acta 624, 78.
5. Peisach, J. and W.E. Blumberg (1974), Arch. Biochem. Biophys. 165, 691.
6. Greenaway, F.T., S.H.P. Chan and G. Vincow (1977), Biochim. Biophys. Acta 490, 62.
7. Chan, S.I., D.F. Bocian, G.W. Brudvig, R.H. Morse and T.H. Stevens (1978), in "Frontiers of Biological Energetics", vol. 2, (P.L. Dutton, J.S. Leigh, Jr. and A. Scarpa, eds.), Academic Press, N.Y., p. 883.
8. Chan, S.I., D.F. Bocian, G.W. Brudvig, R.H. Morse and T.H. Stevens (1979), in "Cytochrome Oxidase", (T.E. King, Y. Orii, B. Chance and K. Okunuki, eds.), Elsevier, Amsterdam, p. 177.
9. Stevens, T.H., personal communication.
10. Stevens, T.H., G.W. Brudvig, D.F. Bocian and S.I. Chan (1979), Proc. Natl. Acad. Sci. USA 76, 3320.
11. Brudvig, G.W., T.H. Stevens and S.I. Chan (1980), Biochemistry 19, in press.